Use of Polyhexanide and Nanomedicine Approach for Effective Treatments of Cutaneous Leishmaniasis

Die Verwendung von Polyhexaniden und Konzepten der Nanomedizin zur effektiven Behandlung kutaner Leishmaniose

Doctoral thesis for a doctoral degree

at the Graduate School of Life Sciences,

Julius-Maximilians-Universität Würzburg,

Infection and Immunity

submitted by

Rebuma Firdessa Fite

from

Wollega, Oromia, Ethiopia

Würzburg, 2015

Submitted on: ……..……..

Office stamp

Members of the *Promotionskomitee*:

Chairperson:	**Prof. Dr. Thomas Hünig**
Primary Supervisor:	**Prof. Dr. Heidrun Moll**
Supervisor (Second):	**AOR Dr. Tobias Ölschläger**
Supervisor (Third):	**Prof. Dr. Richard Lucius**

Date of Public Defence: ……..……

Date of Receipt of Certificates: …….

Table of contents

Figure legends

Table legends

1. INTRODUCTION

1.1 Leishmaniasis

Leishmaniasis is a zoonotic disease caused by obligate intracellular, protozoan parasites of the genus *Leishmania,* which maintain their life cycle through transmission between sandfly and a mammalian host. During their life cycle, *Leishmania* procyclic promastigotes differentiate in sandflies' gut into infective, non-dividing metacylic promastigotes. The female sandflies regurgitate the metacylic promastigotes together with various parasite derived immunomodulatroy agents and salivary components during blood feeding on mammalian host[1]. Once the metacylic promastigotes are in the mammalian host's blood, they are taken up by phagocytes and transformed to the dividing intracellular form called amastigotes. The amastigotes then undergo multiplication within the phagocytes at the infection site until the host cell bursts, allowing the freed parasites to infect other phagocytic cells (Fig. 1). Since *Leishmania* parasites have several molecular patterns, which can be detected by pattern-recognition receptors (PRRs) of the mammalian host, they should be detected during internalizations by macrophages. Macrophages are coated with various PRRs. The parasites then cause either asymptomatic or a more severe symptomatic outcome by manipulating macrophage's function in multiple ways, including subverting the control of phagosome biogenesis and maturation[1]. The asymptomatic stage of the diseases pathogenesis is a very critical stage where it can either potentially conferring immunity to superinfection or creating the dangerous likelihood of reactivation, which is often associated with a more severe symptomatic outcome[2,3].

Leishmaniasis has persisted for centuries as life-threatening and disfiguring parasitic diseases affecting about 350 million people around the world in 98 countries with an overall estimated prevalence of 12 million and a yearly incidence of 2 million new cases[1,4,5]. It is one of the world's most neglected tropical diseases, affecting mainly very poor people in

developing countries where the patients cannot afford the costs for medication. It encompasses localized (skin lesions) and disseminated infection (cutaneous, mucosal, or visceral). Although little is known about the basic mechanisms of symptomatic divergence, several determinant parameters, such as host response or susceptibility, parasite genetic background and various environmental factors related to the vector have been commonly associated with the disease outcomes[2,6,7]. These factors significantly complicate the diagnosis, treatment and control of leishmaniasis. Despite its high prevalence and huge suffering it causes, the disease remains largely uncontrolled, with few sub-optimum treatment options, little clinical research interest and no effective vaccine[8,9]. The current treatment regimes against cutaneous leishmaniasis (CL) can be either topical or systemic therapy based on *Leishmania* species, geographic regions, and clinical presentations[10]. It has been recently suggested that effective intervention measurements of the disease should consider both the host and pathogen[1].

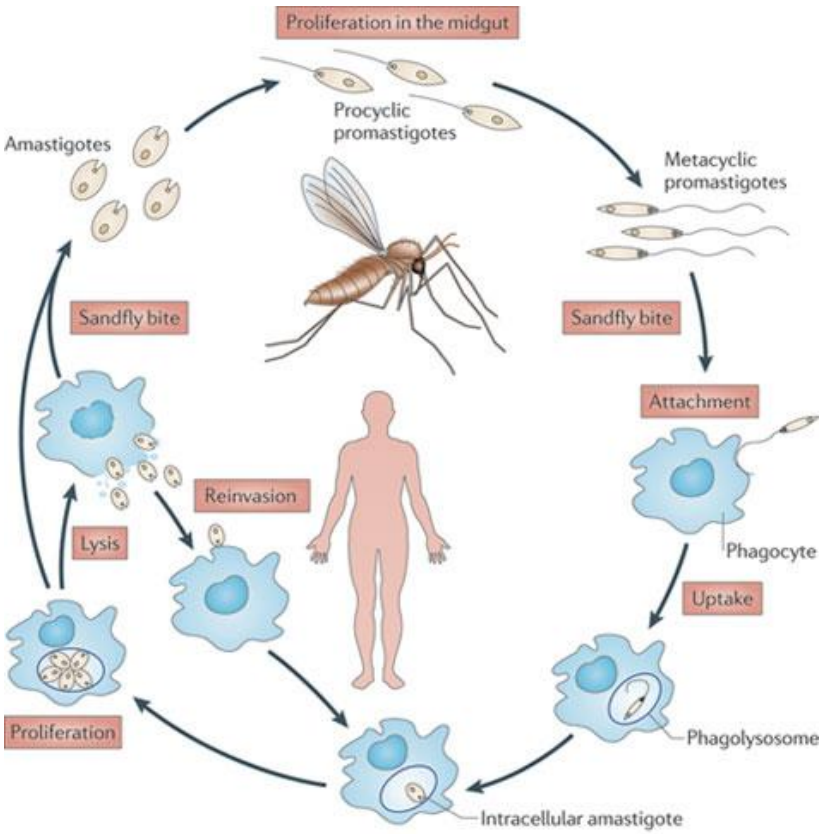

Fig. 1. *Life cycles of Leishmania parasites*[1]

1.1.1 Pathogen factor

Leishmaniasis is generally caused by species of two major *Leishmania* subgenera, namely *Leishmania* (*Leishmania*) and *Leishmania (Viannia*). The two subgenera of *Leishmania* comprise of about 30 species, which can produce a large spectrum of clinical manifestations in humans. Depending on the infecting species, the parasites can induce different disease pathologies in a susceptible host, from asymptomatic to fatal visceral disease[3]. Thus, it is evident that each *Leishmania* species has its own tropism and specific clinical forms[3]. Moreover, it has been shown that virulence factors of the parasite (for example, lipophosphoglycan) are dependent upon leishmanial species[1]. For instance: While *Leishmania donovani (L. donovani)* species complex, including *L. donovani, Leishmania chagasi (L. chagasi),* and *Leishmania infantum (L. infantum),* almost invariably cause life-threatening visceral leishmaniasis (VL) that usually have no cutaneous manifestations in immunocompetent humans, the remaining human-infective *Leishmania* species usually cause CL, with varying degrees of severity: localized cutaneous, diffuse cutaneous, and disseminated or mucocutaneous leishmaniasis[2,7,9]. CL is chronically disfiguring parasitic infections with symptoms of disease commonly caused by *Leishmania tropica (L. tropica), Leishmania major (L. major), L. donovani, L. infantum, Leishmania aethiopica (L. aethiopica)* and *Leishmania mexicana (L. Mexicana),* whereas, the mucocutaneous leishmaniasis (MCL), the extension of local skin disease into the mucosal tissue, is most frequently caused by *Leishmania braziliensis (L. braziliensis)* complex, where metastasis occurs in 5–10% of CL patients[2,9]. These phylogenetic clustering supports the idea that symptomatic tropism is determined by species-specific parasite factors.

Importantly, disease phenotypes of CL and VL can be replicated in mouse models. *L. major* causes progressive footpad swelling in susceptible mouse strains such as BALB/c following subcutaneous or intradermal injection, whereas *L. donovani* injection is associated

with high visceral organ parasite levels. Furthermore, genomic sequencing of *L. infantum*, *L. major*, *L. braziliensis*, and *L. mexicana* highlighted each species with specific genes that may be associated with difference in the disease phenotype[11,12]. For example, in a study comparing *L. major* and *L. donovani*, the ability to colonize internal organs and cause VL has been associated with their thermotolerance ability[12]. The A2 family of proteins, expressed in *L. donovani* but not in *L. major* that has a low thermotolerance, promote resistance to the warmer temperatures found in visceral organs. As a result, the A2 gene was proposed to harbor a 'visceralizing factor', enabling parasites to withstand the heat shock of visceral fever[13]. Indeed, genetic introduction of A2 into *L. major* improves its ability to infect visceral organs while decreasing its ability to cause footpad swelling supporting the notion that visceral colonization is associated with heat tolerance[14,15]. Similarly, it has been also shown that interspecies differences are accounting for variability in treatment response[16,17]. Taken together, the current research data suggest that the clinical outcome of leishmaniasis follow the speciation of *Leishmania* and parasite-related factors.

1.1.2 Host Factor

The genetic background of the host plays another important role in resistance or susceptibility to infection with *Leishmania* parasites. It is likely to be a key parameter in the control of parasite burden[18]. Several studies genetically compared populations presenting different evolution patterns of leishmaniasis. Some studies identified significant associations between human gene polymorphisms and expression of the disease[19,20]. Based on the clinical manifestation and exposure to different *Leishmania* species, different patterns of immunological response are also observed. The phagocytes represent some of the most potent players in innate and adaptive immunity to infection with *Leishmania*, as these cells have the capacity to eliminate the invading pathogen due to their microbicidal effector mechanism. However, once *Leishmania* parasite is inside the host cells, it can manipulate phagocytic cells

by subverting their responses to its own advantage and, thereby, successfully escape their microbicidal effector mechanisms[21–24]. The mechanisms are not fully resolved, however; it is believed to be multi counterbalancing mechanisms. Particularly, the cellular host immune system has a major role in the control of infections with *Leishmania. L. major* infection has been shown to shift a cellular immunity that is associated with cytokines such as interleukin-(IL)-12, interferon (IFN)-γ and tumor necrosis factor (TNF)-α producing Th1 CD4+ T lymphocytes to humoral immunity associated with (Th2) CD4+ T lymphocytes responses that prevents parasite removal and facilitates its survival and multiplication in phagocytes[18,25,26]. IL-4, IL-10, and IL-13 (Th2 cell-associated cytokines) and transforming growth factor β (TGFβ) are capable of suppressing Th1-type responses and deactivating macrophages[25,27,28]. Moreover, modulation of leishmanicidal activity of macrophages by generation and suppressive effects of cytokines are well studied. The outcome of leishmanial infections is determined by two functionally distinct T-helper cell populations, Th1 and Th2 showing its dependence on the immune response of the host. While resistance to the disease is associated with the development of Th1 type of immune responses, susceptibility is associated with Th2. Indeed, this has been confirmed when pretreatment of macrophages with IFN-γ and IL-12 induced resistance to *L. major* in otherwise susceptible mice, showing how potently immunological cross-talk is able to alter the disease pathogenesis or outcomes[8].

Leishmania infections stimulate the innate arm of the immune system and critically modifies the maturation, activation and development of host phagocytes through a mechanism dependent on TLR[29,30]. It has been shown that TLR3/7/9 knock-out in genetically resistant mice strain become highly susceptible to *L. major* infection[18]. This study clearly showed the critical role of nucleic acid-sensing TLR in the Th1 and Th2 polarization that determines susceptibility and resistance to *L. major* infection. Likewise, it has been recently shown that the current antileishmanial drugs such as sodium antimony gluconate, amphotericin B, miltefosine and paromomycin have also immunomodulatory properties that can stimulate the

innate arm of the immune system and critically modifies the maturation, activation and development of host dendritic cells (DCs) through a mechanism dependent on TLR9[29,30]. Moreover, it has been revealed that *Leishmania* spp. interfere with both the innate and adaptive immune systems through the exosome secretion and attenuate the phagocytic cells in the hosts[31,32]. However, our current understanding of host immune responses generated against *Leishmania* parasites is mainly based on the studies in animal models and the lack of large-scale or systematic human studies leaves many questions regarding the effect of host factors[33]. Therefore, translation of ideas from animal models to clinical settings is a major remaining challenge. However, a general consensus is that the host immune response and host-related factors are also critical in determining the diseases outcomes in humans. Altogether, the recent findings suggest the feasibility and consideration of immunotherapy/immunochemotherapy, aimed to modulate and activate the immune response in a strategy to challenge the diseases or obtain a therapeutic cure.

1.1.3 Environmental Factors

The clinical outcomes of leishmaniasis further vary by geographical region. Geographical boundaries remain the clearest demarcation among symptomatic outcomes of the disease, and the parasite-specific endemic regions that often corresponds with the parasite phylogeny[2]. For instance, although *Leishmania* is found worldwide, the majority of infections occur in the Paleotropics (Eurasia and Africa), whereas species of the *Viannia* subgenus are exclusively endemic in the Neotropics (the Americas), suggesting the outcomes of the disease follow geographical patterns[2]. CL is endemic in numerous regions of the subtropics and is most frequently caused by *L. major, L. tropica, and L. aethiopica* in the Paleotropics, whereas in the Neotropics it is caused by *L. mexicana* and *Leishmania amazonensis (L. amazonensis),* or *L. (Viannia) braziliensis*, *L. (Viannia) panamensis*, and *L. (Viannia) guyanensis.* It suggests that environmental factors are also playing their part in the complexity of the disease and

should be taken in to account in designing the control measures against leishmaniasis. Moreover, the data suggests that one endemic area of the disease may need different control measures than the others.

1.1.4 Control and Therapy

Two-third of all forms of leishmaniaisis prevalence is CL presentations. It is a major tropical infection caused by vector-borne protozoa of the *Leishmania* species. Its control strategies primarily rely on a few chemotherapeutic agents that lack appropriate efficacy, safety and affordability. Old world CL lesions can spontaneously heal without any need for therapeutic intervention in certain cases while local therapies (thermotherapy, cryotherapy, paromomycin ointment, local infiltration with antimonials) are WHO recommended options with less systemic toxicity. For complex cases, systemic treatments such as miltefosine, antimonials and amphotericin B formulations are recommended regimens. However, the efficiency of such traditional antileishmanial systemic agents is limited by toxic side effects, parenteral route of administration and emerging drug resistance[34]. The most commonly used drugs faced major drawbacks and the current chemotherapy tools are in a critical issue. For examples: Pentavalent antimonials were commonly employed as first line of treatment for many years, but serious side effects such as cardiotoxicity, pancreatitis, nephrotoxicity and increasing parasite resistance in endemic regions has limited their use[33,35]. Similarly, the uses of pentamidine, paromomycin, miltefosine, or ampohotericine B are limited by toxic side effects, long courses of treatment and low efficacy[24,36]. Furthermore, resistance to the existing drugs has been reported and withdrawing some drugs that are currently used in the clinic[37–39]. Although the relatively newer oral miltefosine has shown some efficacy and tolerability, the use of systemic pharmacotherapies against CL in general remains limited by their relative high cost in developing countries[34]. Moreover, the intracellular locations of *Leishmania* add more challenge in impairing the accession of therapeutic drugs. As people cured

of *Leishmania* infections develop lifelong immunity, prophylactic vaccination seems to be feasible but an effective vaccination strategy against the diseases has not yet been successful. Therefore, the current control measures and therapies against leishmaniasis are inefficient and suboptimal, warranting a need for other alternative control measures. Discovering novel antileishmanial compounds as well as nanomedicine approaches with a combination therapy are believed to be appropriate to bridge the gaps.

1.2 Nanomedicine

Nanomedicine is an emerging interdisciplinary field involving application of nanotechnology for the prevention, diagnosis and treatment of disease at the molecular level. Recent rapid advancement in innovation and discovery in sciences including fields of materials and life sciences are leading to exciting progress in the development of nanomedicines[40]. Many diseases originate from changes in biological processes that result from mutated genes, misfolded proteins, and infections caused by microbes at the molecular or nanoscale level[41,42]. Moreover, many biological molecules including oligonucleotides, polysaccharides, and proteins that function as antigens, allergens or pathogen-associated molecular patterns have nanoscale sizes[42]. The size, charge, shape and chemical properties of these nanoscale size molecules/pathogens appear to dictate their transport to distinct cellular compartments, interactions, immune response and their biomedical applications[41,42]. For example, regardless of their great promise for a significant improvement of treatment against many diseases, nucleic acids therapies are severely hindered by their large size, instability in biological fluids and negative charge that will result in poor cellular uptake and inefficient biomedical applications[43]. Thus, many synthetic and natural cationic polymers are commonly used as nucleic acids carriers by forming polyplex (any complex of a polymer and DNA) nanostructures due to their ability to condense nucleic acids into smaller particles, while allowing it to dissociate once inside the cell[44,45]. Loading or enclosing the nucleic acids within

a polymer or nanoparticles (NPs) could overcome the challenges in their applications by crossing the physiological or cell barriers and achieve delivery to the target cells. NPs are nanoscale in size and can be engineered due to their unique physical and chemical properties to improve the distribution and performance of the target molecules. The development of novel NPs has received much attention in recent years. It is expected that physicochemical properties such as size, shape, and surface chemistry of the NPs will dictate their carrier behavior within the body or cellular interactions and responses. This NPs' behavior consequently affects the functions of the target molecules. NPs can be prepared from a variety of materials such as proteins, polysaccharides, metals, organic compounds, nucleic acids, synthetic polymers or hybrid systems (Fig. 2). Among the various nanomedicine approaches, the development of medicines containing NPs suspension has enabled to increase the therapeutic index of many drugs[46,47]. Due to their smaller size (one million times smaller in size than a millimeter), NPs can effectively transport molecules/drugs to the target site by overcoming the physiological or cellular barriers. Consequently, once they are loaded with the functional molecules/drugs, NPs can effectively transport them to the target site. The loading is incorporation of functional molecules into the systems without any chemical reaction; this is an important factor for preserving the drug/molecule activity. Moreover, NPs can be used *in vivo* to protect the target molecules entity in the systemic circulation, restrict access to the chosen sites and to deliver them at a controlled and sustained rate to the site of action. Furthermore, production of highly potent drugs or imaging agents often possess physicochemical and/or biological characteristics that make their use suboptimal in humans[48]. NP-based delivery platforms have many applications in biomedical sciences such as imaging, clinical diagnostics and therapeutics by virtue of NPs' large surface area to volume ratio. Therefore, nanomedicine approaches may overcome pitfalls in sensitivity of diagnostic tools, therapeutic effectiveness, toxicity of drugs, or immunogenicity of vaccines[46,49,50].

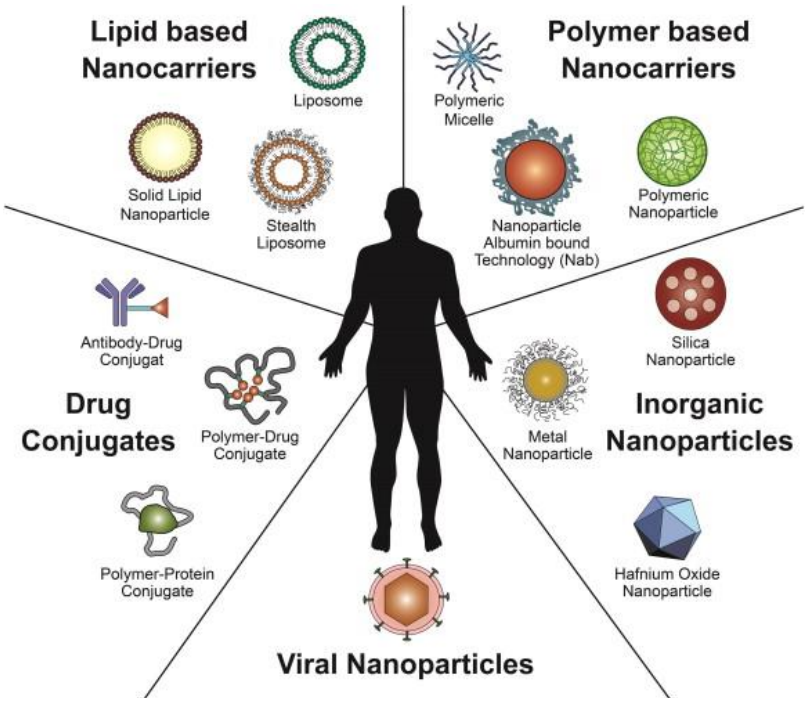

Fig. 2. *Schematic illustration of various types of nanotherapeutic platforms that are being used in clinics*[51].

1.2.1. Nanomedicine applications in drug delivery systems

The applications of nanomedicine in drug delivery systems have become a key tool to overcome the main drawbacks of chemotherapeutics and to enable their selective targeting to specific diseased cells and tissues. Many promising drugs or drug candidates have the problem of reaching their target site and the concept of NP-based drug delivery systems can play a significant complementary role in shaping these modern medicines. For drug delivery applications, selection of appropriate NPs and drugs are very crucial. Major factors such as inherent properties of the target drug, e.g., aqueous solubility and stability, biocompatibility and toxicity, surface characteristics such as charge and permeability, degree of biodegradability of the NPs or nature of drug release profile desired should be considered during the initial design for nanomedicine applications. The major goals in designing NPs for drug delivery systems are to control particle physicochemical properties and release of the drug to achieve the site-specific action at the therapeutically optimal rate and dose regimen. Excluding many more drugs that are being studied in clinical trials, NP-based

chemotherapeutics for six cancer and more than 11 other diseases have been so far approved for clinical use[52]. Among which, liposomal drugs and polymer drug conjugates are two dominant classes of formulations.

The delivery of therapeutics with intracellular sites of action for which cellular uptake is inefficient may be best achieved with targeted delivery vehicles[53]. Targeted drug delivery is a method of transporting drugs to a patient in a manner that increases the concentration in some parts the body organ or cells relative to others. Moreover, multidrug resistance (MDR) is the common treatment challenges in many human diseases including leishmaniasis. Some of the mechanism of MDR includes a decreased influx of drug, increased efflux of drugs and altered drug targets. In the case of leishmaniasis, for instance, drug resistance against miltefosine has been reported in the last few decades and the resistance mechanisms are exclusively associated with dysfunction in miltefosine uptake system or poor access to intracellular targets[54]. Thus, intracellular delivery approaches and/or modulating macrophage uptake have been suggested to overcome the drug resistance problem against miltefosine[54–56]. Currently, NP-based drug delivery systems provide alternative strategies to circumvent MDR in several diseases[57,58]. Moreover, nucleic acid-based therapeutic molecules are a new approach for targeting of specific, prominent and essential genes responsible for causing diseases. Thus, they have specific anti-sense and anti-gene inhibition effect on target molecules due to sequence selectivity toward DNA and RNA for silencing. Such therapeutics are currently representing a growing number of applications in drug development pipelines[59]. However, the major limits in the use of nucleic acids therapeutics are their poor ability to penetrate across the cell membrane into the cytoplasm and insufficient capability to reach intracellular targets. Therefore, effective drug delivery systems could able to convert these poorly soluble, poorly absorbed and labile substances into promising deliverable drugs for efficient uptake and better results. In general, advanced NP-based drug delivery system is superior to existing therapeutic strategies and a more effective method to induce enhanced cellular uptake, maintain sustained

drug release, and improve bioavailability[60]. It is also possible to deliver large macromolecule drugs to intracellular sites of action or co-delivery of two or more drugs or therapeutic modality for combination therapy through nanomedicine approach[53].

Efficient drug loading and controlled release mechanism are other important determinants to establish effective drug delivery platforms. Efficient drug loading may be achieved through encapsulation, covalent linking and non-covalent or self-assembly methods. Internal stimuli-responsive NP formulations by keeping a check/control over certain specific parameters like pH, hydrolytic, enzymatic degradation, ionic strength, temperature, as well as externally applied stimuli such as magnetic field, ultrasound or light have been developed to trigger site-specific drug release[61,62]. Intracellular delivery, with efficient intracellular release, have become important design considerations in NP formulations[63]. In cancer, the tumor microenvironment like low pH, elevated redox potential, over-expressed enzymes and hyperthermia has helped to design NP which can respond to such variety of intrinsic circumstances. Therefore, nanomedicine approaches is a promising strategy to overcome the current challenge of traditional chemotherapy and effectively target human diseases including CL.

1.2.2. Nanomedicine applications in vaccine

The technology of vaccine development has been radically changing and there are currently several successful vaccines available. Despite the huge success, there are still a large number of diseases including leishmanisis against which there is still no effective vaccine currently available. This is because the pathogens causing such diseases are mastering either immune escape or immune evasion[64]. To address such challenges, increasing both the basic immunological knowledge and also the development of advanced materials and techniques in the field of vaccinology (nanovaccine) are needed[65]. Three critical elements are essential in the composition of an effective vaccine; an antigen which induces an adaptive immune

response, an adjuvant which stimulates the innate immune system and influence the profile of the elicited immune response, and a delivery system which insures optimal delivery of antigen and/or adjuvant for effective activation of the immune system. Once a useful set of antigens and adjuvants are selected, they should be formulated in such a way that a robust immune response is induced. Although the subunit vaccines have an excellent safety over other traditional vaccine formulations such as live-attenuated or inactivated/killed pathogens, they have inherently weak immunogenicity and short-term immune responses that necessitate for novel formulation with immunopotentiating adjuvants.

The evolving use of nanomedicine in vaccination has resulted in several promising formulations that increases effectiveness by inducing a more efficient immune response[42,66]. NP mimic invading pathogens and provide adjuvant activity by either enhancing the delivery of antigens to the immune system or by potentiating innate immune responses via their intrinsic immunostimulatory properties[42,67]. They activate antigen-presenting cells (APC) via TLR signaling and/or autophagy induction pathways with increasing corresponding cytokines and subsequent induction of innate immunity[68–71]. By such approaches, particularly nucleic acid-based adjuvants with intracellular targets like unmethylated cytosine-phosphate-guanine oligodeoxynucleotides (CpG ODN) have been shown to enhance vaccine efficacy at a low adjuvant dose for inducing potent and long-lived cellular immunity[50,72]. Several groups have shown that NP-based co-delivery systems also reduce the amount of antigen and adjuvant required to activate T cells as compared to concomitant administration of equal amount of respective antigen and adjuvant *in vitro* and *in vivo*[68,69,73]. Several molecules can also be combined for optimum efficacy of a nanovaccine. Thus, in order to ensure the optimum presentation to both innate and adaptive type of immune system, use of nanovaccine such as vaccine formulations containing liposomes, polymers or NPs are of great importance. Nanovaccines have multi-fold advantages over traditional vaccines; 1) they can serve as a point source for antigen retention and release in a sustained manner so that not only the

quantity, but also the quality of immune responses is enhanced; 2) they have the capacity to induce presentation of antigens through both MHC class I and MHC class II complexes; 3) they protect the immunogens from rapid degradation and clearance while increasing their stability; 4) they are readily taken up and processed by APC; 5) they mimic the natural process of infection and give a possibility of codelivery of several immunogens, being either several antigens or antigens and adjuvant molecules and 6) they permit organ- and cell-specific targeting via surface modifications of particles with functional moieties and targeting ligands[67,74,75]. Moreover, side effects might be decreased upon encapsulation of the adjuvant or the concomitant delivery of antigen and adjuvant[64].

1.2.3. Nanomedicine applications in diagnosis

Application of nanomedicine in diagnosis includes engineering NPs in order to achieve enhanced or novel magnetic, optical, and electronic properties that can operate at the biomolecular level[76]. Incorporating NPs into the existing clinical diagnostic and detection systems have demonstrated improved sensitivity and specificity of diagnosis compared to traditional approaches[77]. It greatly enhances early and accurate diagnosis. Moreover, it has been recently shown that NP-based diagnosis is rapid and offers clinicians the opportunity to diagnose multiple human pathogens within hours of sample collection[78]. NPs usually have rich surface chemistry that allows a variety of other molecules to be loaded or attached for the introduction of specific functionalities. Functionalizing the NPs in combination with targeting agents (antibodies and their fragments, nucleic acids, or other receptor ligands like peptides, vitamins, and carbohydrates), and probes for fluorescent and/or magnetic resonance imaging can be used to develop novel sensing and diagnostic techniques. However, there are limitations in the density and selectivity of these targeting molecules on target cells relative to normal cells so as to deliver enough concentration of molecules needed for efficient diagnosis. Moreover, the blockage of NPs tumor targeting ligands by a serum proteins or

protein corona from binding to tumor cell receptors in the blood. As a result, less than 10% of all systemically administered NPs formulations accumulates in tumor[79]. In contrast, serum proteins adsorb onto NPs encourages uptake by macrophages, which makes easier to target pathogens residing inside macrophages. Recently, theranostics, a combination of diagnostic and therapy by incorporating drugs to the integral components needed for diagnosis is becoming of great interest in order to simultaneously perform the disease identification and therapy.

1.2.4. Interactions of NPs with biological systems

Consensus has been reached by now that NPs are not only carriers for biomedical applications, but can also play an inherent active role in mediating biological effects[80]. For instance, some NPs can inherently induce immunological responses while others have antimicrobial effect in addition to their carrier activity[44,45]. NPs have two interdependent identities for such effects: the synthetic identity which is comprised of its intentionally designed physicochemical properties such as its size, shape, surface chemistry, and surface functionalization, and the biological identity which is produced after adsorption of blood proteins onto the NPs surface (protein corona) after introduction into the biological systems. The synthetic identity is used to design a desirable biological identity. However, the biological identity is determinants of its behavior and function within the body by causing unexpected changes in cellular interactions, cellular uptake, biodistribution, and immunogenicity[79]. The knowledge of how NPs properties change within a biological environment can lead to the rapid development of key applications, including improved delivery system, and resolution of their potential threat to organisms and the environment. It can also determine the performance of NPs by impacting on its transport and drug release.

In biological fluids, proteins bind to the surface of NP to form a coating known as the protein corona, which can critically affect the interaction of NPs with living systems, and,

therefore, further cellular/tissue responses depend on the composition of corona[81,82]. The structure and composition of the protein corona depends on the physicochemical properties of NPs, the nature of the physiological environment (blood, interstitial fluid, cell cytoplasm, etc.), and the duration of exposure[83]. For example: NPs surface charge is an important factor in protein interaction and it has been reported that increasing the surface charge of NPs increases the protein adsorption[84]. As a result, the protein corona alters the size and surface properties of the particle, giving it a new biological identity and, consequently, increases the NPs size by 3–35 nm, and changes the surface charge to −10 to −20 mV[84–86]. This biological identity determines the physiological response including agglomeration, cellular uptake, circulation lifetime, signaling, kinetics, transport, accumulation, and toxicity. Moreover, targeted therapy is a central concept in nanomedicine research. It exploits the (over)expression of surface receptors in target cells by ligand incorporation. However, the main challenge is after introduction in the bloodstream, the NPs surface is immediately modified by protein corona and it would be difficult to preserve the surface functionality[87]. Thus, parameters including evasion of the immune system, stability in physiological media, control over the interaction of NPs with biological entities such as proteins and cell membranes, low toxicity, and optimal bioperformance are critical factors for efficient design and applications of NPs in nanomedicine[76].

Over the past years, considerable numbers of studies have been conducted to understand the route through which NPs are taken up by different cells. The results indicate that NPs entry predominantly takes place through endocytosis mechanisms operating in mammalian cells[88,89]. These distinct endocytotic pathways have been characterized on the basis of their differences in ultrastructure, pharmacology, cargo (membrane protein, or receptor plus ligand) and coat protein composition[90–92]. The ultrastructural morphology of nascent endocytic intermediates at the plasma membrane provides a crucial parameter for classifying endocytic pathways[90]. Typically, endocytosis occurs by multiple mechanisms that

fall into two broad categories: 'Phagocytosis' or cell eating by which cells internalize large solid particles, and 'pinocytosis' or cell drinking, where cells take up both fluid and solutes from their environment. Phagocytosis is an endocytic process exhibited by several types of cells, including epithelial cells, fibroblasts and immune cells. Its unique characteristics includes a larger size of the endocytosed vesicles (>250 nm) known as phagosomes. Phagocytosis can be induced either through receptor-ligand interactions or through receptor-soluble factors interactions that recognize the foreign agent and facilitate opsonization[40]. Pinocytosis can be further sub-classified and at least four basic mechanisms can be distinguished: macropinocytosis, clathrin-mediated endocytosis, caveolae-mediated endocytosis, and clathrin- and caveolae-independent pathway[93,94]. Macropinocytosis is an actin-driven endocytic process by which many types of cell internalize considerable volumes of extracellular fluid through large vesicles (diameter of 0.5–10 μm) known as macropinosomes[95]. It is plasma membrane protrusions or ruffles that collapse onto and fuse with the plasma membrane by trying to generate large endocytic vesicles (unlike phagocytosis, these protrusions do not 'zipper up' along the NPs). Clathrin-dependent endocytosis is the most studied process for trafficking of materials into eukaryotic cells which vesicle formation starts with membrane invaginations forming a more or less homogenous, symmetric polygonal lattice. Caveolin-dependent endocytosis are a smooth flask-shaped invaginations (60–80 nm) of plasma membrane that are abundant in several types of cells, such as fibroblasts, smooth muscle cells, adipocytes, and endothelial cells, and are absent in neurons and leukocytes[40]. Clathrin- and caveolin-independent pathways are several entry pathways characterized by polymorphous or tubulovesicular membrane invaginations. Unlike Clathrin- and caveolin, it does not require the presence of coat proteins for vesicle formation and internalization; however, the actin and actin-associated proteins are important players for vesicle formation. The identification of several uptake routes and pathways complicates the study of the cellular uptake of NP. Furthermore, these uptake mechanisms have been shown

to be highly influenced by the physicochemical properties of NPs including size, surface functionalization, geometry and other factors like concentration, time or cell types[96–99] making the comparison of different findings even more difficult.

In multicellular organisms, the distinct endocytic pathways are highly regulated to control all aspects of intercellular communications including hormone-mediated signal transduction, immune surveillance, antigen presentation, and cellular and organismal homeostasis[93,100]. As a result, one of the goals of designing NP-based delivery systems is to be able to correlate uptake routes with the physicochemical properties of the engineered NPs in order to guide the entry into the cell and, consequently, control the cellular responses[40]. For example, it has been shown that the cellular uptake rate is higher in cationic (e.g. with COOH surface charge) as compared to in the neutral (plain) or anionic (e.g. with NH_2 surface charge) NP in different cell types, concluding that the particle size and surface charge are critical factors in influencing cellular uptake[83,101,102]. Ligand-targeted NPs for receptor-mediated cellular internalization are also a good strategy for modulating the cellular uptake and have been the main impetus behind the progress of nanomedicines towards the clinic. Moreover, Karlson *et al.* described that bone marrow-derived dendritic cells use caveolin-dependent pathways to take up 40-50 nm polystyrene NPs[70]. Thus, unlike most other NPs, they do not induce extracellular signal-regulated kinases that mediate inflammatory pathways during their applications in vaccines. Moreover, since the targets of many therapeutic agents are localized in subcellular compartments, modulation of NP-cell interactions is needed for their precise delivery to subcellular compartments[40]. Thus, understanding the interactions of NP with biological systems at the cellular and subcellular level is a prerequisite for their efficient and safe application in biomedical sciences. It aids in the design of NPs for effective biomedical applications by controlling their physicochemical properties, composition, and formulation process[82].

2. RATIONALE AND OBJECTIVES OF THE STUDY

The control of leishmaniasis mainly depends on a few chemotherapeutics that lack safety, efficacy and affordability. Unfortunately, vaccination against leishmaniasis has not been yet successful either. There is no optimum treatment option against leishmaniasis. Particularly, the treatment of CL is very challenging as its treatment needs both reducing the size of the ulcers on exposed parts of the body for healing with minimal scarring as well as eradicating the intracellular parasite causing the lesions. Hence, wound healing processes are important determinants of CL treatment[103]. Currently, parenteral administration of antimonials, pentamidine, amphotericin B or oral miltefosine is the standard systemic treatments measures against CL. However, due to their severe unwanted side effects that often lead to unfavorable risk-benefit ratios, a topical or local treatment has been recently recommended as first line treatment approach for CL patients[5,10,104,105]. Paromomycin ointment and local infiltration with antimonials are good alternatives for local treatment against CL; however, they have not yet provided a strong consistent result. Although such local treatment usually allows higher drug concentration at the site of infection, reduced systemic toxicity, faster time to healing and reduced cost, the treatment of CL remains sub-optimal. Overall, there is a lack of evidence for potential benefit of the current CL treatments. WHO recommended a simple wound management as a first line treatment approach for non-complicated CL cases. Moreover, after decades of research, there is still no new commercial drug for use in the near future against CL. The ongoing research on CL treatment is also one of the areas of neglected tropical diseases research. Furthermore, there is no assurance that the development of new drugs can catch up to the pathogens' fast and frequent development of resistance in a timely manner. In addition, leishmaniasis mainly affects the poorest regions of the world where the patients cannot afford the costs for medication, a fact that severely discourages the pharmaceutical industry to invest in this field. Hence, there is an urgent need for discovery of

novel antileishmanial compounds and/or alternative treatment approaches against CL. However, due to the high costs associated with drug identification and development, discovery of novel drugs against CL may not be attractive.

Topical or local treatment has been recommended by WHO as a first line treatment approach for CL patients[5]. However, the efficacy of the drugs are generally hindered by the intrinsic antileishmanial activity of the drugs and the amount of drug available in the dermis, suggesting a need for improved drug absorption and retention strategies[106,107]. Importantly, it has been shown that liposomes loaded with drugs enhanced *in vitro* drug permeation across stripped skin and improved the *in vivo* antileishmanial activity in experimentally infected mice[35,56,108]. Insights into the most promising delivery strategies to improve treatment of CL could enhance skin delivery and efficacy of conventional antileishmanial drugs[35]. Moreover, the challenge of the current conventional leishmaniasis treatment is partially because of the failure of drugs to penetrate macrophages where the parasite hides[24,49]. Since macrophages are prominent sites for microbial infections such as *L. major*, particle formulations that are easily taken up by macrophages would be highly advantageous for macrophage-targeting drug delivery. The particle formulations can be efficiently taken up by macrophages and consequently, increases intracellular drug concentration for an efficient pharmacological effect against intracellular *L. major*. Thus, an effective therapy could be achieved through delivering antileishmanial drugs to the site of infection and releasing the drug in a controlled manner. However, in the past 35 years of research in the field of drug delivery, AmBisome (Amphotericin B liposome for injection, Astellas Pharma US, Inc.) is the only drug delivery system currently used against leishmaniasis[109,110]. Though AmBisome is decreasing its uptake by kidney cells and thereby reducing its nephron toxicity, it is relatively less active and more expensive than free amphotericin B and also associated with central nervous system toxicity[111,112]. As a result, practically there is no optimal drug delivery system that may

enhance the antileishmanial activity of drugs through crossing the physiological or cell barriers while reducing or avoiding their host toxicity.

The emerging nanomedicine approaches, particularly advanced drug delivery systems, have currently been found to increase the antimicrobial efficacy in many cases. However, their successful applications require a thorough understanding of NPs' physical and chemical properties and how they interact with host cell. This is because in order to transport pharmaceutically active compounds in the body, NPs should interact with all sort of biological systems that determine their safety and applications to achieve a desired therapeutic effect. It has been suggested that alterations in the physicochemical properties of NPs can regulate uptake mechanisms and the intracellular fate of NPs[94,97,99]. A great deal of scientific efforts have focused on understanding and controlling the NPs internalization pathways to facilitate the development of NPs that can perform precise intracellular targeting with enhanced therapeutic outcomes[40]. Regardless of the efforts, a complete understanding of how cells interact with nanostructures of well-defined sizes, at the molecular level, remains poorly understood and there is little consensus in the literatures regarding this issue. It has been suggested that the accurate knowledge of NP uptake mechanisms and NP-cell interactions are an important criterium to progress in the field of nanomedicine[88,89,94].

On the other hand, recent data suggested that immunotherapeutic approaches are promising methods for effective treatment of leishmaniasis[10,106]. *Leishmania* parasites resides in phagocytic cells that include neutrophils, macrophages and dendritic cells; therefore, an immunomodulatory compound could be potentially leishmanicidal by virtue of its potential to activate phagocytic cells[113]. A curative response against leishmaniasis depends on the classical activation of phagocytes and the IL-12-dependent onset of an adaptive type 1 response characterized by the production of IFN-γ[6,26]. It has been shown that CpG ODN alone or in combination with other antileishmanial drugs show a promising efficacy against *L. major*[114]. This can be further verified by the fact that many antileishmanial compounds

including current conventional drugs have either immunomodulatory activity, or rely on the host immune system for their effect[113]. Thus, besides discovering new compounds and establishing advanced drug delivery systems against leishmanaisis, a combination therapy that employs both host- and pathogen-directed treatment may represent feasible alternatives. This may include a combination therapy that comprising chemotherapy and biological therapeutics that act through manipulating the host immune system (immunotherapy). Although considerable success has been attained using combination therapies, none has yet achieved commercial status. Well-designed mechanism-based combinations therapies (drugs acting through different mechanisms) that target the host and the parasite may improve treatment by reducing the length of treatment, relapse, and risk of toxicity and increases the therapeutic index. As a result, combination therapy that is targeted to simultaneously kill the parasites and manipulate the host immune system in favor of cellular parasite removal (killing) is of particular interest.

Developing an effective topical treatment for CL using antileishmanial drugs still remains a great challenge[35]. Regardless of the advances in basic scientific research, there has been little progress in new drug development, and the overall outcomes of current treatments for CL are far from ideal therapy. Effective and safe therapies that are readily accessible to third-world countries are urgently needed. It requires effective killing of intracellular amastigotes and enhancing lesion or wound closure caused by CL. In these contexts, polyhexamethylene biguanide (PHMB; CAS# 27083-27-8; alternative chemical names: polyhexanide, polyamino propylbiguanide, M_w = 2780 g/mol)[115] is an "old" antimicrobial polymer and wound antisepsis that is widely used in clinics, homes and industry was investigated for CL treatment. It is a very cheap synthetic polymer that is recommended as a treatment choice for locally infected and critically colonized wounds with no evidence for the development of resistance against several bacteria in many parts of the world including Europe and the US for over 50 years[116]. It is also widely used as preservative, contact-lens

multipurpose solutions and general care purposes, with excellent tolerance and a low-risk profile lacking any systemic toxicity[117–119]. Furthermore, PHMB is being frequently used in clinical treatment of Acanthamoeba keratitis patients[120,121]. However, there is no information about the use of PHMB as treatment for trypanosomatid protozoan diseases in general and *Leishmania* infection in particular, and there have been no attempts to evaluate PHMB as treatment for CL. Given its cheap cost and excellent toxicity profile, PHMB may be a promising candidate for effective treatment of CL.

Taken together, exploring potential strategies to identify novel, effective and affordable chemotherapeutic agents in parallel to exploring alternative treatment approaches to improve the existing drugs against leishmaniasis are urgently needed. It has been suggested that current nanomedicine approaches are believed to be an appropriate alternative to address the treatment challenges against CL[35]. In light of the time required to bring a new drug to market and the cost involved, a combined therapy with alternative advanced drug delivery systems seems to be feasible options for effective treatment of leishmaniasis. This strategy includes designing novel NP carrier and loading it with the components of combination therapies for safe and effective treatment. It would then lead to reductions in the duration of conventional treatment, better patient compliance, and the prevention of antileishmanial drug resistance or toxicity. Therefore, the general objectives of my PhD research project were aiming at identifying novel antileishmanial agents and using a nanomedicine approach to address the current treatment challenges of CL. The specific objectives of the study were to:

- Discover novel and affordable topical antileishmanial compound for the treatments of CL patients,
- Systematically understand how NP interacts with mammalian cells for safe and effective usage in nanomedicine,

- Establish a mechanism based host- and pathogen-directed combination therapy with innovative NP-based drug delivery systems against CL.

3. MATERIALS AND METHODS

3.1 Nanoparticles and drugs

Two different types of polymer NPs were used in this study. Primarily, fluorescent polystyrene latex beads of different sizes (0.02 μm, 0.1 μm, 0.2 μm, 0.5 μm, 1 μm and 2 μm) were purchased from Life Technologies (F-8888, Darmstadt, Germany) at 2% solids and used without any further modification. They were used as a model to analyze the uptake and endocytosis pathways, which play a key role in the clearance of drugs. The NPs were sonicated (Bandelin Sonorex Super RK 106, Berlin, Germany) for 10 min immediately prior to every experiment. Secondly, PHMB was kindly provided by Dr. Liam Good, University of London, and Tecrea Ltd, London UK, at stock concentrations of 1 mg/ml and 200 mg/ml.

Standard antileishmanial drugs including amphotericin B (A2942), pentamidine isothionate (P0547) and paromomycin sulfate (P9297) were purchased from Sigma-Aldrich (Deisenhofen, Germany) and were used as positive controls. Similarly, miltefosine (1-hexadecylphosphorylcholine) from Cayman Chemical Company, Ann Arbor, MI, USA was used as standard antileishmanial positive control compound. FM4-64FX dye (F34653) which is a fixable analog of FM 4-64, Hoechst 33342 (H3570) and LysoSensor Blue DND-167 (L-7533) were similarly purchased from Life Technologies and used according to the supplier's instructions. AlamarBlue cell viability assay reagent was purchased from Trinova Biochem GmbH (Giessen, Germany) and was used according to the manufacturer's instructions. To investigate the cellular uptake mechanisms of polymer NP based on specific pharmacological inhibitors, chlorpromazine hydrochloride (C8138), cytochalasin D (C8273), ikarugamycin (SML0188), wortmannin (W1628), and dynasore (D7693) were purchased from Sigma-Aldrich (Deisenhofen, Germany). Oligodeoxynucleotides containing unmethylated cytosine-phosphate-guanine (CpG ODN 1668, M_w = 6058 g/mol) and rhodamine red-labeled CpG ODN (CpG-R, M_w = 6891 g/mol) lyophilisates with the same sequence

TCCATGACGTTCCTGATGCT were purchased from Eurofins MWG Operon (Ebersberg, Germany) and were diluted in distilled water and used at various concentration.

3.2 Cell culture

Primary bone marrow-derived macrophages (BMDM) were generated from bone marrow of BALB/c mice (Charles River Breeding Laboratories, Sulzfeld, Germany) as previously described[122]. The particular mouse was sacrificed by cervical dislocation in laboratory animal facility at Institute for Molecular Biology (IMIB), University of Würzburg and taken to laboratory. After disinfecting all external surfaces with 70% ethanol, tibia and femur were surgically removed by using pre-heat sterilized scissors and forceps without damaging the epiphysis. After brief disinfection in 75% ethanol, the bones were placed into a 50 ml polypropylene tube containing phosphate-buffered saline (PBS). The bone marrows were then opened by cutting both tips of the bones with a sharp sterile scissor in conditioned Dulbecco's Modified Eagle Medium (DMEM). The conditioned medium contains supplementary nutrients or compounds such as 10% heat-inactivated fetal calf serum (FCS), 5% horse serum (heat-inactivated), 50 μM β-mercaptoethanol, 10 mM HEPES buffer, 4 mM L-glutamine, 1% non-essential amino acids and 15% L929 macrophage-colony stimulating factor (M-CSF) that was generated from L929 fibroblasts as indicated below. The bone marrows were flushed with the conditioned medium in a 1 ml syringe (with 26G needle) by inserting the needle into the tip of the bones. The stem cells were then collected in 50 ml polypropylene tube and washed at 300 × g (10 min, 4°C) and counted by using a Neubauer chamber (0.1 mm depth) after 1:10 dilution in trypan blue solution. After the stem cells numbers were adjusted to 1.2×10^5 cells per ml by the same conditioned medium, 10 ml of cell suspension was added to culture dishes (20 × 100 mm suspension plates; Sarstedt, Nümbrecht, Germany) and incubated at 37°C and 5% CO_2 for 6 days. The primary BMDM were harvested by using cell scraper and maintained in complete Roswell Park Memorial Institute (RPMI) medium containing 10% FCS (heat-inactivated), 2

mM L-glutamine, 10 mM HEPES buffer, 0.05 mM β-mercaptoethanol solution, gentamicin (50 µg/ml) and penicillin G (100 u/ml). The percentage of BMDM was confirmed by flow cytometry after staining with F4/80 macrophage marker and more than 85% cut off value were considered acceptable as compared to the isotype control. At this point, BMDM are ready for biological experiments.

M-CSF supernatant was generated from L929 fibroblasts (Leibniz DSMZ, German Collection of Microorganisms and Cell Cultures, DSMZ-No ACC-2, Braunschweig, Germany) in special medium containing 500 ml 1×DMEM (Gibco 21969), 0.25 µM 2-mercaptoethanol (Sigma Aldrich M-7154), 1% non-essential amino acids (Gibco 11140), 5% heat-inactivated FCS, 1% penicillin/streptomycin solution (Gibco 15140), 4 mM L-glutamine (Biochrom AG K0282) and 10 mM HEPES buffer. The subculture tube containing L929 cells were taken from the stock in liquid nitrogen tank. The tube was put in pre-warmed water bath to thaw subculture cells until only a bit of frozen cells left at the bottom of the tube. 700-800 µl of pre-warmed medium was added to the cells, resuspended and transferred into 15 ml polypropylene tube containing 10 ml of the pre-warmed medium. The bottom of the tube containing cells was washed once more with 200-300 µl of medium and added to the rest of the cells. The cells were then briefly centrifuged at 68 × g, 4°C for 10 min to wash out the DMSO. The supernatant was discarded and the pellet was resuspended with 30 ml medium. The cells were then transferred to culture flasks and cultivated at 37°C, 5% CO_2 for two to three days (1st passage). When the L929 cells were about 70-80% confluent, the passages were continued for second and third times. On the fourth passage, the cells were harvested by gently scraping, centrifuged at 300 × g, 4°C for 10 min and counted in trypan blue. The cell numbers were adjusted to1×10^5 cells/ml. 30 ml of the cell suspensions were added to flasks and further incubated for about 10 days to get enough M-CSF productions. Finally, the M-CSF supernatant were transferred into 50 ml tubes, centrifuged at 300 × g, 4°C for 10 min, filtered and stored at -20 °C in a desired aliquot until used.

For 293T kidney epithelial cell lines (DSMZ-No ACC-635, Braunschweig, Germany) and L929 fibroblasts (Leibniz DSMZ, German Collection of Microorganisms and Cell Cultures, DSMZ-No ACC-2, Braunschweig, Germany) were cultivated and maintained in high glucose (4.5 g/l) DMEM without L-glutamine and phenol red but containing 10% fetal calf serum (heat-inactivated), 200 mM L-glutamine and sodium pyruvate for at least two consecutive passages before use. The epithelial cells were trypsinized to obtain single cell suspensions, diluted 1:10 in trypan blue and counted in the same Neubauer chamber. The numbers of cells in all the three cell types were adjusted to 2×10^5 cells per ml for all cell types and respective experiments.

3.3 Flow cytometry

Cells were grown as described in cell culture and were harvested, treated with different concentrations of fluorescent NPs (Polystyrene and PHMB), CpG-R, PHMB/CpG-R polyplexes and PHMB-FITC/CpG polyplexes for different time points. The cells were pre-treated with five different pharmacological inhibitors before they were exposed to the fluorescent compounds for detailed uptake mechanism studies. After exposure for required period of time with the fluorescent compounds, the cells were then washed, fixed with 4% paraformaldehyde and washed three times (300 × g, 10 min, 4°C) with ice cold PBS. 1×10^6 fixed cell suspensions were transferred into fluorescence-activated cell sorter (FACS) tubes and centrifuged (750 × *g*, 4°C, 10 min). The cell pellets were resuspended in 1 ml buffer (0.1% sodium azide, 2.5% FCS in PBS) and washed again in 1 ml buffer. The pellet was then finally resuspended in 300 µl of the buffer for measurement and 20,000 total events were acquired per sample.

Similarly, the fluorescence intensity of promastigotes treated with propidium iodide (PI) and YO-PRO®-1 dyes (Life Technologies, Darmstadt, Germany) were measured by flow cytomtery as indicators for membrane integrity[123]. *L. major* promastigotes were treated with 2 µM PHMB for various time points and then washed at 3,000 × g for 10 min. The

promastigotes were stained by incubating with PI or YO-PRO®-1 dyes for 15 min in the dark at room temperature (RT) according to manufacturer's instructions. The dyes can enter and stain the parasite only after loss of membrane integrity. The promastigotes were then washed with FACS buffer and a total of 100,000 total events were immediately acquired by the flow cytometry. The MACS Quant Analyzer (Miltenyi Biotec, Bergisch Gladbach, Germany) based on the same instrument setting for all measurements were used. The data were analyzed using FlowJo software (Tree Star Inc., CA, USA).

3.4 Transmission electron microscopy

To investigate the uptake mechanisms of NPs, the BMDM, L929 or 293T kidney epithelial cells were allowed to take up polystyrene NPs at different time points. The cells were then harvested from culture plate, transferred to 15 ml polypropylene tube and washed with PBS at 300 × g, 4 °C for 10 min. The cells were fixed by incubating with 1 ml of 2.5% buffered 0.2 M cacodylate in glutaraldehyde at 4°C overnight. At the next day, the cells were washed five times (300 × g, 5 min at RT) in 0.5 ml of 50 mM cacodylate buffer (pH 7.2) while incubating at RT for 3 min in between each washing step. The cells were further treated with 0.2 ml of 2% buffered OsO_4 containing 25% H_2O, 25% 0.2 M cacodylate and 50% OsO_4 at 4°C overnight for further fixation. The cells were then similarly washed five times in 0.5 ml of H_2O (1200 × g, RT, 5 min). The cells were further incubated with 0.1 ml of 0.5% aqueous uranyl acetate (Sigma-Aldrich) overnight at 4°C for contrast and nucleus staining. The cells were again washed five times in 0.5 ml of H_2O while incubating at RT for 3 min in between each washing step.

After successful fixation steps, the cells were dehydrated by incubating and washing in various ethanol concentration. Briefly, the cells were incubated in 0.5 ml of 50% ethanol concentrations for 30 min at 4°C before washing at 1200 × g, 4°C for 5 min. This dehydration step was repeated for each 70%, 90%, 96% and 100% ethanol concentrations, respectively.

The cells were again incubated in 0.5 ml of 100% ethanol concentrations for 30 min at RT. They were then incubated in 0.5 ml readymade 100% propylene oxide at RT for 30 min and washed at 1200 × g, RT, for 5 min. Finally, the cells were incubated in 0.5 ml readymade 100% propylene oxide at RT for 30 min and transferred to small embedding tube. Then, the embedding step followed by centrifuging the cell suspension at 1200 × g, RT, for 5 min and carefully discarding the supernatants. Embedding was done by adding Epon 812 to propylene oxide at 1:1 ratio carefully without disturbing the cell sediment. The cells were incubated at RT overnight for evaporation of propylene oxide. After removing the mixed Epon and propylene oxide supernatant on the next day, the cells were embedded again in pure Epon for 21 h at RT and allowed to polymerize at 60°C for 2 days. Note that for morphology characterizations of the PHMB/CpG polyplexes by TEM, all fixations, dehydration and embedding were not necessary but the polyplexes were directly stained with uranyl acetate and lead citrate for imaging. Imaging was performed after the polyplex suspension or ultrathin sectioned cells were mounted on 300-mesh grids, and stained with uranyl acetate and lead citrate. TEM (JEOL JEM-2100, Germany) at an accelerating voltage of 80 kV with 200 kV with TVIPS F416 4k x 4k and Olympus Veleta 2k x 2k camera systems were used. The TEM procedures for experiments with *L. major* promastigotes were the same as for the mammalian cells except centrifugations were performed at 3,000 × g, 10 min at RT and concentration of the parasites used were 10^7 parasites per ml.

3.5 Luciferase reporter assay

The virulent *L. major* parasites expressing the *luciferase* reporter gene called luciferase-transgenic strain (Luc-tg) containing the firefly luciferase reporter gene was generated as previously described[124]. Luc-tg strain was maintained by continuous passage in female BALB/c mice and was grown in 96-well blood agar cultures at 27°C, 5% CO_2, and 95% humidity. The metacyclic Luc-tg promastigotes were grown in 96-well blood agar cultures

and the fourth passage was used for infecting macrophages. The parasites were collected into a 50 ml polypropylene tube and washed twice with 20 ml of PBS at 3,000 × g, 10 min at RT. After suspending the parasite pellet in 2 ml of complete RPMI medium, the parasites numbers were adjusted to 3×10^6 parasites per ml to achieve an infection rate of macrophages to promastigotes (cell/parasite ratio) of 1:15. Meanwhile, BMDM were harvested and counted according to the described cell culture protocol. The numbers of the macrophages were then adjusted to 2×10^5 cells per ml and 200 µl of the cell suspension was seeded into 96-well plates. The plate was pre-incubated for 4 h to allow adherence of macrophages to the surface of the plate before the supernatant was discarded and replaced with an equal volume of complete RPMI medium containing 3×10^6 parasites per ml promastigotes suspension. After incubating (37°C, 5% CO_2) for 24 h to allow full differentiation of the promastigotes into amastigotes, the medium containing the extracellular parasites was removed and the wells were washed 3-5 times with the same medium. During washing, the plates were observed under optical microscopy to confirm complete removal of all extracellular parasites. And consequently, the washing supernatant (medium) was removed from the wells and replaced by five serial dilutions (1:5) of each target substance in complete RPMI in duplicate. Three controls were used: A growth control containing complete RPMI and infected BMDM in triplicate, a general control comprising uninfected BMDM, equal volume of water with the target substance and medium in duplicate, and a color control for each substance which comprises the highest dilution of the target substance and complete RPMI medium only. After further 24 h of incubation at 37°C and 5% CO_2, the infected BMDM were lysed with a luciferin-containing buffer (Britelite, PerkinElmer, Germany) to release the luciferase enzyme into solution. The free luciferase enzyme then catalyzes a reaction that generates light. Thus, the assay is based on bioluminescence measurement of firefly luciferase enzyme that catalyzes the formation of light from ATP and luciferin. The luminescence was then measured with a luminescence plate reader, Victor X Light 2030 luminometer (PerkinElmer). This is

proportional to the amount of *luciferase* gene expression or the number of the parasites. The IC_{50} values of the compounds against intracellular amastigotes were calculated based on the intercept theorem as previously described[124,125].

3.6 AlamarBlue assay

AlamarBlue assay is a redox-sensitive assay that quantitatively measures cell viability and proliferation using colorimetric detection strategies. The cytotoxicity of various NPs, compounds and nanoformulations were assessed against mammalian cell (BMDM or 293T epithelial cells) as previously described[126]. 4×10^4 cells per well were co-cultured with five serial dilutions of each compound in 96-well plates at 37°C for 24 h. Similarly, 10×10^6 virulent *L. major* isolate promastigotes (MHOM/IL/81/FE/BNI strain) per well were co-incubated with five serial dilutions of each compound in 96-well plates at 27°C for 24 h. After the co-cultures, alamarBlue cell viability assay reagent was added to each well at 10% final concentration and incubated for further 48 h. The optical density (OD) was then measured by using Multiskan Ascent ELISA reader at a wavelength 550 nm and 630 nm. The OD value or % dye reduction is proportional to viable cell/parasite number and was used for IC_{50} calculation based on the intercept theorem.

3.7 Electrophoretic mobility shift assay (EMSA)

EMSA is used to detect complexes of polymers or proteins with nucleic acids and widely used for the characterization of two interacting molecules[127]. We used for physicochemical characterization of PHMB/DNA interactions (polyplexes) of different types of DNA. Namely, high-purity genomic DNA (gDNA) that was isolated from 1.5×10^9 *L. major* promastigotes using silica-based, microcentrifuge spin-column (Purelink® Genomic DNA kit K1820-01, Life Technologies, Germany) and CpG ODN with sequence TCCATGACGTTCCTGATGCT purchased from Eurofins MWG Operon, Germany. For

gDNA from the parasites, the DNA concentration and purification were assessed and quantified by NanoDrop 2000 spectrophotometer (Thermo Scientific, Germany). PHMB/gDNA complex formulations were prepared by adding and mixing 4.5 μg of gDNA with PHMB (0-54 μg) in a final volume of 30 μl water. After thorough mixing by pipette, the polyplexes were left stabilizing at RT for 2 h prior to any of the experiments. The polyplexes were mixed with 6× Blue/Orange loading dye (Promega, Germany) at 4:1 sample to dye ratio and loaded to 1% agarose gel containing SYBR® gold nucleic acid gel stain (S11494, Life Technologies, Germany) for electrophoresis at 100 Volts for 3 h. To investigate PHMB/CpG interactions and their physicochemical characterization, PHMB/CpG ODN and PHMB/CpG-R polyplex formulations were prepared in the same manner by mixing 30 μg CpG ODN 1668 or 15 μg of CpG-R with PHMB (0-54 μg) in a final volume of 30 μl water, respectively. After the polyplexes were stabilized for more than 20 min, the samples were then combined with 6× Blue/Orange loading dye (Promega, Germany) at 4:1 sample to dye ratio and loaded to 1% agarose gel containing SYBR® gold nucleic acid gel stain for electrophoresis at 100 Volts for 45 min. 2-Log DNA ladder (0.1-10.0 kb, New England Biolabs) was used as a positive control. Intas Science Imaging gel reader (Germany) and Luminescent Image Analyzer (GE Healthcare Life Sciences, Imagequant LAS 4000, Germany) were used for Gel documentations of non-fluorescent and fluorescent molecules, respectively.

3.8 Dynamic light scattering and electrophoretic light scattering

Dynamic light scattering (DLS) is a well-established technique for measuring the size and size distribution of particles dispersed in a liquid. The Brownian motion of particles in suspension causes laser light to be scattered at different intensities and the intensity fluctuations yields the velocity, which have relationship with the particle size. Likewise, electrophoretic light scattering (ELS) measures the electrophoretic mobility of particles in dispersion. It is based on the fundamental physical principle of electrophoresis, in which an electrical field is applied

to the electrodes, and particles with a net charge or a net zeta potential will migrate towards the oppositely charged electrode with a velocity (mobility). For further characterizations of PHMB/CpG ODN polyplexes, particle sizes and zeta potential were measured by using a Beckman coulter Delsa Nano C (Beckman Coulter, Krefeld, Germany). CONTIN analysis mode and Smoluchowski equation were used to determine the size and the zeta potential, respectively. The polyplex formulations were first prepared by mixing appropriate relative weight ratio of PHMB/CpG ODN. The size distributions with their polydispersity index (PDI) and zeta potential measurements were performed using DSL and ELS in clean disposable cuvettes containing 500 µl Millipore water and ISA water (KCl 0.15M), respectively. All measurements were carried out at 25ºC. Scattered light was detected in an angle of 165° (particle size) and 15° (zeta potential). The measurements were done in triplicates and reproduced at least three times.

3.9 Isothermal titration calorimetry

Isothermal titration calorimetry (ITC) is used to study the binding behavior of biomolecules and is applicable in wide varieties of biomedical researches including the characterization of molecules mechanism of actions. The nature of interactions between PHMB and CpG ODN were investigated by ITC (MicroCal™ iTC200 System, GE Healthcare Northampton, MA, USA) by directly measuring the heat released or absorbed during binding events. The samples were diluted to desired concentrations in Millipore water and degassed by ultrasonication for 15 min prior to measurements. A 40-µl microsyringe was filled with PHMB as a titrant and injected at a rate of 2 µl/injection into cell sample containing 200 µl CpG ODN for a total of 20 individual injections. Different concentrations of the titrant with at least 20-fold higher concentration of the cell sample (CpG ODN) than the titrant (PHMB) were tested and optimized to have good saturation curve. During the injection and measurement, the reaction was facilitated by using the titrant syringe as the stirrer with the speed of 400 rpm. The

stabilization delay of the heat signal before the first injection was adjusted at 3 min with 150 seconds injection interval and 5 ± 0.5 μcal/sec calibration power. The measurements were performed at 25°C in triplicates and all experiments were repeated three times. Background titrations were carried out by using identical PHMB titrant solution but the cell filled with Millipore water and also successive Millipore water additions to the CpG ODN solutions to determine the background heat to be subtracted from the main experiment. All data were automatically collected and analyzed using Origin® Software to get thermodynamic parameters associated with the interaction. The binding isotherm (ΔH) was used for fitting to an appropriate model.

3.10 Fluorescence microscopy and confocal microscopy

Localizations and colocalizations of fluorescent molecules or particles in mammalian cells and promastigotes were performed by a live video fluorescence and/or confocal microscopy imaging system (Wetzlar, Germany). In mammalian cells, the cells were harvested by either scraping or trypsinizing methods after incubating the culture dishes on ice for 10 min and washing with PBS. The cells were transferred to 50-ml tubes and washed with 20 ml of PBS (300 × g, 10 min, 4°C). The supernatants were discarded and the pellet was re-suspended in 3 ml cold RPMI. The cells were then counted in Neubauer counting chamber (0.1 mm depth) by making a 10-fold dilution in Trypanblue (10 μl of cells to 90 μl of Trypanblue) and the number of cells were adjusted to 2×10^5 cells/ml. The cells were then co-cultured with the molecular probes by incubating at 37°C, 5% CO_2 for required time points depending on the time required for the uptake and attachments to bottom of culture dishes or chamber slides. After washing in ice-cold PBS (300 × g, 10 min, 4°C) for three times, the cells were fixed in 4% paraformaldehyde for 10-15 min at RT and further washed with PBS. Finally, 10─20 μl of solution containing the cells were added to slides and covered with cover slips for microscopic examinations. However, for chambers slide, the imaging was performed directly

after fixing and washing steps. For promastigotes, the procedures were similar to the mammalian cells as indicated above. The few exceptions are that the washings of the promastigotes were performed at 3,000 × g, 10 min at RT. Moreover, the concentration was adjusted at 3×10^6 parasites per ml and the experiments were performed in culture dishes.

3.11 Determination of cytokine productions

Initial recognition by the immune system is an essential determinant for the fate and distribution of materials inside the body[100]. The effect of CpG ODN on the host immune system and its influence on proinflammatory cytokine productions have been investigated by many groups. In order to investigate immune modulation property of the polyplexes compared to free CpG ODN or PHMB, BMDMs were generated from female BALB/c mice. The number of BMDM was adjusted to 2×10^6 BMDM and 0.5 ml of the volume was seeded in 24-well plates and incubated at 37°C for 30 min in the presence/absence of CpG ODN (1.5 µg/ml). PHMB, CpG ODN or PHMB/CpG ODN polyplexes of various concentrations were prepared and added to the pre-activated or control cell wells. The plate was further incubated for 48 h for the production of proinflammatory cytokines. The supernatants were then collected from all wells and IL-6, IL-10, IL-4 or TNF-α (BD Biosciences, Wiesbaden, Germany) concentrations were measured by sandwich enzyme-linked immunosorbent assays (ELISA) while IL-12p70 was measured by using the IL-12p70 ELISA Ready-SET-Go kit from eBioscience according to the suppliers' instructions.

3.12 Statistical Analysis

Normalization and percentage calculations were done based on mean fluorescence intensity (MFI) of the treated cells as compared to the control in flow cytometry data analyses. The values are given as mean ± standard error (SE). Statistical significance was determined by using one sample t-test or Student's *t* test (Microsoft Excel Software). For quantitative colocalization analysis, ImageJ (freely available software) was used.

4. RESULTS

4.1 Chapter one: Discovery of polyhexanide as novel antileishmanial agent

4.1.1 Efficacy of PHMB against L. major

To investigate its potential use as topical therapeutic agent against CL, PHMB, a widely used antimicrobial polymer and wound antisepsis, was tested against the extracellular form of *L. major* (promastigotes) by using AlamarBlue cell viability assay as previously described[126]. The results showed that PHMB can effectively kill the promastigotes at sub-micromolar concentrations in a dose-dependent manner as compared to the growth control (Fig. 3).

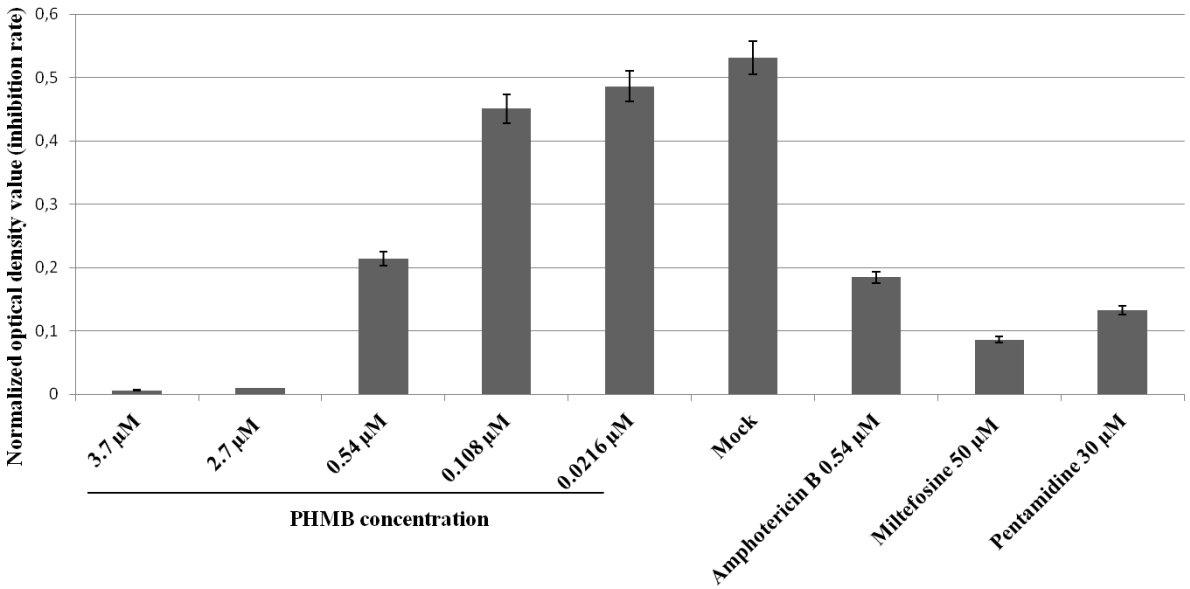

Fig. 3. *Dose-dependent antileishmanial activity of PHMB against L. major promastigotes. Growth inhibition was determined in vitro using an AlamarBlue assay. Miltefosine, pentamidine and amphotericin B were used as positive controls while distilled water was used as negative control (mock). The error bars show standard error of three independent experiments to the mean*.

Determination of the 50% inhibitory concentration (IC_{50}) results confirm that PHMB is active against *L. major* promastigotes *in vitro* with IC_{50} = 0.41 µM. Moreover, it provides evidence that PHMB show higher potency than the current standard antileishmanial drugs

used in clinics. PHMB is about 69- or 39-fold more potent than miltefosine or pentamidine, respectively. Surprisingly, it is more than 1,000 fold more potent than paromomycin, the currently recommended drug for topical treatment of CL. It has been shown that PHMB eliminates *Aspergillus* growth starting at a dose of 4 µg/ml[128], which is higher than the doses needed to kill *L. major* promastigotes. Furthermore, efficacy of PHMB was assessed against the intracellular form of *L. major* (amastigotes) in BMDM infected model. The results showed that the activity of PHMB against the intracellular amastigotes (IC_{50} = 4 µM) was equal to the IC_{50} against BMDM, suggesting no relative selectivity towards the promastigotes as compared to macrophages (Table 1).

Substances	**IC_{50} (µM) promastigotes**	**SI promastigotes**	**IC_{50} (µM) amastigotes**	**SI amastigotes**
PHMB	0.41 ± 0.25	9.75	4 ± 0.65	1
CpG ODN	>150	ND	>150	ND
PHMB/CpG (1:2 w/w)	2.54 ± 0.5	52.7	1.12 ± 0.23	119.4
PHMB/CpG (1:1 w/w)	2.2 ± 0.28	22.7	2. 82 ± 2.8	17.7
PHMB/CpG (2:1 w/w)	1.45± 0.33	22.8	1 ± 0.55	15.89
Paromomycin	>500	ND	1500 ± 12.5	ND
Miltefosine	28.33 ± 5.2	2.67	54 ± 8.1	1.4
Pentamidine	16.19 ± 31	7.9	6.38 ± 2.4	20
Amphotericin B	0.42 ± 0.5	>50	0.099 ± 0.05	>208

IC_{50}= minimum concentration of the substances required to kill 50% of the population; SI = mean IC_{50} against BMDM /mean IC_{50} against *L. major* promastigotes or amastigotes; ND = not determined.

Table 1. *Antileishmanial efficacy of PHMB, polyplexes and standard drugs. The selectivity index (SI) and IC_{50} values against promastigotes or amastigotes as compared to standard antileishmanial drugs are shown. The tables are the average IC_{50} values of 3-6 independent experiments for each compound.*

To further confirm the potency of PHMB against *L. major* promastigotes, the parasites were treated with 2 µM PHMB for 24-48 h and the samples were prepared for transmission electron microscopic and light microscopic examinations as compared to the untreated controls. Our visual examinations by light microscopy and TEM clearly showed morphological and behavioral changes in PHMB-treated promastigotes as compared to untreated parasites (Fig. 4). It confirms that PHMB has observable activity against *L. major* promastigotes.

Fig. 4*. Effects of PHMB on L. major morphology and behavior. (a-d) TEM images of L. major promastigotes (right) showing morphological changes such as shrinkage, extensive cytoplasmic vacuolization (V), marked loss of cytosolic contents and condensed nucleus (N). Images b and d were taken after treatment with 2 µM PHMB for 48 and 24 h, respectively. The untreated controls (left) show normal elongated morphology of promastigotes with intact and clear distinct kinetoplast (kDNA), N, mitochondrion (M), lipid vacuoles (LV) and glycosome (G). (e-h) Light microscopy images showing morphological and behavioral changes (no more clamp formation as indicated by arrowheads) after treatment with 2 µM PHMB for 24 h. Scale bars = (a) 1.1 µm, (b) 0.6 µm, (c and d) 0.25 µm, (e and f) 7.5 µm and (g and h) 25 µm.*

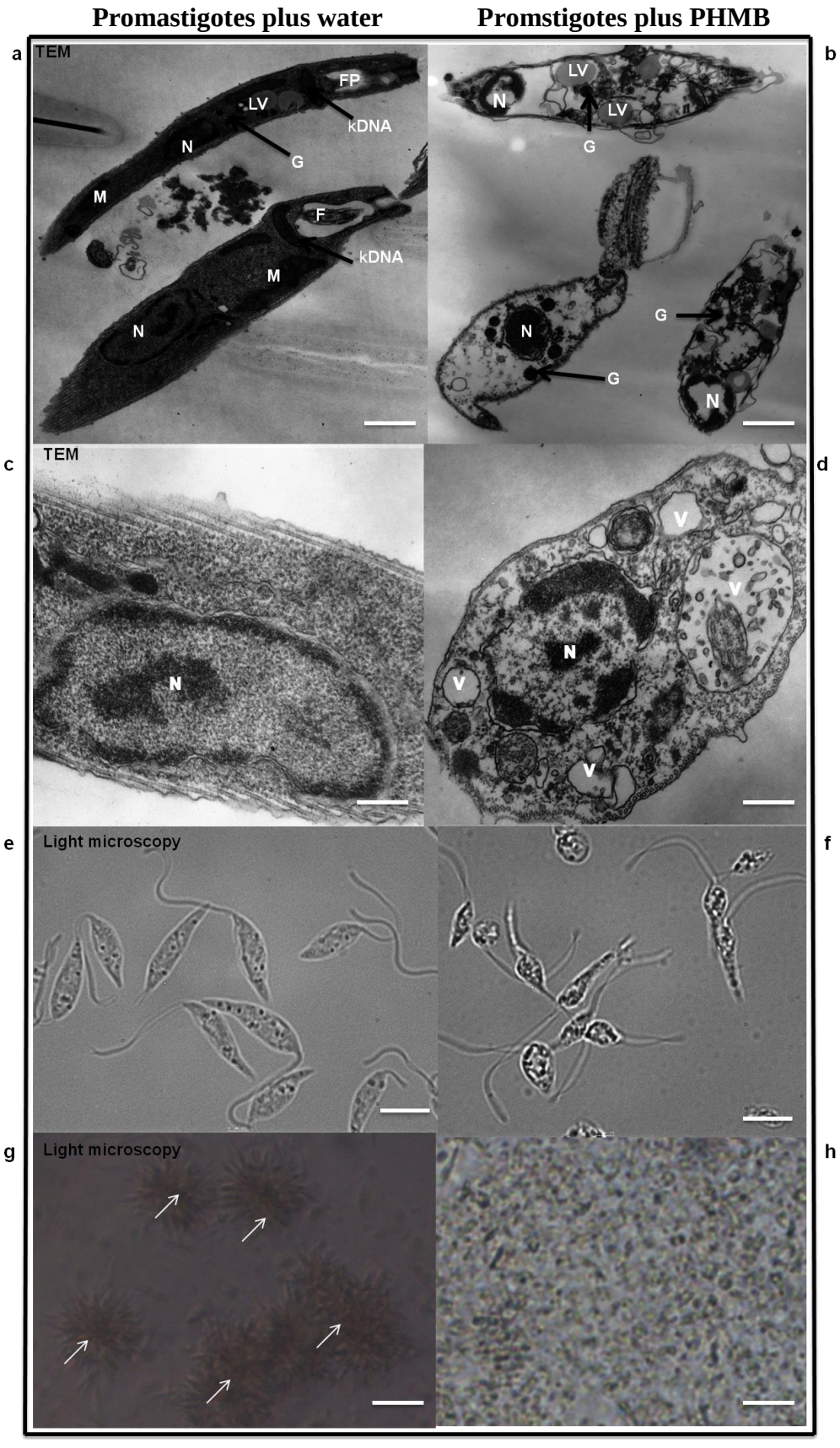
Promastigotes plus water
Promstigotes plus PHMB
a
TEM
FP
LV
kDNA
N
G
M
F
kDNA
M
N
b
LV
N
LV
G
G
N
G
N
c
TEM
N
d
V
V
N
V
V
e
Light microscopy
f
g
Light microscopy
h

To determine the level of host/pathogen selectivity of PHMB, we measured its cytotoxicity against BMDM and 293T epithelial cells using the AlamarBlue assay. Surprisingly, the IC_{50} value obtained indicate that PHMB is about 6.5-fold more toxic against BMDM (IC_{50} = 4 μM) than 293T epithelial cells (IC_{50} = 26 μM), resulting in selectivity indexes (SI) of 9.75 and 63.4 against these cell types, respectively (Table 2). The results show that the toxicity of PHMB is different in different host cell types. We speculate that phagocytic cells such as macrophages take up more PHMB than 293T epithelial cells, which may consequently result in higher toxicity.

Substances	**IC_{50} against BMDM (µM)**	**IC_{50} 293T epithelial cells (µM)**
PHMB	4± 0.65	26 ± 6.8
PHMB/CpG (2:3)	196 ± 80	ND
PHMB/CpG (1:2)	134 ± 40.2	ND
PHMB/CpG (1:1)	50 ± 10.4	185± 22.5
PHMB/CpG (2:1)	33± 9.5	90.3± 23.5
Paromomycin	>1500	ND
Miltefosine	75.6 ± 6.5	ND
Pentamidine	127.9 ± 23.2	ND
Amphotericin B	>21	ND

The concentration given to the polyplexes represents the concentration of PHMB

ND= not determined.

Table 2. *Cytotoxicity effects of PHMB and PHMB/DNA polyplexes as compared to standard antileishmanial drugs. The table shows cytotoxicity of each compound. The IC_{50} values of each compound against BMDM and 293T epithelial cell line are shown. The tables are the average IC_{50} values of 3-6 independent experiments for each compound.*

4.1.2 Uptake mechanisms of PHMB by BMDM and its proposed mechanisms of action against L. major

After determining the potency and selectivity of PHMB against *L. major* promastigotes, we were interested to know its underlying mechanism of action. To have a clue where to start, we reviewed literature on PHMB's mechanisms of action against other microbes. It suggested that PHMB's microbe-selective toxicity is due to preferential disruption of microbial membranes rather than mammalian membranes[121,129]. We then hypothesized that PHMB kills *L. major* parasites by this mechanism. Two plasma membrane permeability markers were used to test the effects of PHMB on the membrane integrity of the promastigotes. PI, a dye that can enter the parasite and stain DNA only after loss of membrane integrity, and YO-PRO®-1 dye, another plasma membrane permeability marker which selectively passes through the plasma membranes of apoptotic cells but it does not label living cells[123]. After incubating the promastigotes with 2 μM PHMB for only 30 min, more than 20% of the parasite population was stained by PI and the staining increased at later time points (Fig. 5a). This dye exclusion experiment was repeated by using YO-PRO®-1 dye according to the manufacturer's instructions. The results similarly showed time-dependent permeabilisation of the parasite even at early time points (Fig. 5b). Taken together, the dye exclusion assay results clearly show that PHMB damages the membrane integrity of the parasite in a time-dependent manner. Moreover, as it can be clearly seen from the figure (Fig. 5), it shows that permeabilized parasites can be observed within 30 minutes of PHMB treatments, supporting the hypothesis that PHMB disrupts parasite membranes.

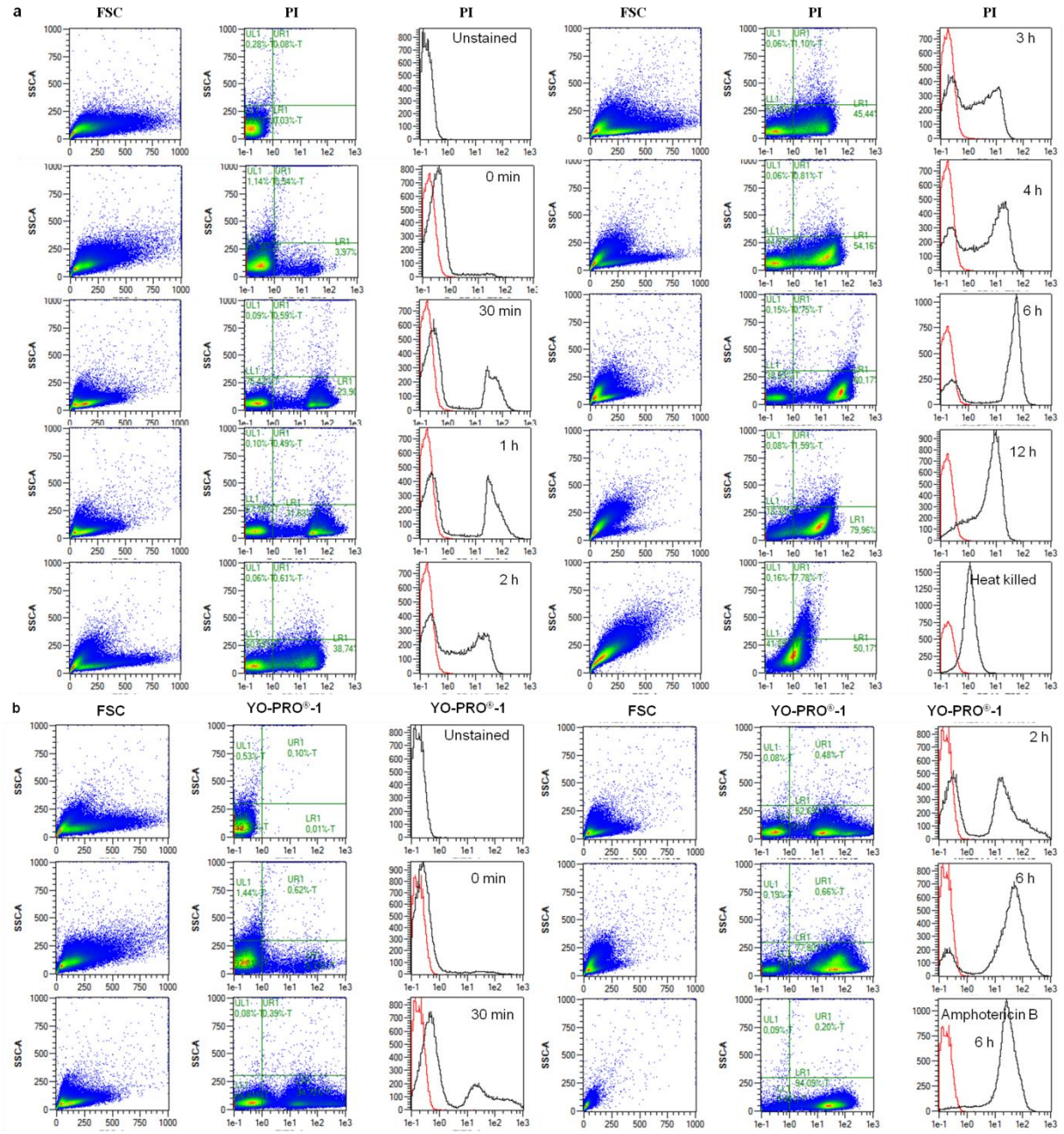

Fig. 5*. Time-dependent effect of PHMB on membrane integrity of L. major promastigotes. Representative detailed FACS data of (a) PI and (b) YO-PRO®-1dye staining of promastigotes after treatment with 2 µM PHMB for indicated time points, showing time-dependent effect of PHMB on the membrane. Amphotericin B at 2 µM concentration and hat killed promastigotes were used as positive control.*

Furthermore, we consistently observed condensation of parasite nuclei after incubation with 2 µM PHMB for 24–48 h in our TEM pictures (Fig. 4). In line with this observation, PHMB's mechanism of bactericidal action was associated with its strong and cooperative interaction with all forms of nucleic acids *in vitro*[130]. These observations led us to consider

that killing mechanisms of PHMB may be more complex, and we further investigated whether PHMB also targets DNA inside parasites. Cellular DNA of *L. major* promastigotes was stained with Hoechst 33342 after treated with 2 μM PHMB for 48 h. Confocal and fluorescence microscopy study results show that PHMB condenses and disrupts chromosome structures in the parasites (Fig. 6).

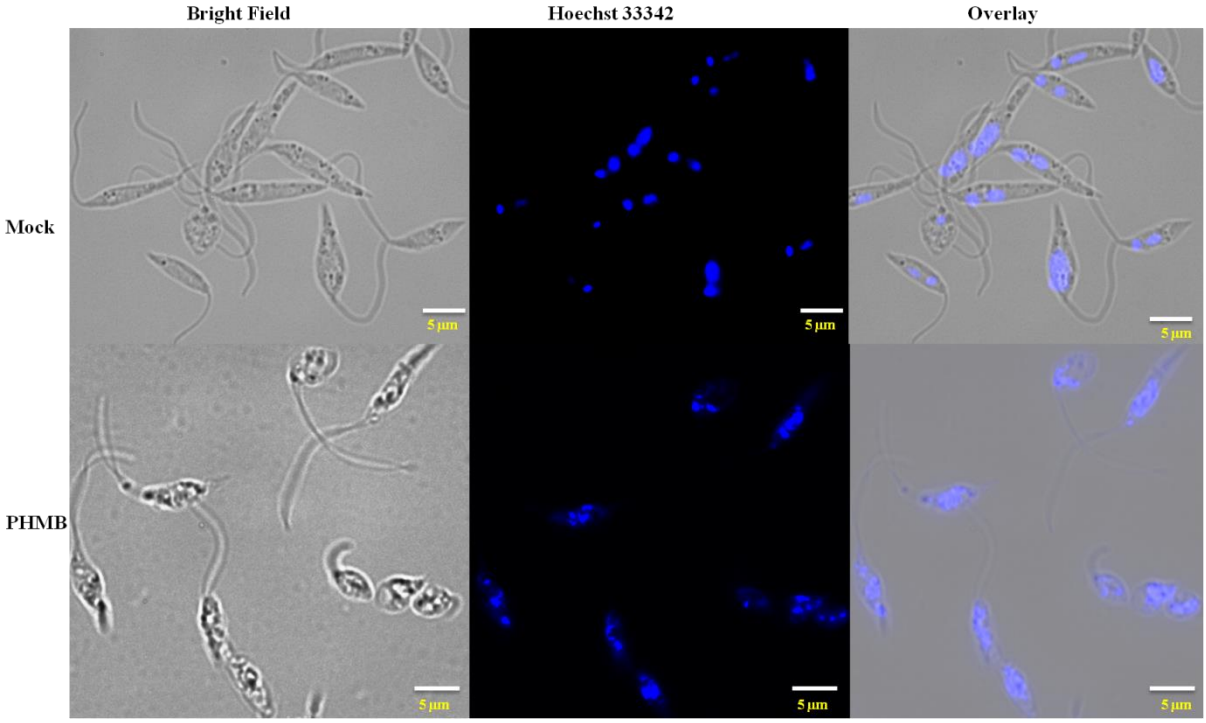

Fig. 6. *Fluorescent microscopy analysis showing condensed and damaged DNA materials of L. major promastigotes after treatment with PHMB. The concentration of PHMB used was 2 μM for 48 h while the mock control was distilled water.*

We further confirmed our observation of PHMB effects on DNA materials of the parasites by supposing that if the observations are correct, then it should also bind isolated parasite genomic DNA (gDNA). To test this hypothesis, genomic DNA of *L. major* promastigotes was isolated from 1.5 × 10^9 parasites using Purelink® Genomic DNA kit (K1820-01, Life Technologies, Germany) and was quantified by using a *NanoDrop 2000* spectrophotometer (Thermo Scientific, Germany). PHMB/gDNA polyplex formulations were prepared and electrophoretic mobility shift assay (EMSA) was performed. The results confirmed that PHMB has an excellent binding affinity towards isolated genomic DNA and

forms PHMB/gDNA polyplexes at relative weight ratios ≥ 0.25, confirming that PHMB can bind gDNA from parasites, and, thus, may also bind chromosomal DNA within parasites (Fig. 7).

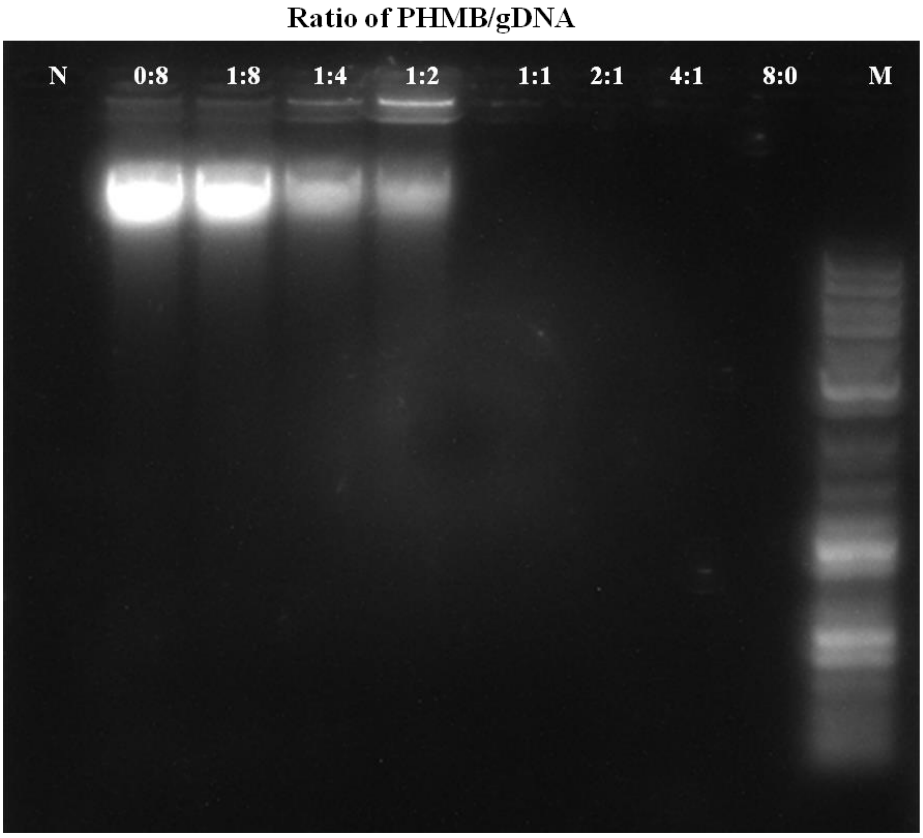

Fig. 7*. Formation of PHMB/gDNA polyplexes as confirmed by 1% agarose gel, showing PHMB/gDNA interactions. With the exceptions of negative control and PHMB alone, all wells contained equal amounts (weight) of DNA with various concentrations of PHMB. M represents 2-Log DNA ladder (0.1-10.0 kb, New England Biolabs) and N represents water for negative control. All indicated PHMB/gDNA ratios are in relative (w/w).*

We next asked a question that if the mechanisms of action of PHMB against *L. major* promastigotes involve DNA binding and disruption, how it selectively condenses or disrupts only the chromosomes of the parasites without affecting the DNA of the mammalian host cells. To address this question, PHMB-FITC was produced by covalent conjugation of PHMB with fluorescein isothiocyanate (FITC). First, we then investigated the uptake properties of PHMB-FITC into *L. major* and macrophages, and checked where it localizes. For this purpose, BMDM cells were incubated with 1 μM PHMB-FITC, counterstained with Hoechst

33342, and internalization was investigated using confocal microscopy. The results confirmed that PHMB-FITC is readily taken up by macrophages (Fig. 8). However, PHMB-FITC exclusively localized in the cytoplasm without entering nuclei in mammalian cells, indicating failure to transit across the nuclear envelope (Fig. 8).

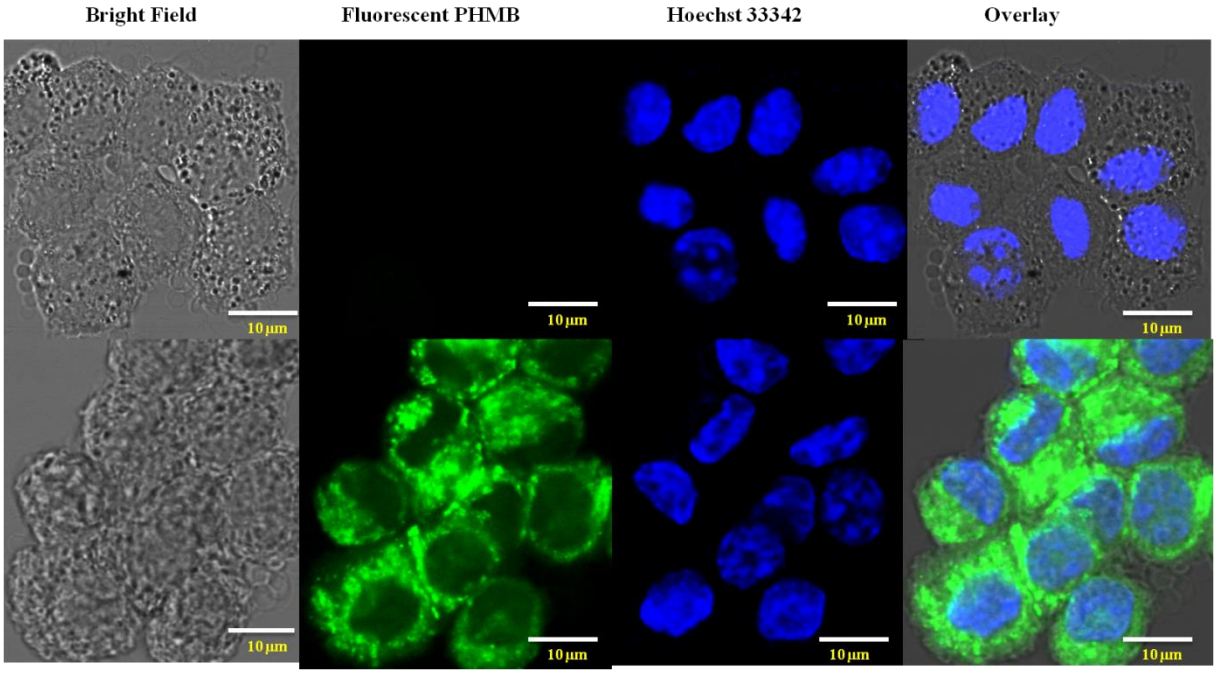

Fig. 8. *Cell localization of PHMB-FITC in BMDM. Laser scanning confocal images showing uptake of PHMB-FITC by BMDM (lower) and control cells (upper). Note apparent nuclear exclusion in BMDM cells, scale bars = 10 µm.*

In the same manner, BMDMs were incubated with 1 µM PHMB-FITC, washed three times with PBS (300 × g, 10 min, 4°C) and uptake was quantified by flow cytometry. The results revealed that about 100% of the macrophages accumulate enough PHMB-FITC that could be detected by flow cytometry as early as 1 h, indicating their ability to entry into BMDM. Moreover, the results also showed that BMDM take up PHMB-FITC in a time-dependent manner (Fig. 9a). BMDM cells were also incubated with 1 µM PHMB-FITC/CpG ODN polyplexes for different time points and intracellular intensity was quantified by flow cytometry. The results show that the cellular uptake of PHMB-FITC/CpG ODN polyplexes is time-dependent (Fig. 9b).

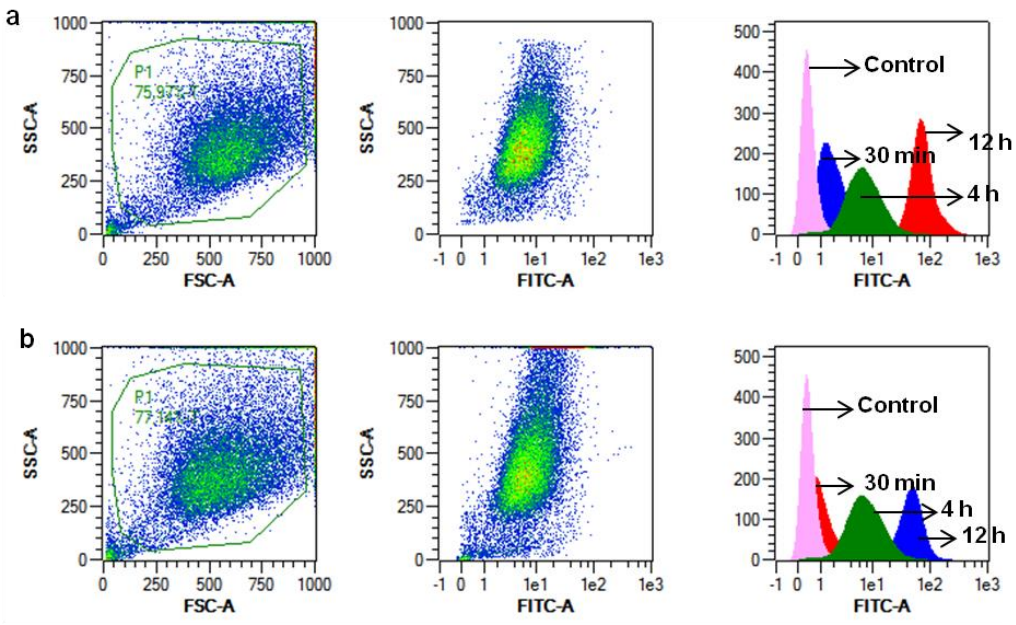

Fig. 9*. Time-dependent cellular uptake of PHMB-FITC and PHMB-FITC/CpG ODN polyplexes by BMDM. The representative flow cytometric data show uptake of (a) PHMB-FITC and (b) HMB-FITC/CpG ODN polyplexes into macrophages, and the histograms show the overlay of their uptake at 0 h, 30 min, 4 h and 12 h.*

Similarly, *L. major* promastigotes were incubated with 0.35 μM fluorescent PHMB (sub-IC_{50}) to investigate whether they take up PHMB-FITC or not. Our results confirm that *L. major* parasites take up PHMB-FITC without apparent exclusion from their nucleus (Fig. 10). Therefore, the intracellular localization of PHMB appears to differ in BMDM and parasites, with PHMB gaining access to parasite chromosomes.

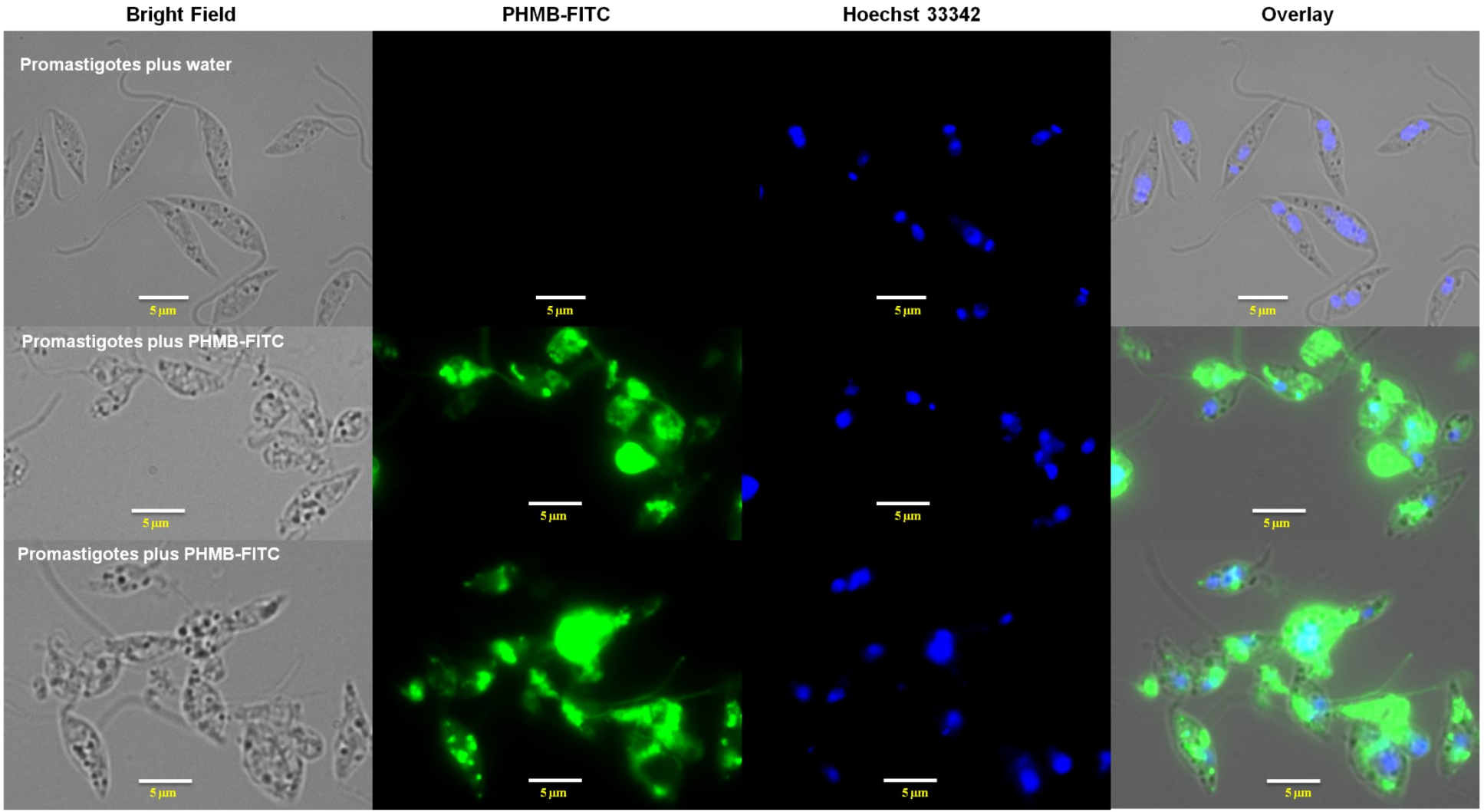

Fig. 10. *Localizations of PHMB-FITC in promastigotes. Fluorescence microscopy images showing uptake of PHMB-FITC by promastigotes (lower) and control cells (upper). Note no apparent nuclear exclusion in the parasites, scale bars = 5 µm.*

Understanding the uptake mechanisms of PHMB into macrophages is very important to control its intracellular antileishmanial activity and toxicity. We showed that PHMB-FITC was readily taken up and localizes in the cytoplasm of macrophages; however, we did not know the mechanism(s) of how BMDM take up PHMB. To address this question, different approaches were employed. First, we checked whether the uptake of PHMB-FITC was energy-dependent or not. BMDMs were treated with PHMB-FITC and incubated at 4°C under equivalent cell culture conditions for 4 h. The uptake of PHMB was then quantified by flow cytometry after washing three times with PBS, fixation with 4% paraformaldehyde and further washing with PBS. The results showed that the uptake of PHMB was strongly reduced (87%) at 4°C as compared to incubating the cells at normal 37°C (Fig. 11). This indicates that the predominant uptake mechanism of PHMB-FITC by BMDM is an energy-dependent cellular process or endocytosis but not energy-independent pathways such as direct penetration or diffusion. To further know the specific endocytosis pathway(s) involved in the uptake, five different selective endocytosis inhibitors were employed, as recently described[122]. These includes wortmannin, a potent inhibitor of phosphatidylinositol kinase (PI3K) that is commonly used as inhibitor of macropinocytosis at a dose of 12.85 μg/ml, cytochalasin D, a commonly used inhibitor of phagocytosis by blocking the actin polymerization at a dose of 5 μg/ml, dynasore, a cell-permeable small molecule that inhibits dynamin GTPase activity needed for dynamin-dependent endocytosis at a dose of 25.8 μg/ml, chlorpromazine hydrochloride that inhibits a Rho GTPase which is essential for the formation of clathrin-coated vesicles in clathrin-dependent endocytosis at dose of 10 μg/ml, and ikarugamycin, an inhibitor of clathrin coated pit-mediated endocytosis at a dose of 1 μM . Moreover, alexa-448-labeled transferrin and FITC-labeled dextran were used as positive control for clathrin-dependent endocytosis and to exclude the effect of FITC that might interfere with the cellular uptake mechanisms of PHMB, respectively. BMDMs were pre-incubated with each of the five specific endocytosis inhibitors for 30 min and exposed to PHMB-FITC, dextran or

transferrin followed by incubation at 37°C for 4 h. The results show that only dynasore effectively inhibited the uptake of PHMB-FITC (80% inhibition), showing that the PHMB-FITC uptake mechanism is dynamin-dependent endocytosis (Fig. 11). Similar results were obtained for PHMB-FITC/CpG ODN and PHMB/CpG-R polyplexes (Figs. 11 and 12), suggesting the uptake pathways of PHMB by BMDM was not affected by a polyplex formation process. However, neither the uptake of alexa-448-labeled transferrin or FITC-labeled dextran by BMDM was inhibited by equal concentrations of dynasore. Taken together, the data shows that the uptake mechanism of PHMB is predominantly via dynamin-dependent endocytosis rather than other endocytosis pathways. Moreover, the data confirmed that dynasore effectively blocks the uptake of PHMB or its polyplexes into macrophages.

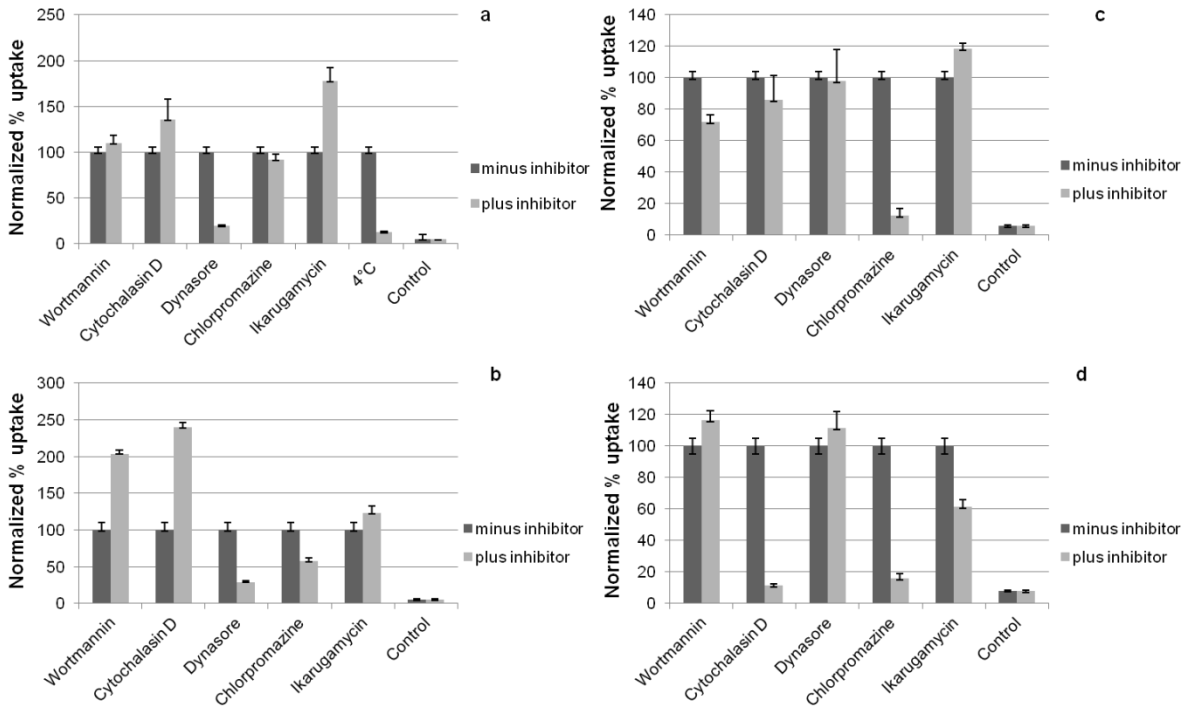

Fig. 11. *Cellular uptake mechanisms of PHMB-FITC and PHMB-FITC/CpG ODN polyplexes based on effects of selective endocytosis inhibitors. The bar graphs show the effects of different inhibitors and temperature on cellular uptake of (a) PHMB-FITC, (b) PHMB-FITC/CpG ODN polyplexes, (c) dextran/FITC and (d) alexa-448-labeled transferrin used as positive controls. Normalized mean fluorescence intensity (MFI) values of three independent flow cytometry experiments are shown and the values are given as mean ± SE.*

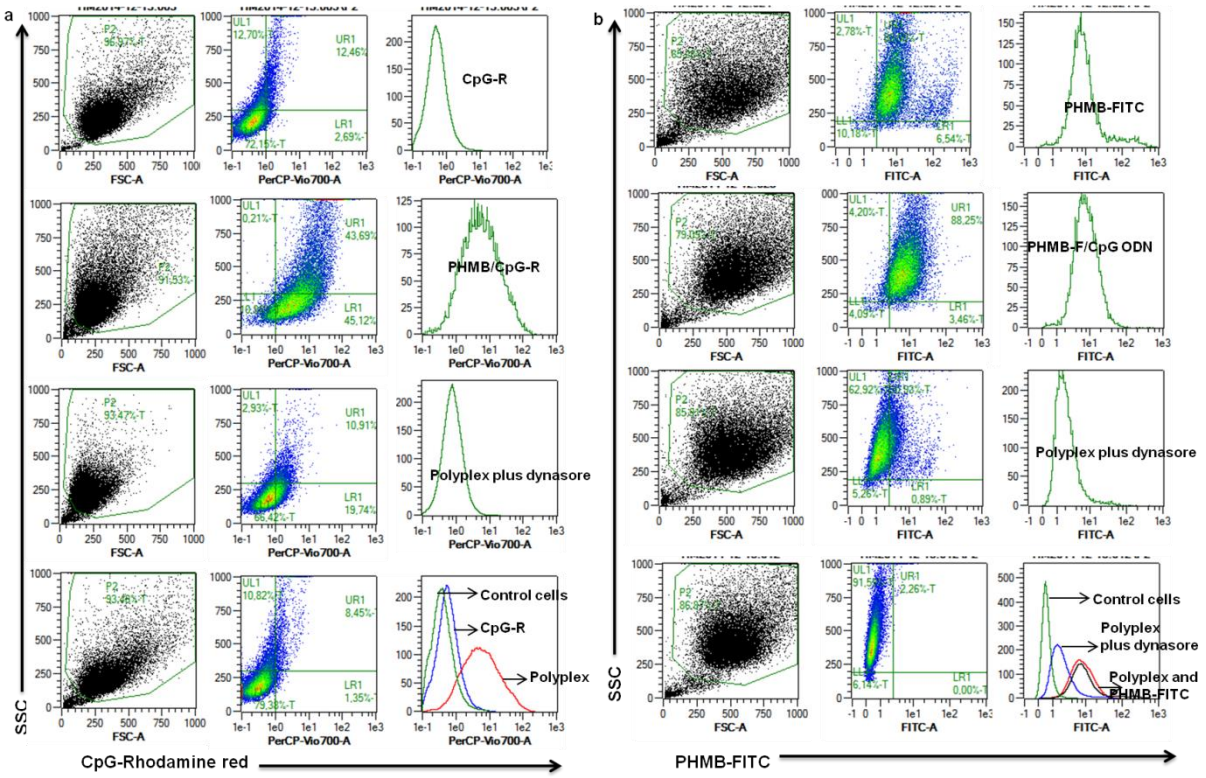

Fig. 12. *Uptake mechanism(s) of PHMB/CpG polyplexes and CpG ODN delivery into macrophages. The cellular uptake potential of (a) PHMB/CpG-R and (b) PHMB-FITC/CpG ODN polyplexes, and inhibition by dynasore. Free PHMB-FITC, PHMB-FITC/CpG ODN and PHMB/CpG-R polyplexes were efficiently blocked by dynasore. Based on their MFI, the uptake of CpG-R was enhanced by about 15 folds as polyplex form compared to its free form.*

We next hypothesized that if dynasore inhibited the uptake of PHMB or its polyplexes, it should also suppress PHMB's intracellular killing of amastigotes. To test this hypothesis, we determined the efficacy of PHMB or its polyplexes against intracellular amastigotes using luciferase reporter assay in the presence/absence of dynasore (80 µM). The results show clearly that dynasore inhibits PHMB-mediated killing of amastigotes (Table 3). In the presence of dynasore (80 µM), the IC_{50} value of PHMB against the intracellular amastigotes was increased twice and the polyplexes were completely inactive until the maximum dose tested (14.2 µM), while the activity of PHMB and the polyplexes were enhanced against the promastigotes in the presence of dynasore (80 µM). Dynasore alone didn't show any cytotoxicity against both amastigotes and promastigotes. The result suggests that dynasore

rescued the parasites from the intracellular antileishmanial effects of PHMB by blocking polymer uptake into host cells. The results also confirm our earlier evidence for PHMB intracellular killing of amastigotes.

Substances	**IC_{50} (µM) amastigotes**	**IC_{50} (µM) amastigotes + dynasore**	**IC_{50} (µM) promastigotes**	**IC_{50} (µM) promastigotes + dynasore**
PHMB	4 ± 0.7	8.1 ± 2	0.41 ± 0.25	0.114 ± 0.15
PHMB/CpG (1:2)	1.12 ± 0.23	>14.2	2.54 ± 0.5	0.11 ± 0.53
PHMB/CpG (1:1)	2.82 ± 2.8	>14.2	2. 2 ± 0.28	0.21 ± 0.14
PHMB/CpG (2:1)	1 ± 0.6	>14.2	1.45 ± 0.33	0.14 ± 0.23
Dynasore (80 µM)	No activity	No activity	No activity	No activity

The concentration values given are for PHMB with polyplexes.

Table 3. *Dynasore rescues killing of L. major amastigotes inside macrophages. The table shows that dynasore inhibits killing of the intracellular L. major amastigotes by PHMB or PHMB/CpG ODN polyplexes through blocking their uptake into macrophages. However, the dynasore enhanced the antileishmanial effects PHMB and the polyplexes against promastigotes. The table shows summary result of two independent experiments and the values are given as mean ± SE.*

It was then important to analyze whether the internalized PHMB were localized into endosomes of BMDM. We used the most common lysosomotropic agent called chloroquine to rupture endosomes[131]. Rupturing endosomes by chloroquine showed increased mean fluorescence intensity of PHMB-FITC inside BMDM in dose dependent manner, suggesting their localizations in endosomes (Fig. 13). At 150 µM chloroquine concentrations, the uptake of PHMB-FITC by BMDM was increased by about 27%. We speculate that PHMB are rapidly internalized by BMDM and accumulate in acidic vesicles during their trafficking in the endolysosomal cascade. It has been shown that degradation of PHMB could be observed

both in acidic and alkaline conditions (5.2% and 9.4%), while temperature caused no degradation[132].

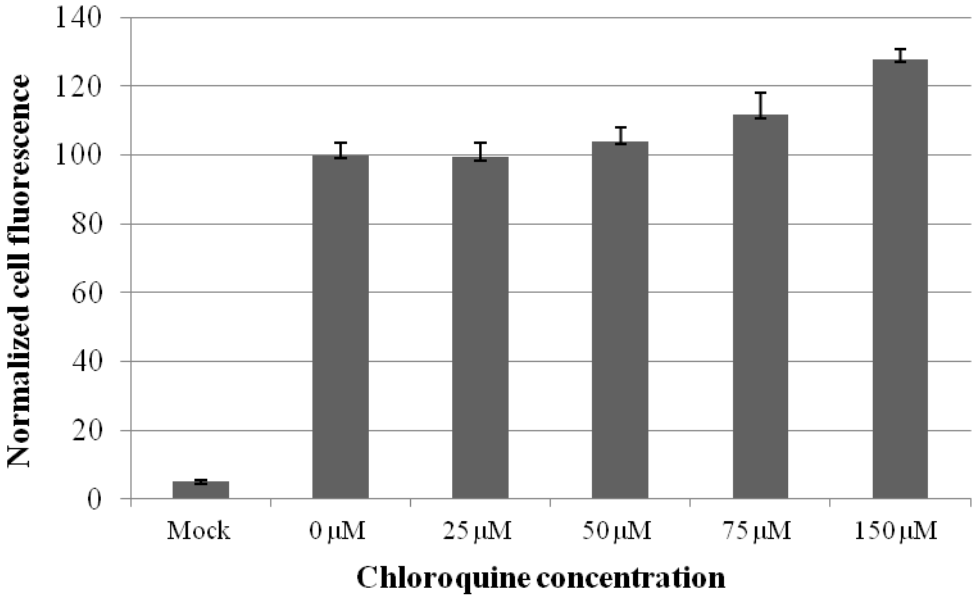

Fig. 13*. PHMB-FITC localizations in the endosomes of BMDM as confirmed by increments of MFI after treatment with different concentrations of chloroquine. The error bars represent standard error of three independent experiments.*

4.2 Chapter two: Understanding the interactions between nanoparticles and host cells

4.2.1 Cellular uptake mechanism of polystyrene NPs based on endosomomal markers

The drug loaded NPs have to overcome a number of transport barriers to reach at and readily taken up by the specific cells. In order to select and load NPs with various antileishmanial drugs for effective drug delivery systems against CL, understanding the cellular interactions and uptake mechanisms of NPs into mammalian cells is a pre-requisite. The type of laboratory techniques applied, the variability in fluorescence of some NPs used for tracking, the lack of uniformity in their physicochemical properties and the toxic nature of some NPs contribute to the complexity and controversial findings regarding the specific endocytic route involved in the cellular uptake of NPs[14]. To avoid such limitations, we used noncytotoxic and

standardized commercial polystyrene NPs which are suitable for quantitative cellular uptake studies and were previously used as model NPs for cellular uptake mechanism studies[18]. We aimed at systematical investigation of cellular uptake mechanisms NPs and exploring the factors affecting their cellular uptake in different host cells. Thus, fluorescent polystyrene latex beads (NPs) of different sizes (0.02 μm, 0.1 μm, 0.2 μm, 0.5 μm, 1 μm and 2 μm) were used to follow their uptake mechanisms in BMDM. According to the supplier's information, the polystyrene NPs were prepared though polymerization reaction with styrene that terminates with a carboxyl moiety and were used without any further modification. The diameters of the NPs were measured by TEM and were shown to be spherical NPs. To create intensely fluorescent signals that show little photo bleaching, polystyrene NPs were loaded with fluorescent dyes by physical absorption. Unlike covalently incorporating dye to NPs, physically absorption methods may potentially create problems such as dye aggregation and leakage. Thus, we initially checked whether the dye is stably retained in the polystyrene NPs without leakage by incubating 100 nm fluorescent NPs with BMDM at 37°C and observing under confocal microscopy. There was no indication for dye leakage and the polystyrene NPs were highly fluorescent with a distinct localization inside the cells, suggesting that this particular dye seems to be stably retained in the polystyrene NPs (Fig. 14). The free dye distribution throughout the cytoplasm as a result of diffusion across cells seems to be very little. The dye is largely hydrophobic, well dispersed and retained within the hydrophobic polystyrene matrix when the beads are kept in an aqueous solution. The fluorescent polystyrene NPs are also widely used as a model for NPs-cell interaction studies.

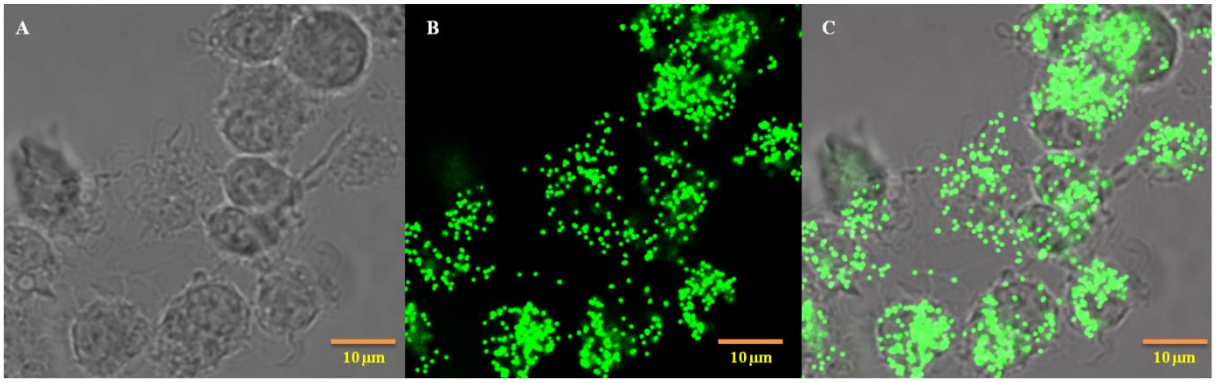

***Fig. 14**: Confocal microscopy image showing a distinct localization of highly fluorescent polystyrene NPs inside BMDMs, indicating no or little indication for dye leakage. The images were taken after BMDMs were incubated with 100 nm fluorescent polystyrene NPs at 37°C and 5% CO_2 for 30 min and washed three times in PBS.*

We then assessed the cytotoxicity of the polystyrene NPs towards host cells by using the alamar Blue® cell viability assay. The beads were sonicated (Bandelin Sonorex Super RK 106, Berlin, Germany) for 10 min immediately prior to every experiment and were used at a 1:1000 v/v dilution. The results showed that the polystyrene NPs were not toxic even at a 10 times higher concentration (1:100 v/v dilutions) than the one used in the experiment (Fig. 15)

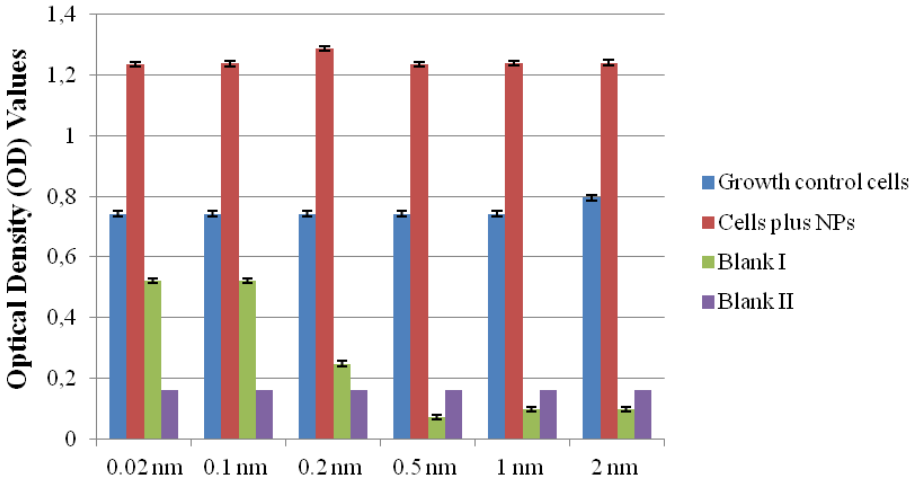

***Fig. 15.** Cytotoxicity assessments of different size polystyrene NPs at 1:100 v/v dilutions against BMDM based on alamarBlue cell viability assay. The error bars represent SE of two independent experiments. Bank I is control containing the highest dilution of the compounds without cells, while, Blank II is control containing water and cells without any compound. Growth control contains BMDMs and medium without any polystyrene NPs.*

Next, we investigated the cellular uptake mechanisms the polystyrene NPs by labeling with endocytosis marker FM4-64FX[133]. FM4-64FX dye stains the plasma membrane by becoming inserted and anchored in the outer leaflet of the plasma membrane lipid bilayer. Only after internalization, the dye becomes localized to the inner leaflet of endocytic vesicles. To this end, BMDMs were incubated with the NPs and 10 μM FM4-64FX for 30 min in phenol-free complete RPMI. The imaging was performed after the cells were harvested, washed three times with PBS and fixed with 4% paraformaldehyde. Under fluorescence microscopy, we observed co-localizations of FM4-64FX with the NPs inside the cells (Fig. 16A-D). The co-localizations of the NPs and FM4-64FX dye indicate internalization via a shared mechanism and suggested endocytosis to be responsible for the uptake of the polystyrene NPs. The results obtained by using the other polystyrene NPs sizes were similar. Moreover, the co-localization result may also indicate intracellular localization.

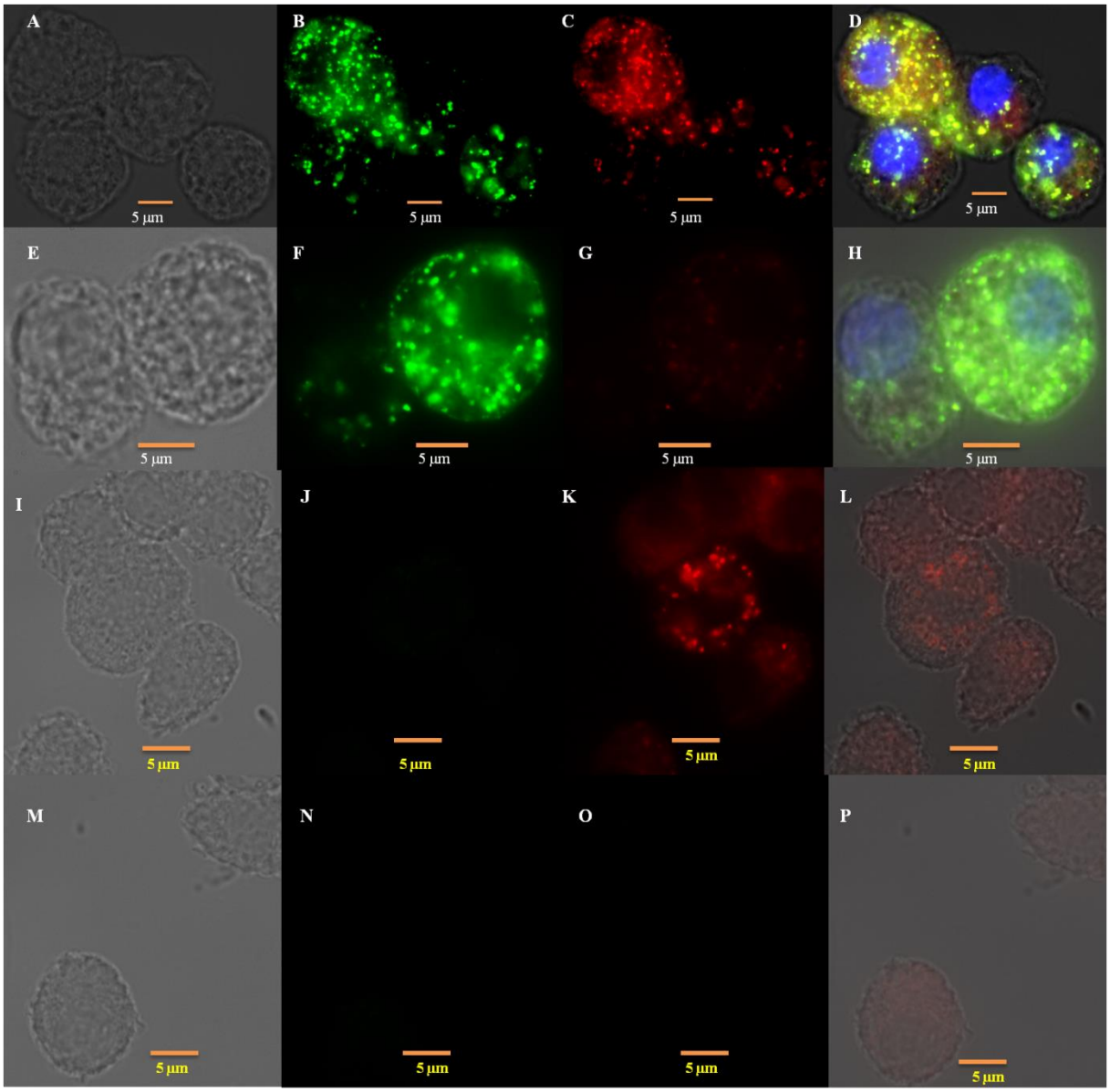

Fig. 16. *Fluorescence microscopy images of BMDMs after 30 min of incubation with 20 nm (A-D) NPs showing co-localization with the endosomal marker FM4-64FX. Images (E-P) are negative control cells treated with only the NPs, FM4-64FX or BMDM, respectively. Bright field (A, E, I and M), the NPs (B, F, J and N), endosomal marker FM4-64FX (C, G, K and O), and merge of the channels (D, H, L and P) are depicted.*

4.2.2 The uptake mechanisms of polystyrene NPs based on effects of energy

Endocytosis is an energy-dependent cellular process. In order to confirm that the NPs uptake was an active process and depends on energy, BMDM were generated and treated with 20 nm or 100 nm NPs for different time points. The plates were incubated either at the physiological

temperature of 37°C in incubator or at 4°C in fridge. After fixation with 4% paraformaldehyde and three times washing with PBS, the NPs uptake was quantified by flow cytometry. After acquiring 20,000 total events, the percentages of uptake were then calculated based on the relative MFI of cells kept at 4°C versus cells kept at 37°C for each time point. For normalization purposes and clarity, the MFI values of cells kept with the NPs at 37°C for 24 h were set as 100% and then compared with the other cells kept at both temperatures. The results of the flow cytometric analyses showed a time- and energy-dependent cellular uptake of the NPs under equivalent cell culture conditions (Fig. 17). With increasing time of exposure to the NPs, the normalized MFI of the cells were increasing from 8.48% at 30 min to 100% at 24 h, showing a time-dependent intracellular accumulation.

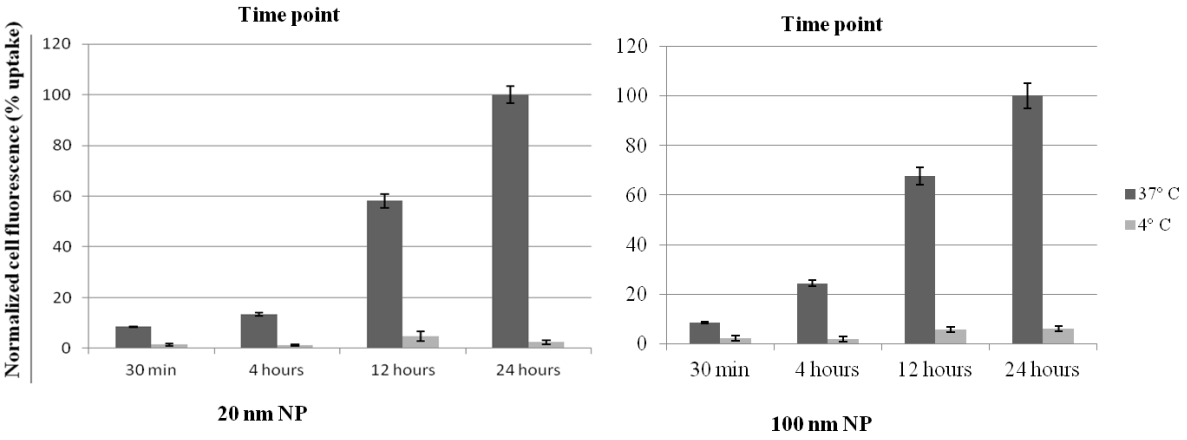

Fig. 17*. Flow cytometric analyses of the effects of temperature and time on the uptake of 20 nm and 100 nm polystyrene NPs by BMDMs. Cells were pre-incubated on ice for 10 min before exposure to NPs followed by incubation at 4°C for further 30 min, 4 h, 12 h or 24 h while the control groups of cells were incubated at 37°C for the respective time points throughout the incubation period. Normalized MFI values of three to six independent experiments are shown and the values are given as mean ± SE.*

To further confirm the time-dependent accumulation of NPs inside BMDMs, fluorescence microscopy and TEM studies were performed. The results clearly showed time-dependent uptake of the NPs inside BMDMs (Fig.18). Nevertheless, incubating the BMDMs with the same dose and batch of polystyrene NPs at 4°C under equivalent cell culture

conditions resulted in a strong reduction of uptake at all considered time points (Figs. 17 and 19). It indicates that at low energy, only limited amount of polystyrene NPs are taken up by cells. Since there is no exocytosis expected at 4°C, we can conclude that the limited accumulations of NPs in cells were as a result of reduced uptake. Thus, the NP uptake is an active process and strongly temperature- and time-dependent. Moreover, regardless of the incubation period, we observed low intracellular fluorescence (about 5%) among cells kept at 4°C (Fig. 17). Likewise, fluorescence microscopy images show similar limited uptake at 4°C at all time points (Fig. 19). The uptake study results for both 20 nm and 100 nm NP sizes were similar (Fig. 17). All together, the results confirm that BMDMs take up polystyrene NPs via endocytosis.

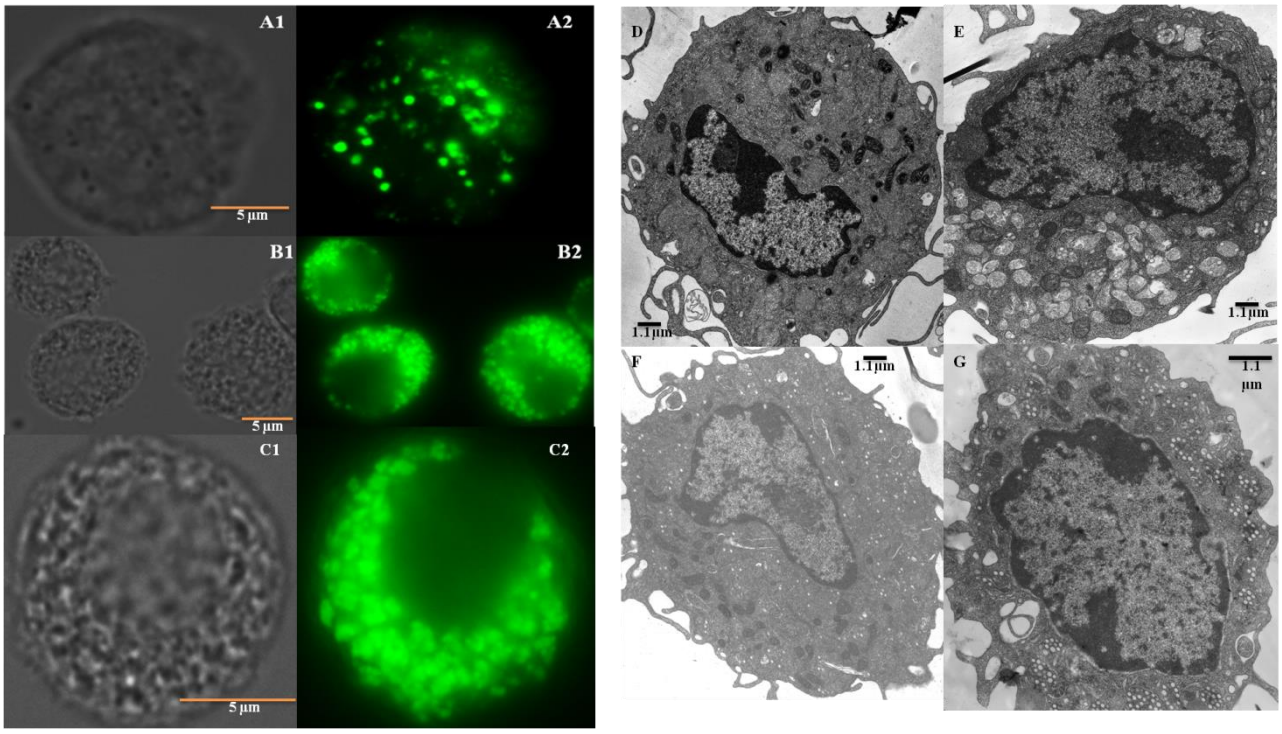

Fig. 18*. A representative fluorescence microscopy and TEM pictures showing time-dependent accumulations of 100 nm polystyrene NPs in BMDMs. Time-dependent differences in relative accumulation of the NPs after incubation with BMDM for 30 min (A1, A2 and E), 6 h (B1, B2 and F) and 12 h (C1, C2 and G) can be observed. The green channel A2, B2 or C2 shows the polystyrene NPs while A1, B1 or C1 represents the bright field. D shows negative control BMDM and the white particle structures in the TEM images are the polystyrene NPs.*

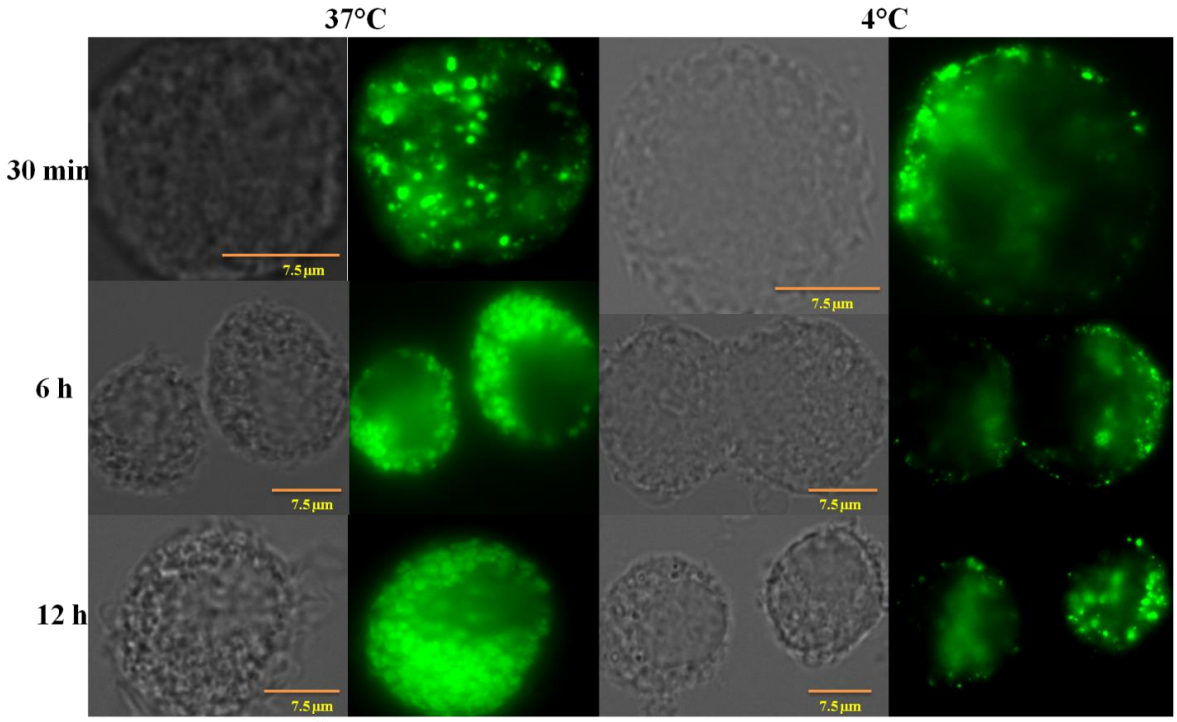

Fig. 19. *Fluorescence microscopy images showing the effect of temperature and time on the uptake of 20 nm polystyrene NPs by BMDMs. The relative uptake of NPs increased in a time dependent manner at 37°C while it was strongly reduced at 4°C. For cells incubated at 4°C, the time difference seemed to have no effect. Bright field and the NPs (green) for each temperature and time point are depicted. The pictures are representatives of three independent experiments*

4.2.3 Ultrastructural analyses of membrane morphology reveal multiple cellular uptake mechanisms

To further confirm endocytosis as uptake mechanism of the polystyrene NPs and investigate the specific routes underlying endocytosis, TEM ultrastructural studies were performed. As macrophages take up extracellular material by a wide range of mechanisms and thus allowed us to study the cellular uptake of NPs via a variety of possible entry routes, BMDMs were used. Macrophages are also an important drug targets as they mediate a wide variety of infectious diseases. BMDMs were exposed to 100 nm polystyrene NPs for 30 min and were prepared for TEM study. The TEM data analyses showed that the NPs are accumulated in

membrane-bound intracellular vesicles as early as 30 min, confirming the involvement of endocytosis in NP uptake (Fig. 20 indicated by EN). The ultrastructural plasma membrane invaginations and protrusions also confirmed that the uptake of 100 nm polystyrene NPs by BMDMs were via endocytosis (Fig. 20A-E). However, a few particles were seen freely localized in the cytoplasm of BMDMs without membrane-bounded. Since the harsh TEM sample preparation processes may affect the membrane surrounding polystyrene NPs and make them fragile, the free localization inside the cytoplasm may not necessarily show the reality. Moreover, due to the level/position of the cell sectioning, it may also difficult to see the membranes surrounding some NPs. Thus, the observation of free NPs in the cytoplasm may not necessarily suggest the involvement non-endocytic uptake mechanisms.

Moreover, we wanted to investigate whether a single cell type employs several uptake mechanisms simultaneously to internalize a given type of NPs. Thus, the ultrastructural morphology of nascent endocytic intermediates were further analyzed to know the specific endocytosis pathway(s) involved in the uptake of 100 nm polystyrene NPs. It appears that different numbers of polystyrene NPs were partially surrounded by plasma membranes invaginations or protrusions forming distinct ultrastructures around the surface of BMDM. These distinct ultrastructures are not seems to be a simple NPs attachment to surface of the cell membrane because we could not observe such NPs containing cell membrane structures throughout the cell membrane surface but localized in particular places. Indeed, by having a closer look at the membrane surface, the coat structures of holding the polystyrene NPs are also observable in some routes (Fig. 20A). Similarly, it has been also documented that the ultrastructural morphology of membrane invaginations and protrusions provides basic criteria for the identification of different endocytic pathways involved in the internalization processes [90,91,134]. Based on such plasma membrane morphology, our TEM results showed that the polystyrene NPs are internalized by BMDMs via multiple endocytic routes simultaneously

(Fig. 20A-E). These include the ultrastructure in Fig. 20B, the cell surface membrane deformations forming cup-like structures by trying to encircle the polystyrene NPs suggests early process of phagocytosis. Similarly, the ultrastrucure in Fig. 20E, plasma membrane protrusions or ruffles that collapse onto and fuse with the plasma membrane by trying to generate large endocytic vesicles indicates macropinocytosis route. The structure in Fig. 20A, a membrane invagination forming a more or less homogenous, symmetric polygonal lattice, shows early clathrin-dependent endocytosis processes. Moreover, Fig. 20D, a typical smooth flask-shaped morphological structure suggests an early caveolin-dependent endocytosis process. Fig. 20C distinct ultrastructures demonstrate other clathrin- and caveolin-independent pathways, routes that are characterized by polymorphous or tubulovesicular membrane invaginations in several entry pathways. Overall, the TEM ultrastructural analyses results shows BMDMs internalizes 100 nm polystyrene NPs via multiple endocytic routes simultaneously.

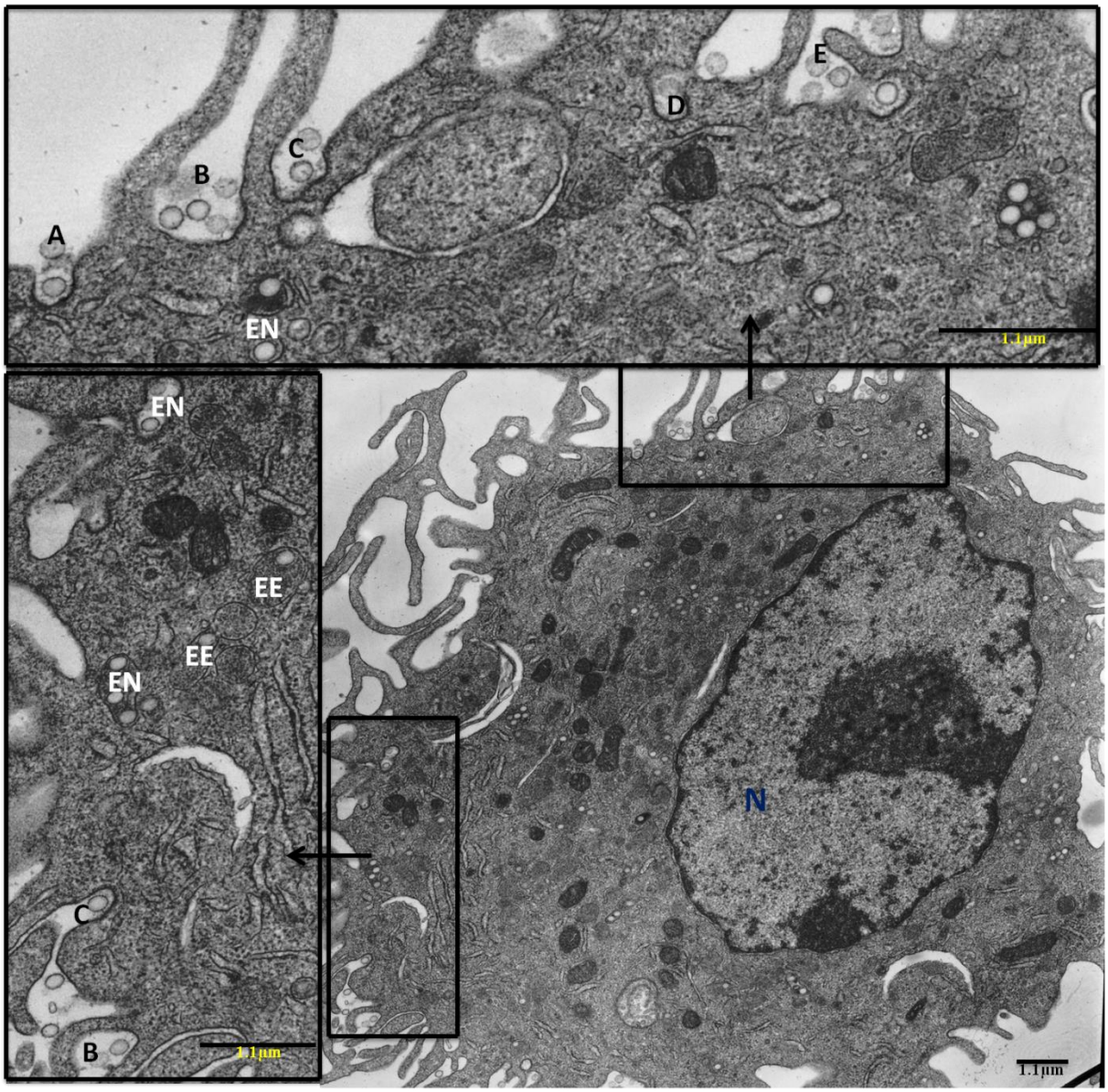

Fig. 20. *Multiple endocytic pathways used simultaneously by BMDMs for uptake of 100 nm polystyrene NPs. Based on the ultrastructural morphology of plasma membrane invaginations/protrusions, clathrin-mediated endocytosis (A), phagocytosis (B), clathrin- and caveolae-independent endocytotic pathways (C), caveolae-mediated endocytosis (D), and macropinocytosis (E) are indicated. Intracellular vesicles containing the endocytosed NPs (EN), localization of the NPs in early endosomes (EL) and the nucleus (N) are also shown. Labeled structures (A-E) are the zoomed out portions of the depicted cell for clarity.*

4.2.4 The ultrastructural morphology of endosomes reveals multiple cellular uptake pathways

The criteria for defining specific endocytic pathways are not yet completely identified. However, it has been suggested that the ultrastructural morphology of endosomes containing NPs may reveal the type of endocytosis involved in the uptake of a given type of NPs[88,135]. To further support our observation of multiple uptake pathways based on the ultrastructural morphology of nascent endocytic intermediates at the plasma membrane, the size and morphology of the endosomes containing NP(s) were analyzed. The result showed that the size and morphology of endosomes containing NPs seems to be correlated with the size and morphology of nascent endocytic intermediates at the plasma membrane (Fig. 21). For instance, the morphology of endosomes formed by clathrin- and caveolin-independent uptake pathways seem to maintain the tubulovesicular structure of the nascent endocytic intermediates at the plasma membrane (Fig. 21E and F). Similarly, the morphology of endosomes formed by caveolae-dependent endocytosis seems to conserve the well-defined flask shape of nascent endocytic intermediates (Fig. 21D). Larger endosomes (Fig. 21B) are associated with macropinocytosis/phagocytosis rather than other smaller size pathways like caveolae- or clathrin-dependent endocytosis. Since the larger size endosomes were observed only after 30 min incubation time, it is less likely that the larger size endosome are as a result of fusion of different endosomes. Furthermore, we also observed endosomes having similar morphology or size but contains different number of NPs (Figure 21E and F). This may suggest that the morphology and size of the endosomes containing the NPs is not necessarily adopted in accordance to the number of NPs they may contain. It suggests that the morphology of each endosome varies not only based on the number of NPs they contained but also the type of uptake routes. This may further suggest that the distinct ultrastructural morphology of nascent endocytic intermediates corresponds to the distinct uptake routes.

Thus, the ultrastructural morphology of endocytic vesicles containing NPs may give a clue about the uptake mechanism of NPs. Consequently, it further supports the notion that BMDM use multiple internalization pathways for 100 nm polystyrene NP(s).

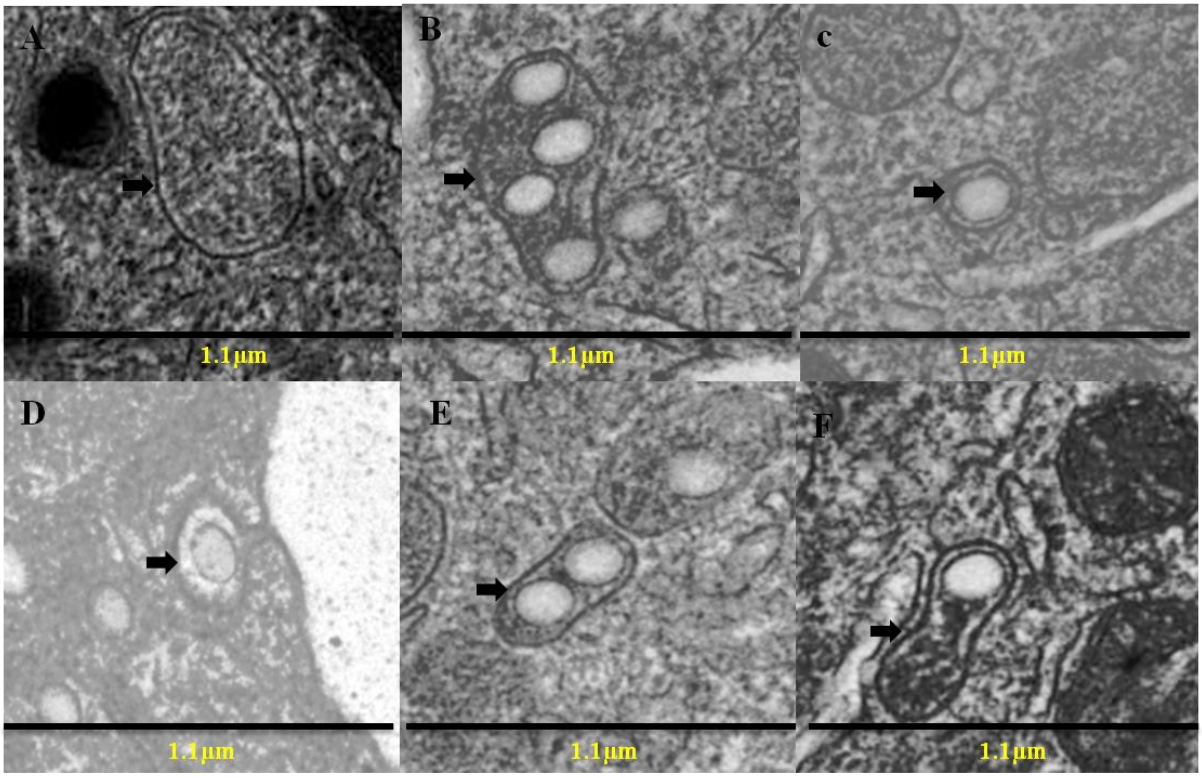

Fig. 21. *Multiple uptake pathways based on ultrastructural morphology of endocytic vesicles. The endosomes contains 100 nm polystyrene NP(s) immediately after their internalization by BMDMs. The cells were fixed for TEM after 30 min of incubation with NPs. The arrows indicate endosomes from NPs untreated cell (A), phagosomes or macropinosomes from NPs treated cell (B), endosomes of clathrin-mediated endocytosis from NPs treated cell (C), endosomes of caveolae-mediated endocytosis from NPs treated cell (D) and endosomes of clathrin-and caveolae-independent endocytotic pathways from NPs treated cell (E and F).*

4.2.5 Analysis of functionally distinct uptake routes by using inhibitors to block different endocytic pathways

To complement the TEM ultrastructural studies of distinct endocytosis pathways involved in the cellular uptake of polystyrene NPs, pharmacological inhibitors of various endocytic processes were employed. We used safe drug concentrations described in previous

studies[97,99,136,137] in order to be sure that the endocytosis inhibitions are due to the pharmacological effect of the inhibitors rather than their toxicity against the host cell. The cytotoxicity of the selected drug concentrations were further tested with BMDMs by using the alamarBue® cell viability assay. The safe concentrations of the inhibitors with relatively high inhibition rates in our system were then used for blocking studies. The inhibitors used include wortmannin (12.85 μg/ml), a potent inhibitor of phosphatidylinositol kinase (PI3K) involved in different endocytic pathways but commonly used as inhibitor of phagocytosis and macropinocytosis[135,138,139], cytochalasin D (5 μg/ml) which blocks the actin polymerization that participates in a variety of endocytic processes but is commonly used as inhibitor of phagocytosis and macropinocytosis[88], dynasore (25.8 μg/ml), a cell-permeable small molecule that inhibits dynamin GTPase activity needed for several mechanisms including clathrin-dependent endocytosis[140,141], chlorpromazine hydrochloride (10 μg/ml) that inhibits a Rho GTPase which is essential for the formation of clathrin-coated vesicles in clathrin-dependent endocytosis[88,136] and ikarugamycin (1 μM), an inhibitor of clathrin coated pit-mediated endocytosis[137]. The BMDMs, L929 fibroblasts, and 293T epithelial cells were cultured and exposed to 100 nm NPs in the same manner as in the TEM study described above except that the cells were pre-incubated with each of the five inhibitors for 30 min at 37°C. The uptake was measured by flow cytometry after 3 h of incubation in order to keep a balance between allowing sufficient time for enough NPs to enter the cells, and for the pharmacological inhibitors to reduce endocytosis without inducing a shift of the pathways. It has been reported previously that blocking one uptake pathway can result in activation of other endocytic mechanisms[142]. The results were then documented as relative uptake (percentage) based on MFI of inhibitor treated cells compared to untreated control cells by setting the average MFI of control cells without inhibitors as 100% (Fig. 22).

The results show that wortmannin inhibited as much as 93.7%, 70.4% and 55.3% of NP uptake in BMDMs, L929 fibroblasts and 293T kidney epithelial cells, respectively. Even though wortmannin is not as specific as other inhibitors, it showed the involvement of phagocytosis and/or macropinocytosis in the uptake of the NPs by all three cell types. Similarly, blocking actin formation by cytochalasin D reduced the NP uptake by 74.3% in BMDMs, 55% in L929 fibroblasts and 50.8% in 293T kidney epithelial cells. Blocking actin formation would inhibit macropinocytosis and phagocytosis. However, it has also been reported to participate in several other uptake mechanisms including clathrin-mediated endocytosis and caveolin-mediated endocytosis[88,143]. Therefore, we consider cytochalasin D as nonselective inhibitor of different internalization pathways, but it can point out the existence of macropinocytosis and/or phagocytosis pathways in this scenario again. Chlorpromazine, a drug considered to block clathrin-dependent endocytosis, inhibited the NP uptake by 77.3% in BMDMs while it only inhibited 47.5% and 42% in L929 fibroblasts and 293T kidney epithelial cells, respectively. However, since the Rho-family GTPases are also involved in other pathways – such as phagocytosis and macropinocytosis[93] – chlorpromazine cannot be regarded as specific either[136]. Nevertheless, it may similarly show the involvement of clathrin-dependent endocytosis. Furthermore, using ikarugamycin, the specific inhibitor of clathrin-coated pit-mediated endocytosis resulted in a 50%, 30% and 57.4% inhibition of NP uptake in BMDMs, L929 fibroblasts and 293T kidney epithelial cells, respectively, highlighting the involvement of clathrin-dependent endocytosis in these cell types. Finally, inhibiting dynamin-dependent endocytic pathways including clathrin-dependent endocytosis and caveolin-mediated endocytosis by dynasore reduced the NP uptake by similar rates in all the three cell types (44%, 44.5% and 45% in BMDM, L929 fibroblasts and 293T kidney epithelial cells, respectively). It also suggests that the remaining 55-56% of the NP uptake were via dynamin-independent pathways indicating that all the three cell types can use both

dynamin-dependent and dynamin-independent endocytic pathways for the uptake of the NPs. Even though it has been shown that the specificity of pharmacological inhibitors is not sufficient to clearly distinguish endocytic pathways[136], the findings support the TEM results regarding the existence and utilization of several distinct endocytic pathways by the three cell types for internalization of NPs.

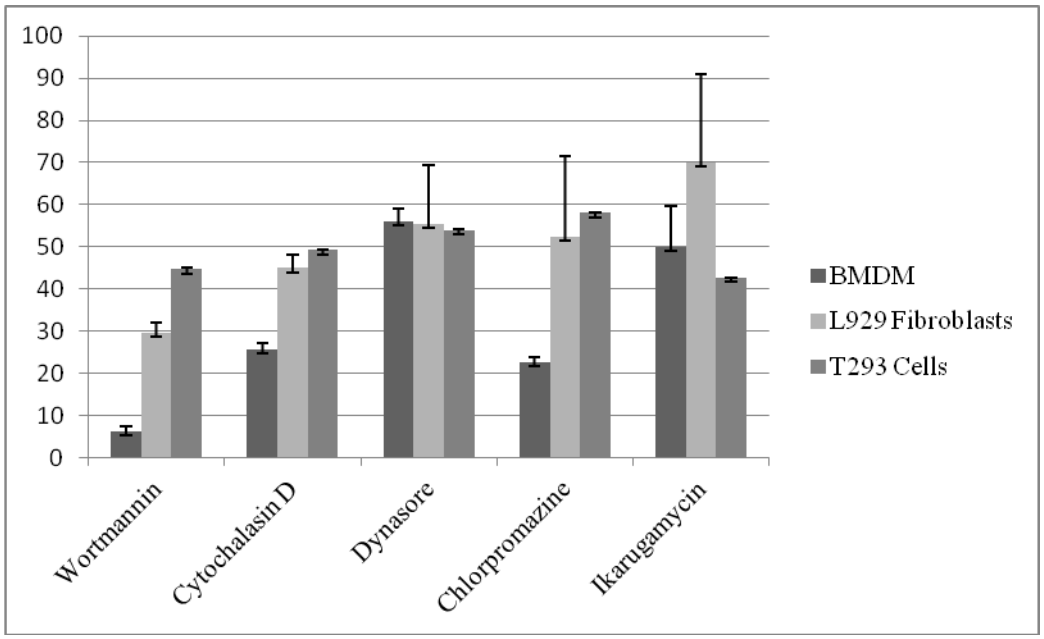

Fig. 22. *Effects of different pharmacological inhibitors on the uptake of 100 nm polystyrene NPs by different cell types (BMDMs, L929 fibroblasts or 293T epithelial cells) after 3 h of incubation. The MFI values of NPs inside the cells were quantified by flow cytometry in the presence or absence of each inhibitor. The average MFI of control cells without any inhibitor were set as 100% for normalization purpose and easy comparison. Normalized MFI values and standard errors of 3 to 6 independent experiments are shown.*

We used Alexa 448-labeled transferrin (2.5 µg/ml) as positive control for clathrin-dependent endocytosis in the same manner for 100 nm polystyrene NPs in BMDMs, L929 fibroblasts and 293T epithelial cells. As expected, the flow cytometry results show that chlorpromazine efficiently blocked the uptake of transferrin in all the three cell types, and cytochalasin D affected the uptake of the transferrin in BMDMs while other inhibitor even increased the uptake of transferrin (Fig. 23). The results validates the specificity of the

pharmacological inhibitors used to characterize multiple endoctotic pathways used by cells to uptake 100 nm polystyrene NPs.

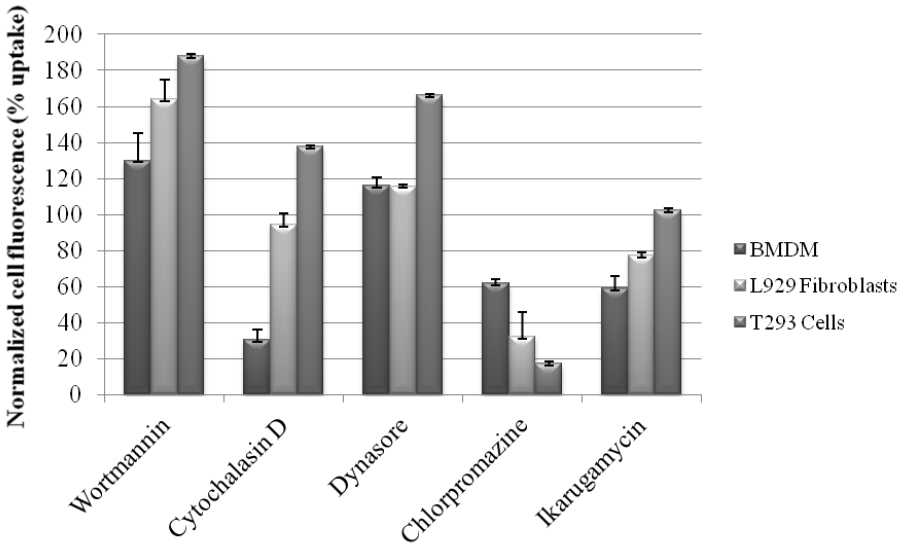

Fig. 23: *Effects of different pharmacological inhibitors on the uptake of Alexa-448-labeled transferrin by different cell types (BMDMs, L929 fibroblasts or 293T epithelial cells) after 3 h of incubation. The MFI of cells treated with Alexa-448-labeled transferrin was set as 100% for clarity in each cell types. The result shows that chlorpromazine efficiently blocked the uptake of transferrin in all the three cell types, while other inhibitor had less effect or even increased the uptake of transferrin. The figure is the summary of three independent experiments with their respective SE.*

4.2.6 Effect of cell types on uptake mechanisms of polystyrene NPs

The uptake mechanisms and pathways of NPs in different cells are not fully known. To investigate polystyrene NPs uptake potentials of BMDM, L929 mouse fibroblasts and 293T epithelial cells, each cell types were cultured and treated with 20 nm polystyrene NPs under equivalent cell culture conditions. Regardless of the differences in their biological properties, such as size and doubling times, all the cell types were treated with the same batch and doses of polystyrene NPs. After incubation for various time points, the uptake potential of polystyrene NPs by each cell types was quantified by flow cytometry. At 24 h of incubation, BMDM had taken up 100 or 5.5 fold more NPs than 293T epithelial cells or L929 fibroblasts,

respectively (Fig. 24). The experiments were also performed using fluorescence microscopy and similar results were observed for each cell type (data not shown), suggesting that the capacity to take up polystyrene NPs significantly differs among different cell types. In order to investigate the uptake kinetics, the uptake rate of NPs was measured at different time points. The results revealed that BMDM take up 33.8, 60.9 or 64 times higher numbers of NPs than 293T epithelial cells at 30 min, 2 h or 4 h incubation periods, respectively (Fig. 24**)**. Compared to L929 fibroblasts, BMDM take up 1.9, 4.7 or 5 times more NPs at 30 min, 2 h and 4 h, respectively (Fig. 24**)**. Even though the kinetics of the uptake varies between the cell types throughout the incubation period, the relative uptake differences were significant at all considered time points. Taken together, the results show that BMDMs take up 20 nm polystyrene NPs much higher than 293T epithelial cells and L929 fibroblasts at all considered time points.

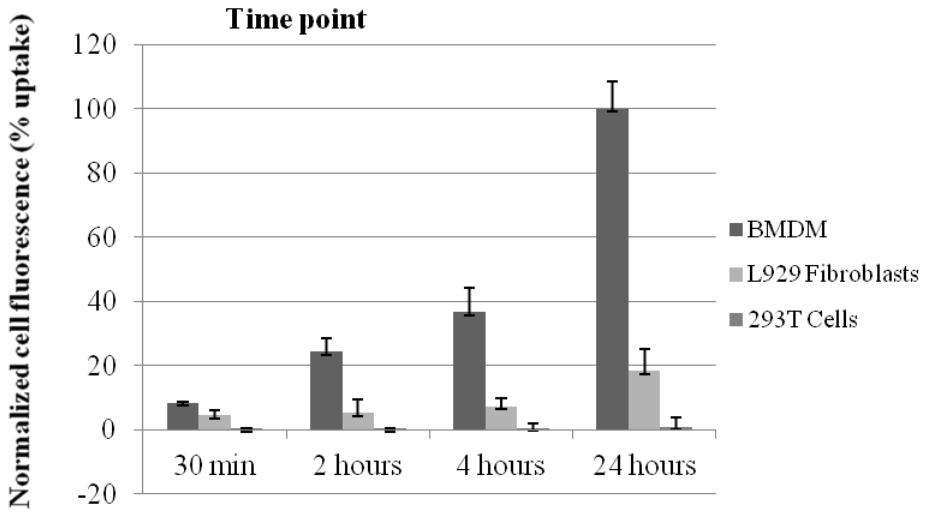

Fig. 24. *A summary of relative uptake levels of 20 nm polystyrene NPs by BMDMs, L929 fibroblasts or 293T epithelial cells. At all considered time points, the flow cytometric analyses showed clear differences in the relative uptake of NPs by the three cell types, being highest in macrophages and lowest in epithelial cells. The results are from three independent experiments and the values are presented as mean values ± SE. Normalization was done based on MFI from flow cytometry data.*

4.2.7 Effect of size on the uptake mechanisms of NPs

Various sizes of polystyrene NPs (200 nm, 500 nm, 1 μm and 2 μm) were used to study whether or not the size of NPs influences the uptake of NPs by BMDM, L929and 293T. Accordingly, cells were cultured and treated with the various sizes of NPs under the same cell culture conditions. The polystyrene NPs uptake potential of the three cell types at different time points were then quantified by flow cytometry. Normalization was done by setting the highest MFI of cells at 18 h as 100% for each NPs size to facilitate easy comparisons. The result showed that the MFI of polystyrene NPs increases according to their size in all the three cell types (Fig. 25). Nonetheless, flow cytometry result showed that the relative uptake efficiency of 293T and L929 are much higher for larger size NPs than smaller size as compared to BMDM (Fig. 25). Conversely, relative NPs uptake efficiency of BMDMs is higher for smaller sizes polystyrene NPs (≤500 nm) than larger sizes (>500 nm) as compared to the two other cell types. This finding suggests that the particle uptake by the three cell types might not follow commonly defined size limits.

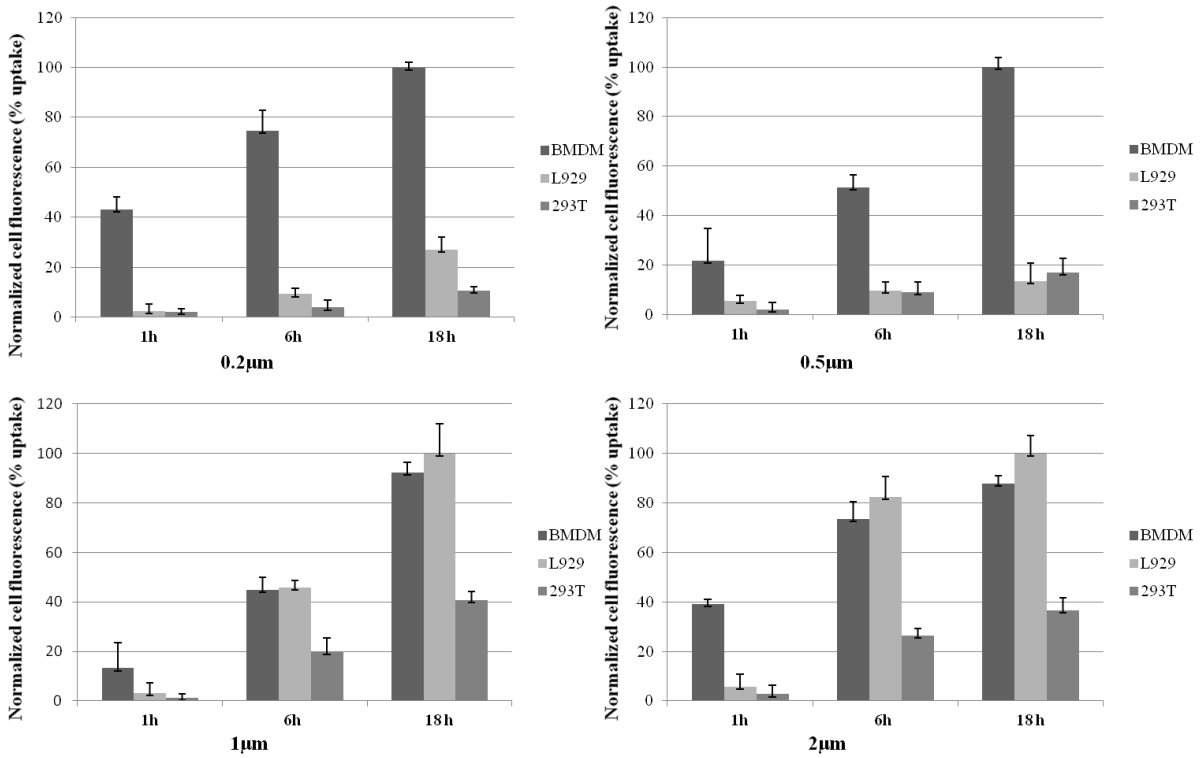

Fig. 25. *The summary of relative uptake kinetics of 0.2 µm, 0.5 µm, 1 µm and 2 µm polystyrene NPs by 293T epithelial cells, L929 fibroblasts and BMDMs at 1 h, 6h or 18 h incubation times. The data were quantified by flow cytometry and the results are the summary of three independent experiments.*

To further confirm the above observation, we conducted confocal microscopy study to see the relative polystyrene NPs uptake variation among the three cell types for the different sizes (0.2 µm, 1 µm and 2 µm). The confocal microscopy results clearly supported the notion that L929 and 293T cells show relatively better uptake tendency towards larger size particles (>500 nm) than smaller sizes (≤500 nm) particles (Fig. 26A-C) as compared to BMDMs. This suggests that the smaller the particle size, the higher the relative uptake potential of BMDMs as compared to L929 and 293T cells. Regardless of the particles' sizes, longer incubation period were accompanied by higher uptake (MFI) in all the three cells types. In general, our data showed that the internalization extent and kinetics of NPs uptake varies based on particles' sizes and cell types.

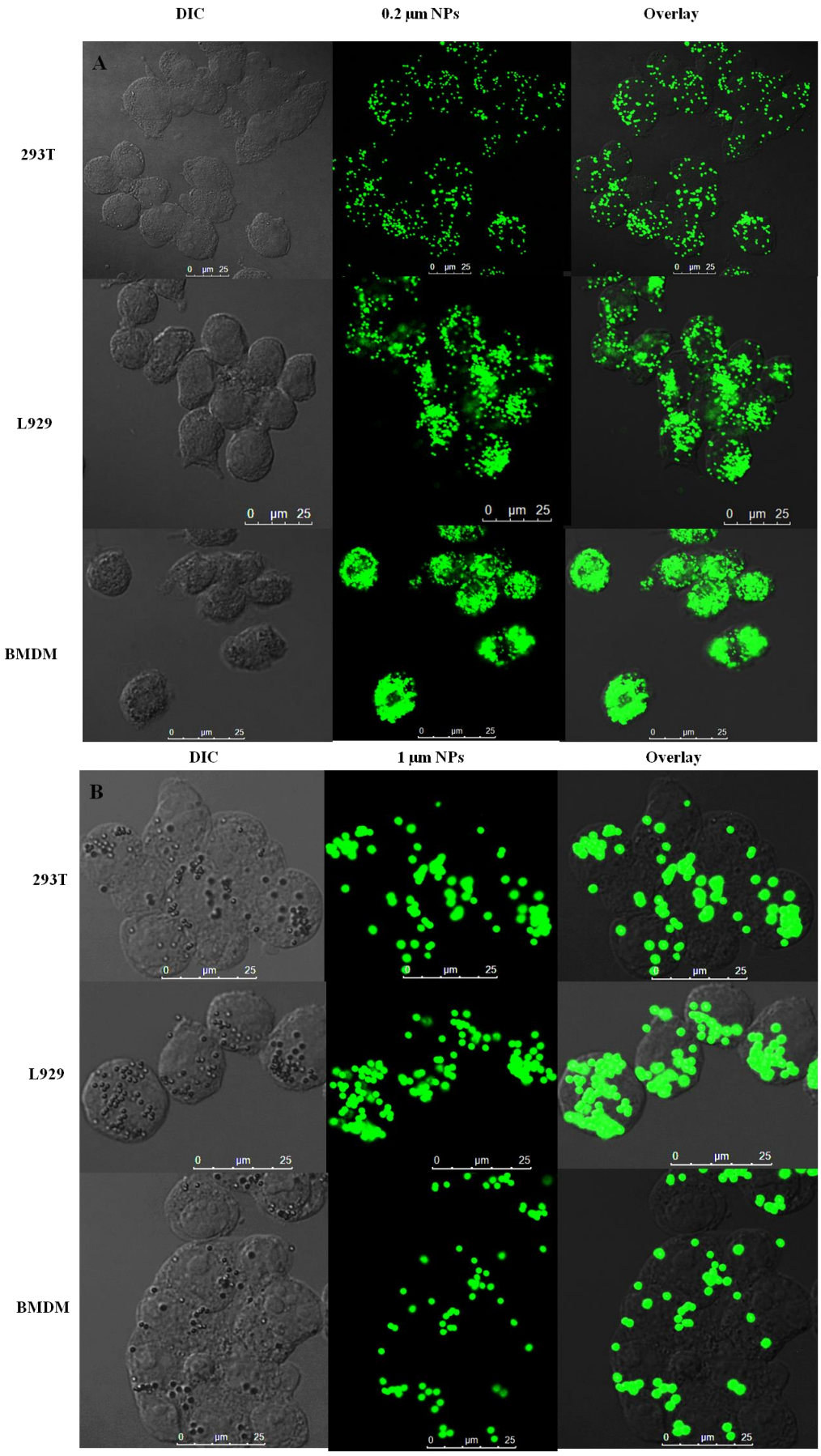
DIC
0.2 µm NPs
Overlay
A
293T
L929
BMDM
0 µm 25
DIC
1 µm NPs
Overlay
B
293T
L929
BMDM
0 µm 25

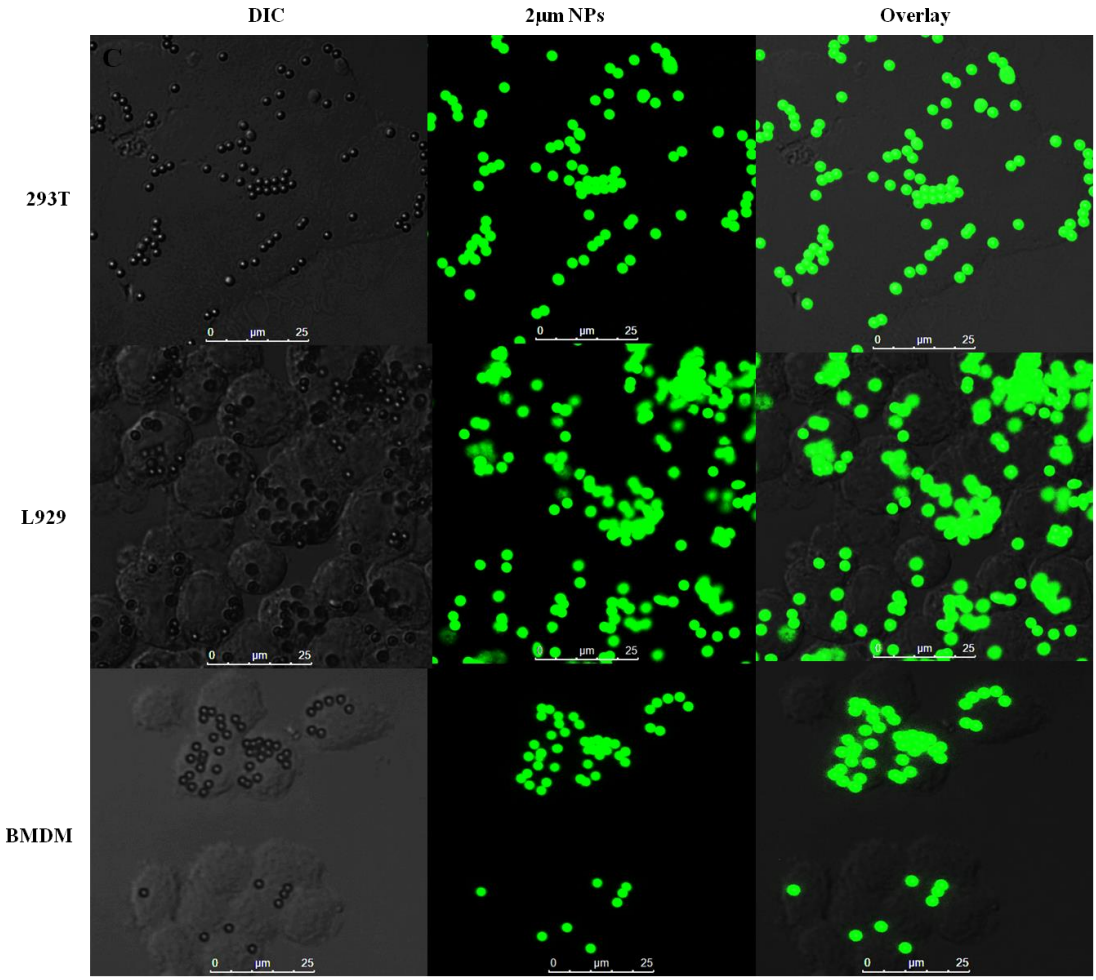

Fig. 26: *Representative confocal microscopy pictures showing the relative NPs uptake potential of 293T, L929 and BMDM cells. The figure shows uptake of 0.2 µm polystyrene NPs (A), 1 µm (B) and 2 µm (C) at 18 h time point. The result indicates that BMDM have relative better uptake tendency for smaller size particles than larger sizes; whereas L929 and 293T cells shows higher relative uptake for larger particle sizes than smaller sizes.*

4.2.8 Effect of Leishmania parasite infection on NPs uptake potential of macrophages

L. major is an obligate intracellular protozoan parasite that causes infection in host macrophages and causes CL. *Leishmania* parasites have developed sophisticated strategies to manipulate the host macrophage responses to establish successful infection and ensure their own survival by triggering several pathways[21,23]. Particularly, it has been shown that macrophage endocytosis capacity is controlled by stimulatory and inhibitory processes[144]. For

instances, some intracellular pathogens overcome host innate immunity by impairing macrophages' endocytosis mechanisms. Moreover, stimulatory molecules like CpG ODN have shown to enhance phagocytic activity of macrophages. We therefore hypothesized that infection of macrophages by *L. major* may negatively influence their NPs uptake potential and consequently affect the application of NPs in drug delivery systems against leishmaniasis. To test this hypothesis, BMDMs were generated, infected with *L. major* for 12 h and exposed to NPs for 24 h at 37°C. We then measured polystyrene NPs uptake potential of the infected BMDMs comparing to non-infected ones. The results from this study showed that the uptakes of NPs by BMDMs were decreased by at least 1.83 fold (from 38.8% to 21.2%) when infected with *L. major* (Fig. 27). The decreased uptake of NPs by *L. major*-infected macrophages may be associated with the pathogenesis of the infection that may suppress physiology of BMDMs.

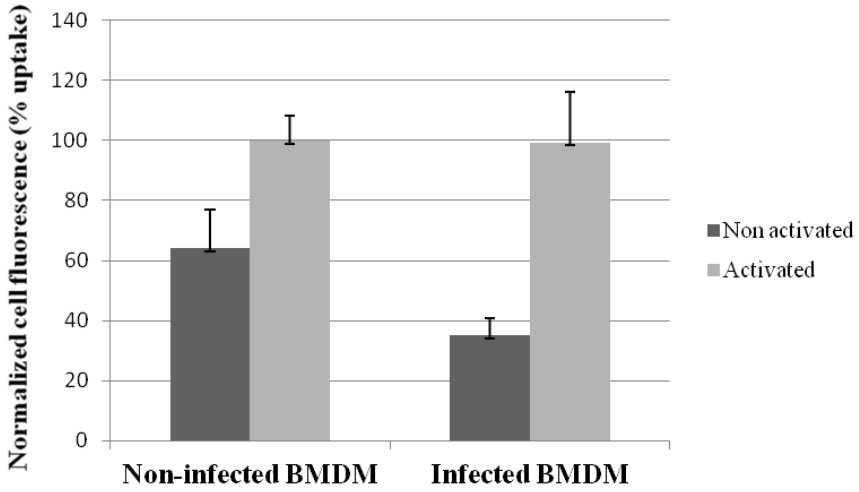

Fig. 27*. Flow cytometric data showing the effect of L. major infection and cell activation status on cellular uptake of 20 nm NPs by BMDMs. The infection significantly reduced the uptake potential of BMDMs while activation by CpG ODN rescued it. The values are given as mean ± SE from three independent experiments. Normalization was done by setting MFI of activated BMDM as 100% for clarity.*

To further investigate whether the reduction in NPs uptake potential of macrophages after *L. major* infection was time dependent or not, the uptake of 0.02 µm polystyrene NPs by BMDM were measured at various time points. At all considered time points, infection of BMDMs with *L. major* resulted in significant decreases of internalization potential of the cells, indicating that the parasite has an inhibitory effect on ability of macrophages to uptake NPs (Fig. 28). We explored whether activation of *L. major*-infected macrophages by CpG ODN may rescue the decrease in the uptake potential of infected macrophages. The BMDMs were either pre-incubated with CpG ODN (25 µg/ml) or solvent control for 30 min. Then, the BMDMs were incubated with the same doses and batch of NPs for 24 h. The flow cytometry data showed that the NP-uptake potential of *L. major*-infected BMDM could be restored by activating them with CpG ODN.

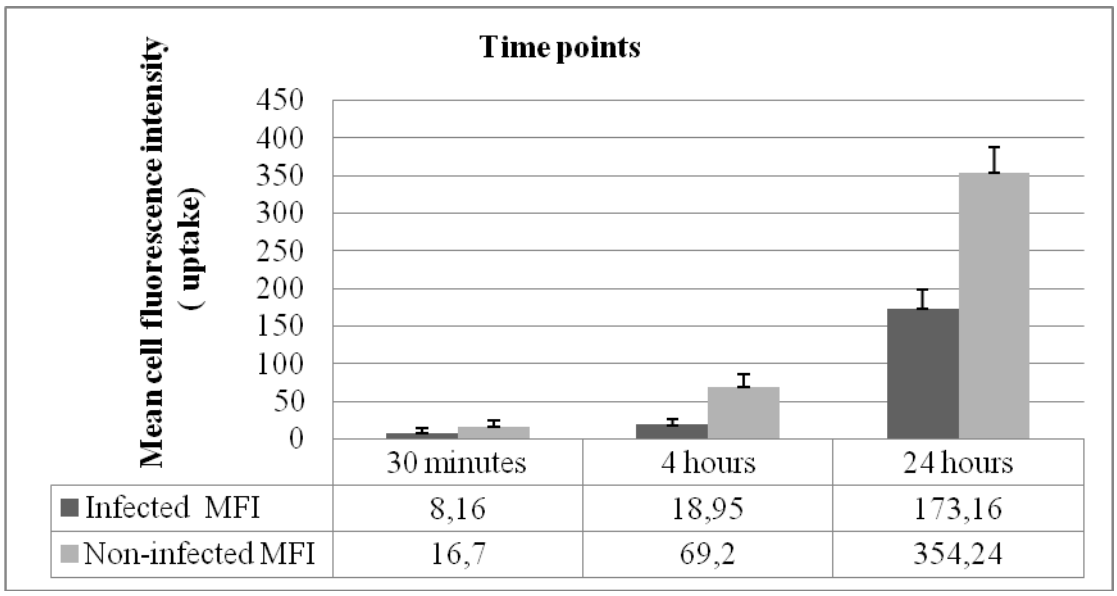

***Fig. 28**: Flow cytometric data showing the effect of L. major infection on the potential of BMDMs to take up 20 nm NPs at different time points. This data shows that the accumulations of NPs inside non-infected BMDMs are higher than the corresponding infected BMDMs at all considered time points. The values are the summary of three independent experiments.*

4.2.9 Intracellular trafficking of polystyrene NPs in BMDMs

Endocytosis is an active cellular process by which living cells uptake nutrient, pathogen or other foreign materials. It also regulates various processes initiated at the cell surface to control all aspects of intercellular communications. These include signaling, immune surveillance, antigen-presentation, and cellular and organismal homeostasis in metazoans. As mentioned before (in Figs. 16, 20 and 21), we confirmed that polystyrene NPs are localized in endocytic vesicles (endosomes) immediately after their internalization. It was therefore important to analyze how the NPs are trafficking inside BMDMs after internalizations. The TEM result (above Fig. 20 and indicated by EE) shows that polystyrene NPs are localized in ultrastructural vesicles suggestive of early endosomes as early as 30 min. Moreover, it indicates that at 30 min time of incubation, only few NPs are transported to early endosomes. To further follow their trafficking inside BMDMs, lysotracker red was used. The dye has high selectivity for acidic pH and is commonly used as a marker for late endosomes/lysosomes[41]. We employed this dye to study whether internalized NPs are further transited through the endolysosomal pathway for attempt to degradation. Upon incubating BMDMs with NPs at 37°C for 6 h, we observed robust co-localizations of NPs with lysostracker red, indicating their accumulation in late endosomes/lysosomes (Fig. 29). The data suggest that the final cellular localization of the NPs is in late endosomes/lysosomes. To further complement our observation, we incubated BMDMs with NPs for 6 h and performed TEM analysis. As can be seen in Fig. 29 (indicated as PL), the results suggest that the final cellular localization of the NPs is in structures suggestive of late endosomes/lysosomes. The NPs distribution inside BMDMs demonstrate that they are exclusively localized in the cytoplasm but not in nuclei, indicating the failure to transit across the nuclear envelope (Fig. 29, also shown earlier in Fig. 20).

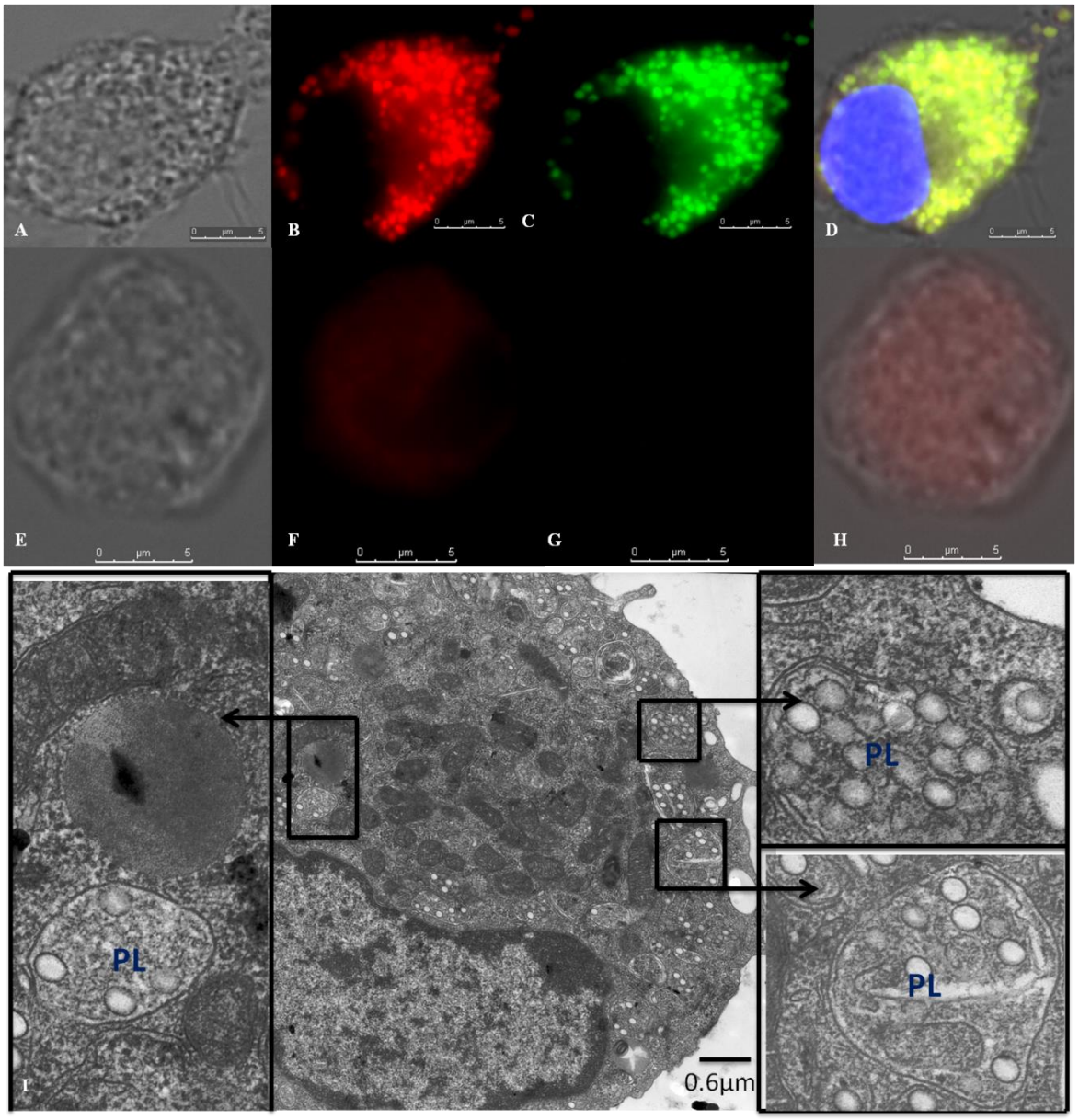

Fig. 29: *Fluorescence microscopy and TEM images of BMDMs showing localizations of the NPs in late endosomes/lysosomes or phagolysosomes after 6 h of incubation. The fluorescent images indicate bright field (A), lysotracker red (B), 100 nm polystyrene NPs (C), overlay including channel for DNA counterstained with Hoechst (D) and their respective channel of NP-untreated control cells (E-H). The TEM image (I) shows localization of the NPs in late endosomes or phago(endo)lysosomes (PL). Scale bars = 5 µm (fluorescence images) or 0.6 µm (TEM images).*

The co-localizations of lysotracker red with NPs also indicated that the particles resided in an acidic compartment (Fig. 29). Lysotracker red is considered to stain vesicles with an acid dissociation constant (pK_a) of less than 5.2[12]. The localization of NPs in acidic

organelles was further validated by lysosensor blue. According to the supplier's information, this dye is almost non-fluorescent except when inside acidic compartments and used to measure pH of vesicles inside cells. The concentrations of dyes were kept as low as possible (5 μM) to reduce potential artifacts from overloading. The results showed that lysosensor blue co-localized with NPs after 6 h of incubation, confirming their localization in acidic pH (Fig. 30). The pK_a of lysosensor blue is ~5.1. Thus, we conclude that the NPs are localized in acidic intracellular vesicles during their trafficking in the endolysosomal cascade of BMDMs. Even though the mechanisms by which internalized particles can escape from endolysosome degradation are complex and not yet fully understood[13], their pH level was found to be in the acidic range. As a result, the changes in pH may be considered as a trigger to activate controlled drug release inside the cytoplasm.

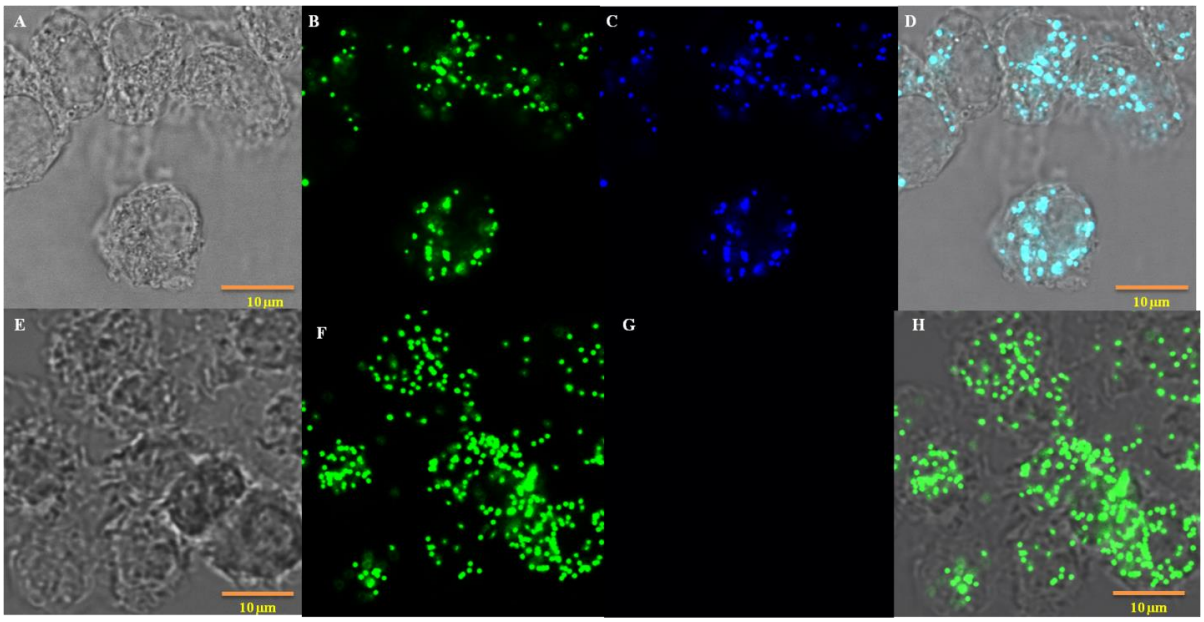

Fig. 30*. Confocal microscopy images of BMDMs showing the colocalizations of 100 nm polystyrene NPs with lysosensor blue staining intracellular acidic pH vesicles. The images indicate bright field (A), green fluorescent polystyrene NPs (B), lysosensor blue (C), overlay (D) and their respective channels for control cells without lysosensor blue (E-H) at 6 h of incubation. The depicted pictures are representatives of two independent experiments.*

4.3 Chapter three: Pathogen- and host-directed PHMB polyplex therapy for CL

One of the recent efforts in addressing the challenges of traditional chemotherapy relies on exploring advanced drug delivery systems. As well as improved drug delivery systems, the host immunity also plays a decisive role for the successful treatments of CL. Thus, a combination therapy comprising of chemotherapy and immune modulators that able to activate host immune systems are of great importance. However, efficient delivery of nucleic acid-based immune modulators into host cells is a key challenge. Enclosing these immune modulators within a polymer could overcome the delivery challenges by improving passage across physiological or cell barriers. Moreover, such formulation could stabilize immune modulatory oligomers against degradation and aid wound repair. In this arsenal, in addition to its potent antileishmanial activity, we showed that PHMB binds the genomic DNA of *L. major* parasites forming PHMB/gDNA complex structures. Similarly, it has also been reported that PHMB can be used as siRNA transfection vehicle in hybrid form with iron oxide[145]. Moreover, CpG ODN have potential applications both as adjuvants and nonspecific immune modulators by triggering innate immunity against intracellular *L. major*[146]. Therefore, we hypothesized that PHMB could be used as carrier of CpG ODN for innovative drug delivery system-based host- and pathogen-directed combination therapy against CL. To test this hypothesis, a range of PHMB/CpG ODN polyplex formulations were prepared and characterized, and their bioactivities were evaluated and compared to the free components (PHMB or CpG ODN alone).

Primarily, before evaluating the potential use of PHMB as a safe and effective carrier for CpG ODN, we first wanted to confirm whether PHMB binds CpG ODN to form stable nanostructures. Following addition of an excess PHMB to CpG ODN, we observed an instant reaction that converted colorless PHMB and CpG ODN in solution to a temporal milk color, suggesting interaction of PHMB and CpG ODN (Fig. 31a). To complements this observation,

we performed EMSA experiments. The results showed that PHMB forms polyplexes with CpG ODN at relative weight ratios of ≥ 0.25 as confirmed by retarded electrophoretic mobility of CpG ODN in 1% agarose gel (Fig. 31b). To clearly show the retention of CpG ODN in the wells, the same CpG ODN sequence but labeled with rhodamine red at 3' termini (CpG-R) were purchased and the EMSA experiments were repeated. The results clearly confirmed that there is retarded electrophoretic mobility and retention of CpG ODN in the wells containing the polyplexes as compared to the free components (Fig. 31 e and f), confirming polyplex formation between PHMB and CpG ODN.

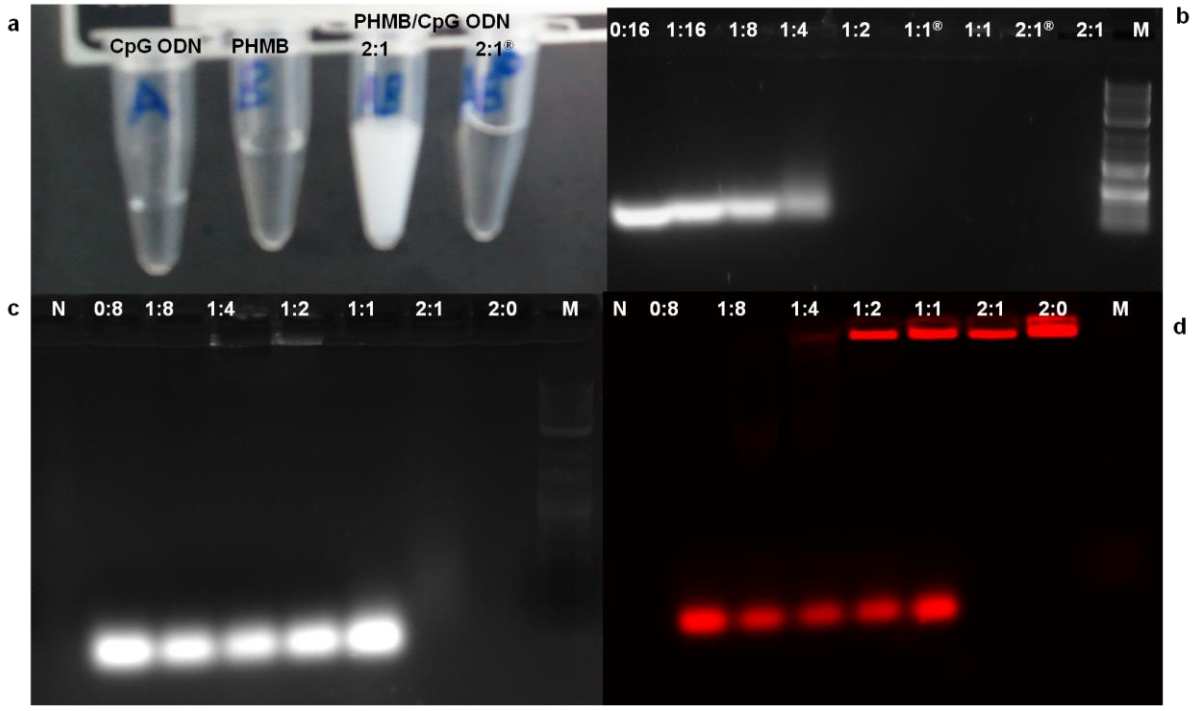

***Fig. 31**. PHMB/CpG ODN interactions and their physicochemical characterization. Formation of PHMB/CpG ODN polyplexes were confirmed by EMSA in 1% agarose gel. The figure shows color change during PHMB/CpG ODN complexation (a), PHMB/CpG ODN polyplexes (b), PHMB/CpG-R polyplexes (c) and the same gel (c) with fluorescence measurement of CpG-R (d). With the exceptions of negative control and PHMB alone, all wells contained equal amounts (weight) of CpG ODN with various concentrations of PHMB. M represents 2-Log DNA ladder (0.1-10.0 kb, New England Biolabs) and N represents water for negative control. All indicated PHMB/CpG ODN ratios are in relative weight (w/w). ®Indicates two month old PHMB/CpG ODN polyplexes.*

To further characterize the particle size and zeta potential of the polyplexes formed between PHMB and CpG ODN, dynamic light scattering (DLS) and electrophoretic light scattering (ELS) were applied. Two formulations of the polyplexes were prepared by mixing PHMB to CpG ODN at relative weight ratio of 2:1 and 1:1, and stabilized by incubating them at room temperature for at least 20 min before measurement. The results showed that the polyplexes have highly reproducible sizes of 310.9 ± 30.5 nm and 285.3 ± 15.0 nm at relative weight ratio of 2:1 and 1:1, respectively (Fig. 32a and b), confirming that PHMB spontaneously bound CpG ODN and formed stable nanopolyplexes. The polydispersity index (PDI) values of the nanopolyplexes were shown to be less than 0.3, indicating a narrow size distribution or their monodispersity (Table 4).

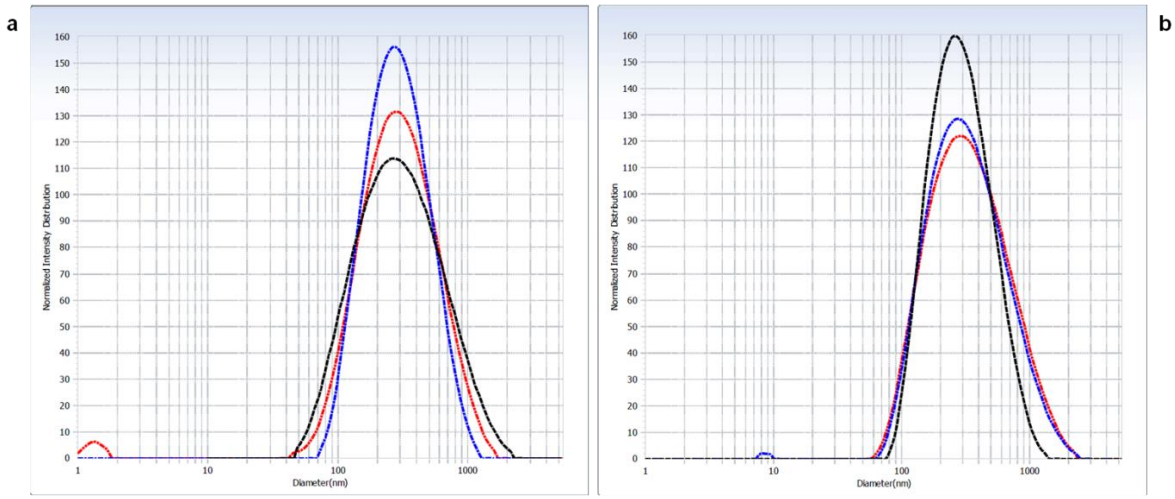

Fig. 32*. A representative intensity distribution curves for particle size determination of PHMB/CpG ODN nanopolyplexes. The figures show intensity distribution curves of PHMB/CpG ODN measured by using DLS at a relative weight ratios of 2:1(a) and 1:1(b) in Millipore water. Each line color represents a single measurement.*

Ratio	**Particle size (nm)**	**PDI**
2:1	310.9 ± 30.5	0.222 ± 0.04
1:1	285.3 ± 15.0	0.260 ± 0.02

Table 4. *Physicochemical characterization of PHMB/CpG ODN nanopolyplexes. The table shows particle size determination by using DLS with their polydispersity index (PDI). The table shows result summary of three independent experiments for each ratio used with ±SE.*

Moreover, to predict the long-term stability of the polyplexes between PHMB and CpG ODN, their zeta potential was measured by ELS. The summary of three independent experiments showed that the zeta potential was determined to be +33.3 ± 1.1 mV (ratio 2:1) and -18.77 ± 0.4 mV(ratio 1:1), and dependant on the ratio of PHMB/CpG ODN (Fig. 33a and b).

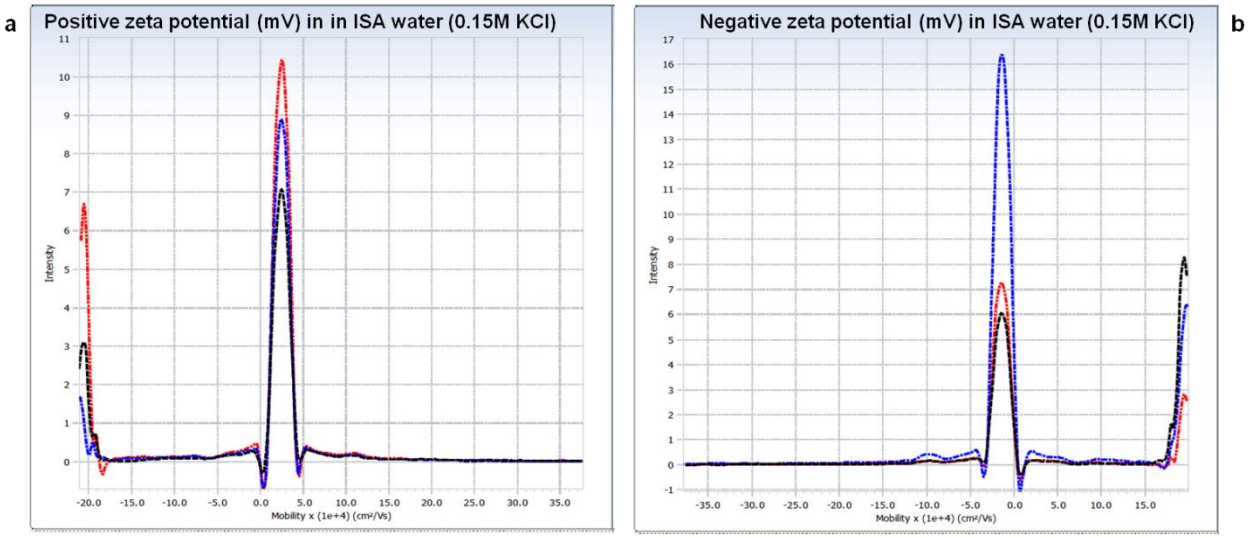

Fig. 33. *Zeta potentail determination of PHMB/CpG ODN nanopolyplexes. The figures show representative examples of intensity mobility curves of PHMB/CpG ODN measured by ELS at a relative weight ratios of 2:1(a) and 1:1(b) in ISA water, showing positive and negative zeta potentials, respectively. Each line color represents a single measurement.*

To further evaluate stability of the nanopolyplexes between PHMB and CpG ODN, the polyplexes were prepared at 2:1 ratio and kept in a refrigerator (4°C) for two months before their physicochemical nature were again characterized by TEM and EMSA. The EMSA results confirmed an excellent stability of the complexes formed between PHMB and CpG ODN (Fig. 31b indicated by ®). Likewise, the TEM results showed that the polyplexes had an excellent stability. In addition, the TEM results suggest that the nanopolyplexes had a nanometer sizes and predominantly spherical morphology rather than cylindrical or rod forms (Fig. 34).

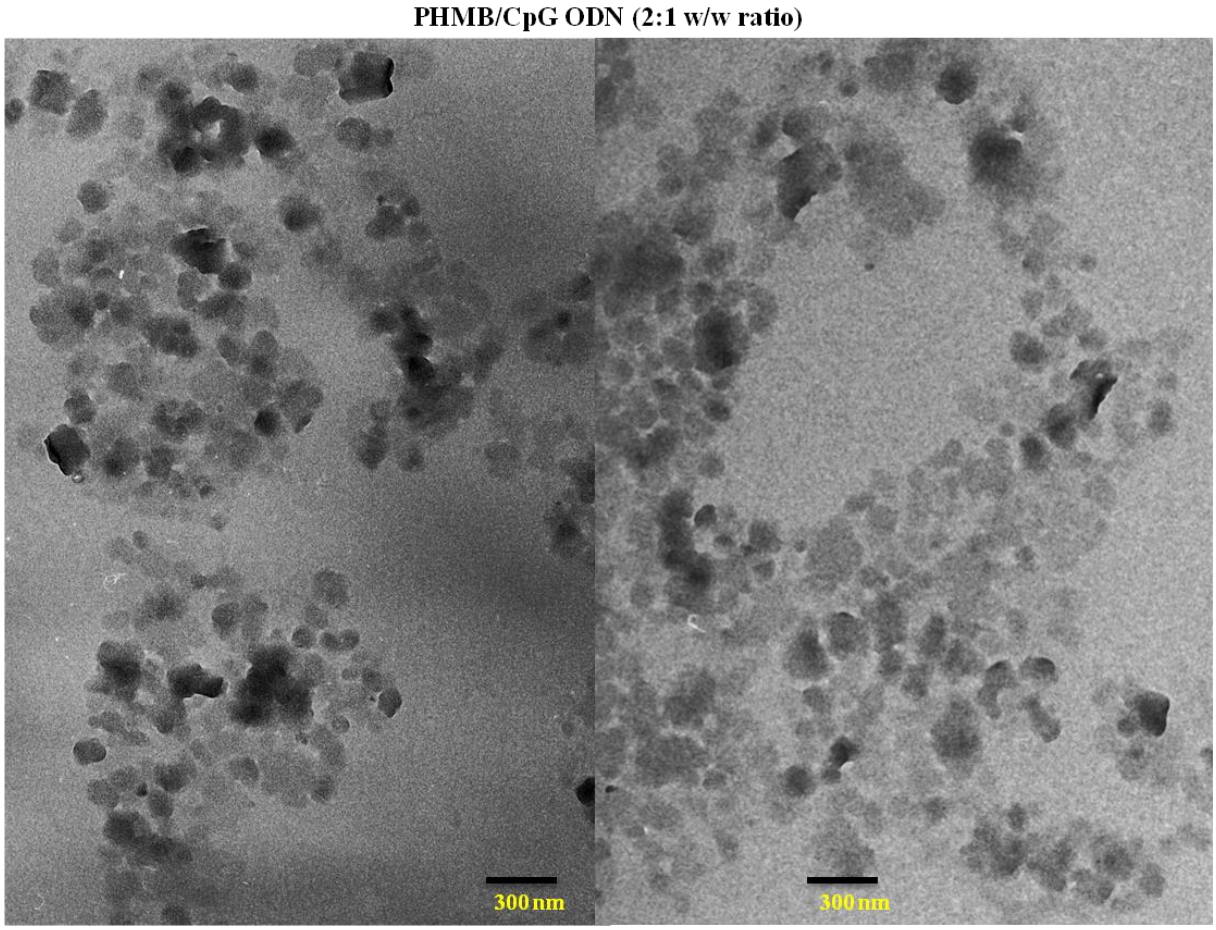

Fig. 34. *Stability and morphology characterization of PHMB/CpG ODN polyplexes by TEM. Two representative TEM pictures showing the stability and spherical morphology of the nanopolyplexes. The polyplexes was prepared and kept at 4°C for two months before the TEM images were taken.*

To quantify the stability and specificity of the interaction between the PHMB and CpG ODN, we used ITC. ITC directly measures the heat generated or absorbed when molecules interact and provides a total picture of binding energetics. The ITC results show that PHMB can strongly bind CpG ODN with sequential binding. The detailed thermodynamic parameters include first binding affinity *(K1=* 2.04E6 ± 3.75E5 M^{-1}*)*, second binding affinity *(K2*=2.62E4 ± 8.0E3 M^{-1}) and third binding affinity *(K3*=2.64E6 ± 1.2E6 M^{-1}) to form polyplexes. The corresponding enthalpy changes *(ΔH)* for each binding affinity include –1.83 ± 0.43 kcal/mol, 16.47 ± 5.19 kcal/mol and –16.71 ± 5.18 kcal/mol, respectively. *ΔH* represents measure of the energy content of the bonds broken and created. The values are

indication of changes in hydrogen and van der Waals bonding. Negative value indicates enthalpy change favoring the binding. Moreover, the respective entropy changes *(ΔS)* for each binding affinity include -32.7 cal/mol/deg, 573 cal/mol/deg and -531 cal/mol/deg, respectively. *ΔS* is positive for entropically driven reactions. Taken together, the detailed thermodynamic parameters confirmed that there is strong interaction between PHMB and CpG ODN that can lead to formation of stable nanopolyplex (Fig. 35)

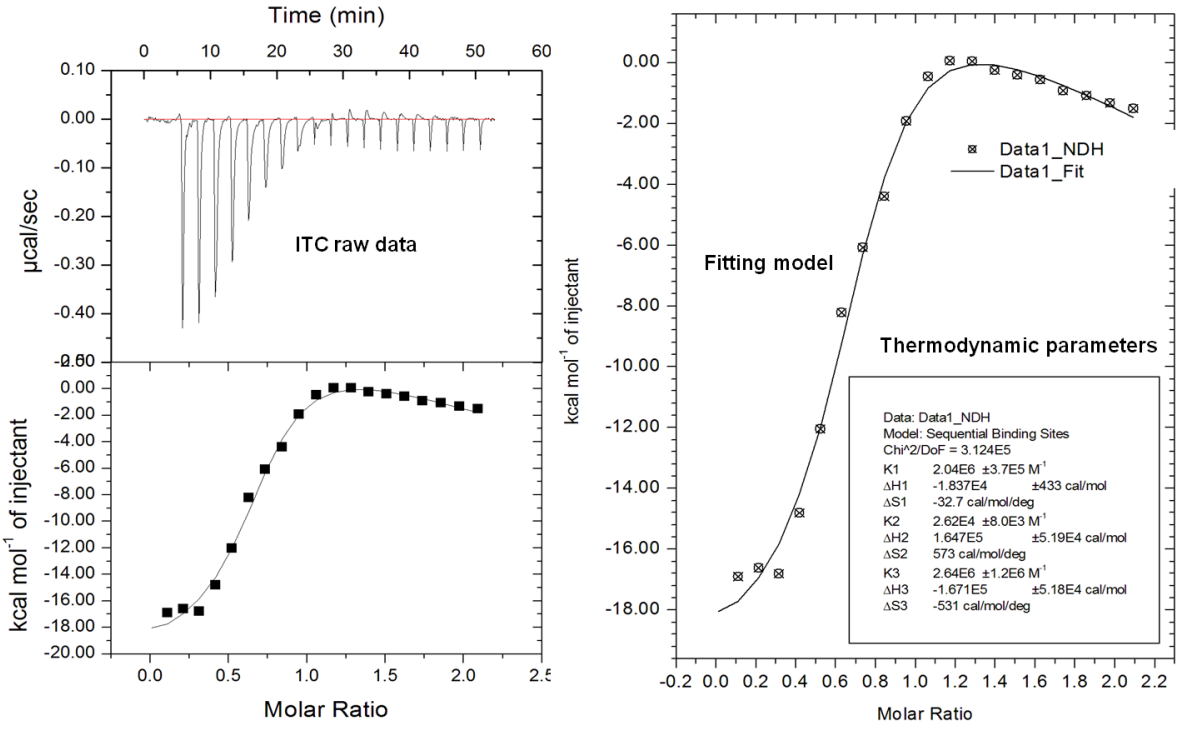

Fig. 35*. Physicochemical characterization of PHMB/CpG ODN nanopolyplexes by ITC. The figures show quantitative measurements of the strength of interaction between CpG ODN and PHMB at 2:1 relative weight ratio. Its corresponding thermodynamic parameters such as binding affinity (K_a), enthalpy changes (ΔH) and entropy changes (ΔS) were shown. The deviation is a result of the fitted curve obtained and the figure is a representative of three independent experiments.*

Furthermore, we investigated immune modulation property of the nanopolyplexes as compared to free CpG ODN or PHMB. We assessed whether the polyplex formation process during formulations positively or negatively affects the immunomodulatory properties of CpG ODN. To this end, the concentrations of several key cytokines were measured by ELISA from

supernatants of co-cultured BMDMs. The results showed that the cytokine productions by BMDMs for the nanopolyplxes and the free component (CpG ODN and PHMB) were increased by increasing their doses (Fig. 36). We were not able to obtain reliable measures for IL-4 and TNF-α in cells treated with the nanopolyplexes or the free components (data not shown). We also observed that PHMB itself stimulated the production of proinflammatory cytokines by activating macrophages (Fig. 36), further supporting its use as therapeutical agent against *Leishmania* infections. It has been consistently shown that the most commonly used antileishmanial drugs have immunomodulatory properties, and activate macrophages and dendritic cells to remove the parasites from the host cells. It has also been shown that PHMB does not induce significant production of TNF-α, IL-1α and the transcription factor nuclear factor kappa B (NF-κB) which can cause either apoptosis or stimulate the growth of transformed cells[147]. Moreover, based on the concentrations of IL-6, IL-12 and IL-10 observed, the nanopolyplexes showed higher or comparable immune stimulation capacity as compared to free CpG ODN (Fig. 36).

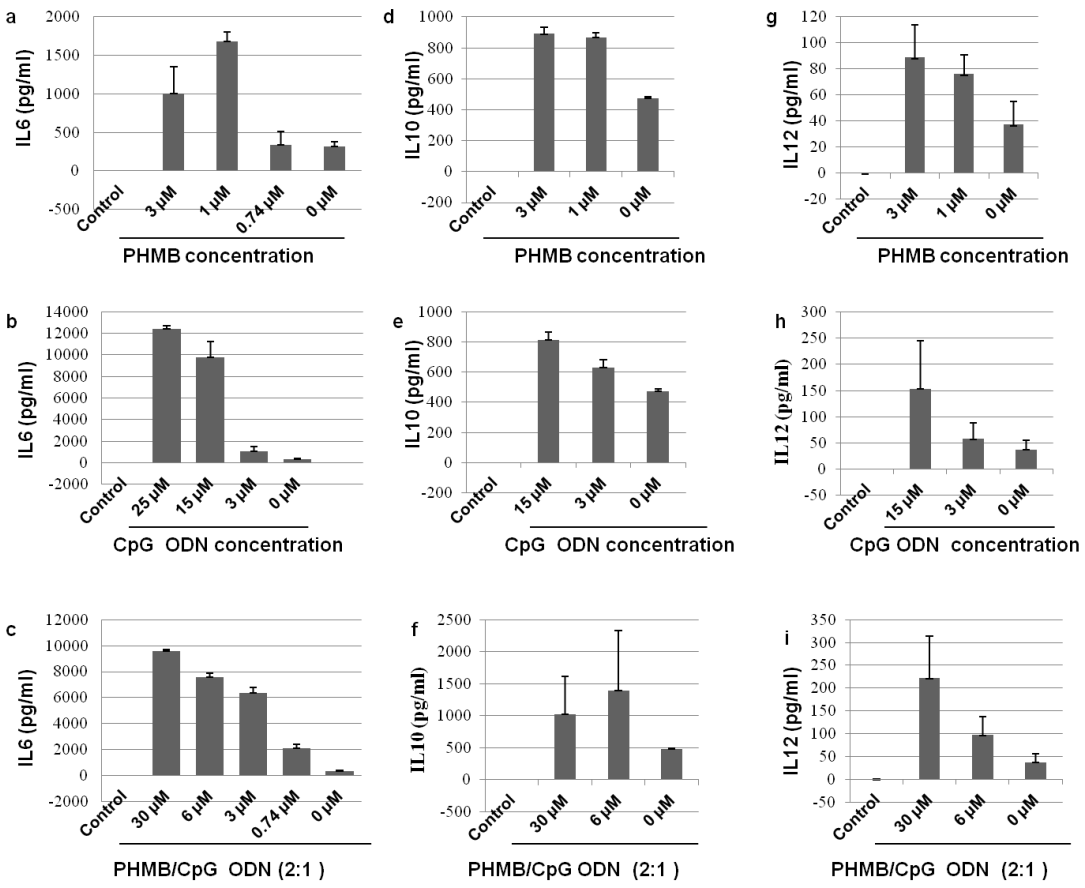

Fig. 36. *Effects of PHMB/CpG ODN polyplex formation process on cytokines production of BMDMs as compared to its free components. The bar graphs show the level of IL-6 (a-c), IL-10 (d-f) and IL-12 (g-i) production after PHMB, CpG ODN or PHMB/CpG ODN polyplex was added to BMDMs that were pre-activated with CpG ODN (1.5 μg/ml) for 30 min and further incubated for 48 h. Controls show cytokines level for non-activated BMDM. The concentrations shown for the polyplexes represent the dose of PHMB and the concentrations of CpG ODN are half of the indicated doses. The error bars show standard error of three independent experiments.*

Finally, we tested the potential to use PHMB with CpG ODN as host- and pathogen-directed combination therapy against CL. This was done by measuring the nanopolyplexes' cellular uptake efficiency, cytotoxicity and antiparasitic efficacy as compared to the free components. To know the uptake efficiency of the nanopolyplexes, flow cytometry analyses were performed. As previous depicted (in Figs. 9b and 11), our results showed that BMDMs take up the nanopolyplexes in time dependent manner. The uptake efficiency of CpG-R in the

polyplex form was enhanced by about 15 fold relative to the free form; while the uptake of PHMB-FITC as a polyplex was not enhanced, confirming that PHMB can deliver CpG ODN into macrophages. Because PHMB and CpG ODN incorporation into polyplex particles may quench the mean fluorescence of PHMB-FITC or CpG-R, the uptake measurements may underestimate the delivery potential. We next tested out if the polyplex formation process reduced the toxicity associated with PHMB or CpG ODN. PHMB has an excellent safety record topically and is widely used as preservative, an antimicrobial and antiseptic agent in clinics, homes and industry for many years worldwide. Nevertheless, as expected for a cationic polymer, cell toxicity was observed at high concentrations. Very recently, the safety of PHMB has been thoroughly reviewed by the Scientific Committee on Consumer Safety of the European Commission. Acute toxicity assessment was reported between 500 to 1000 mg/kg body weight and a NOAEL of 54 mg/kg body weight from a dietary 12-months study in beagle dogs characterized by liver impairment, histopathological findings in the skin and liver among others[148]. In female rats, the systemic toxicity values have been reported to be 1-2000 mg/kg[148]. We hypothesized that PHMB toxicity may be effectively counteracted when interacting with negatively charged CpG ODN. To test this hypothesis, different polyplex formulations of various PHMB to CpG ODN ratios were prepared and tested against BMDMs and 293T epithelial cells. Surprisingly, the results demonstrated that toxicity of PHMB/CpG ODN polyplexes showed a much higher IC_{50} value than PHMB alone against BMDM and 293T epithelial cells (Table 2). Moreover, our results indicated that relative toxicity of PHMB/CpG ODN polyplexes increases with increasing the ratio of PHMB to CpG ODN (Table 2). This finding was further supported by zeta potential determination, and the results similarly showed that the higher the ratio of PHMB to CpG ODN, the more relative zeta potential of the polyplexes (Fig. 33a and b). The cationic nature of polymers (higher positive zeta potential) is typically associated with toxicity against host cells and decationizing is

expected to reduce toxicity[149]. Therefore, our results suggest that polyplex formation process considerably reduces the toxicity of PHMB. Taken together, we speculate that the toxicity properties of PHMB can be further improved by complexation/shielding of its positive charges with CpG ODN.

We next designed an appropriate *in vitro* assay to determine the combined leishmanicidal efficacy of PHMB and CpG ODNA in polyplex and free forms. The IC_{50} values against intracellular amastigotes were determined using BMDMs infected with the luciferase-transgenic *L. major* strain. As previously shown (in Table 1), the polyplexes enhanced antileishmanial activity against intracellular amastigotes while increasing selectivity by many fold. Whereas, the cytotoxicity of the polyplexes against *L. major* promastigotes showed relatively lower efficacy as compared to free PHMB. At the concentration used, CpG ODN alone did not show antileishmanial activity and host cell cytotoxicity activities. In drug development for leishmaniasis, amastigotes are the most important clinical stage of the parasites. Our results generally show that the nanopolyplex therapy against CL is not only improves the uptake of CpG ODN and cytoxicity of PHMB against host cells, it also significantly enhance antileishmanial effect of PHMB. Moreover, our findings suggest that the components of the polyplexes are bioactive after delivery into BMDMs and PHMB releases the CpG ODN from the nanopolyplexes inside BMDMs for overall synergistic effect against CL. In summary, our data suggest that PHMB is an effective nucleic acid entry-promoting vehicle and best synergistic combination therapy with CpG ODN against CL by improving delivery to host cells as wells as targeting both the host immunity and *Leishmania* parasites.

5. DISCUSSION

5.1 Discovery of PHMB as novel antileishmanial agent

Leishmaniasis therapy remains very challenging and relies on only a few chemotherapeutic agents that lack appropriate efficacy, safety and affordability. This situation emphasizes the need for new, effective, affordable and noninvasive treatment options that overcome shortcomings in the present arsenal of CL treatments. In line with these need, we studied the use of PHMB as a potential antileshmanial compond. Our data demonstrate for the first time that PHMB is a potent antileishmanial candidate drug for topical applications against CL. Our results indicated that PHMB is more potent than the current standard antileishmanial drugs *in vitro.* From a clinical point of view, PHMB is one of the most promising substances available today for local treatment of wound[150]. Moreover, PHMB is a very inexpensive compound (about $10-50/kg) that has been widely used in clinics, homes and industry as a disinfectant and antiseptic for over 50 years worldwide[117–119,151], suggesting its affordability in developing world where CL burden is commonly seen. The antileishmanial effects of PHMB here are twofold: it directly kills the parasites that cause the lesions as well as accelerates wound closure and improvement of the cosmetic outcome of CL by preventing secondary bacterial and/or fungal infections. Superinfection commonly causes delay in wound healing in ulcerative CL patients[152]. For topical applications, PHMB shows an excellent safety record[116,153]. There is no evidence for development of resistance against several bacteria[116]. It is also used for clinical treatment of Acanthamoeba keratitis patients[120,121]. A clinical trial results from 100 women diagnosed with human papilloma virus (HPV) infection also shows that the topic treatment with PHMB is a safe and promising approach, and it may avoid the use of invasive treatments[154]. Thus, PHMB could be potentially used as effective topical drug against CL.

Encouraged by the potency of PHMB against *L. major* promastigotes, we wanted to understand PHMB's mode of action. Our results showed that PHMB permeabilized parasite membranes. Moreover, the results revealed that PHMB selectively condenses or damages parasite chromosomes through differential nuclear access as compared to the host cell chromosomes. Recently, it has been similarly shown that PHMB is taken up and kills diverse bacterial species through chromosomal condensation (Chindera et al., submitted). Consistent with our observation of the membrane disruption, PHMB's antimicrobial effect has been associated with its specific interaction with acidic phospholipids in microbial membranes, resulting in possibly forming pores and their disruption, while the neutral phospholipids in human cell membranes are only marginally affected[118,129]. Moreover, PHMB's bactericidal action was also associated with its strong and cooperative interactions with nucleic acids *in vitro*[130]. Nonetheless, lack of any resistance development to the polymer despite many years of use in wide varieties of fields may also indicate its multiple and complex mechanisms of action[118]. Thus, our findings help to explain how PHMB provides a potent broad-spectrum antimicrobial biocide against diverse microbes.

In our attempts to understand how PHMB selectively act on parasites' chromosomes without affecting the DNA of the mammalian host cells, we investigated its uptake mechanism and intracellular trafficking in BMDM. We showed that PHMB or its polyplexes are predominantly taken up by macrophages via dynamin-dependent endocytosis in a time-dependent manner. It then exclusively localized in the cytoplasm without entering the nuclei of mammalian cells, indicating failure to transit across the nuclear envelope. However, there is no apparent exclusion of PHMB from the nuclei of the parasites, indicating its host/pathogen selectivity. Taken together, we described for the first time how mammalian cells internalize PHMB for its broad spectrum intracellular antimicrobial activity and selectivity against the host cells.

In concussion, given its very reasonable cost and long history of safe topical use, PHMB may be repositioned as drug against CL following appropriate *in vivo* experiments and clinical trials.

5.2 Understanding the interactions between NPs and host cells

The use of nanotechnology in every field of science is rapidly spreading. Particularly in medicine, the applications of nanotechnology improve diagnosis and therapy of diseases through effective delivery of drugs, biopharmaceutical molecules and imaging agents to target cells or tissues at disease sites[41,42,155]. For such applications, initial recognition of NPs by the immune system is essentially determinant for the fate and distribution of materials inside the body[100]. Thus, a better understanding of how cells take up NPs may lead to the development of enhanced antigen-, drug- or other molecules- delivery tools. In this scenario, we tried to elucidate the internalization mechanisms of various size commercially available polystyrene NPs by different mammalian host cells and to explore the factors affecting their uptake. Our results show that as many as 95% of NPs are generally taken up via an energy-dependent process at all considered time points in BMDMs. Although lowering the culture temperature affects both an active and a passive mode of entry (diffusion), it has been demonstrated previously that diffusion is not the rate-limiting step for NPs uptake into cells. Thus, blocking uptake pathways by drugs leads to inhibition of active transport, rather than a reduced NPs diffusion[156]. This finding is in accordance with studies from other group which showed that cellular uptake of NPs is predominantly mediated by endocytosis[88,98]. In contrast, it has also been reported that NPs are taken up via non-endocytic pathways. For instance, Mu et al. suggested a passive mode of entry after observing NPs inside cells at 4°C[157]. We also observed about 5% uptake in cells kept at 4°C at different time points. However, the status of the cells before exposure to NPs may have some influence for such uptake at 4°C. Because

the cells might have limited energy from pre-incubation at 37°C that may be exhaustively used for such active cellular processes during the early period of incubation at 4°C. Indeed, we observed a decrease in uptake at 4°C when we increased the pre-incubation on ice from 10 min to 30 min before exposing the cells to the NPs. Altogether; we conclude that NP uptake is predominantly achieved by endocytic processes in an energy- and time-dependent manner.

The cellular uptake mechanism of NPs is influenced by multiple factors[158], among which the physicochemical properties of NPs are considered to be the main determinants of the import and subsequent intracellular trafficking of the NPs. Particle size and charge is likely the primary factor that governs endocytic uptake of particles. Our *in vitro* cellular uptake experimental results indicated that the relative uptake efficiency of 293T and L929 increases with sizes of NPs as compared to the BMDM. On the contrary, relative NPs uptake efficiency of BMDMs is higher for smaller sizes polystyrene NPs as compared to 293T and L929 cell types. Many groups have showed that cellular uptake of NPs is size dependent and is significantly faster for smaller particles than larger particles in antigen-presenting cells[159,160]. However, the non-professional phagocytes like epithelial cells uptake smaller NPs more efficiently than large particle size[161,162]. Interestingly, in line with our finding, it has also been shown that cells non-specialized for phagocytosis were able to internalize as large as 2 µm NPs[96]. Our result suggests that the particle uptake might not follow commonly defined size limits for uptake processes by different cells. The difference of our findings from the others might be resulted from the approaches we followed. Many size dependent uptake studies simply compare the uptake efficiency of different size NPs by measuring the percentage of uptake by particular cell type without first considering the differences in fluorescence intensity among the different NP sizes themselves. However, we compared the relative uptake potential of the three cell types for particular particle size at a time so as to

insure that the variations in MFI among the cells types are resulted from the difference in uptake potentials rather than fluorescence intensity deviations among the different NP sizes.

Moreover, it has been shown that increasing surface charges of NPs (positive or negative) have been shown to increase particle uptake in comparison with uncharged ones[163]. It has been also suggested that NPs with positive surface charge are taken up more efficiently than negatively charged NPs[164]. Another important factor is the degree of aggregation and protein corona. The arrival of NPs into the dynamic extracellular environment may change the protein corona, size or aggregation. These change may consequently affects many aspects of NP-cell interactions including mode of particle uptake because the biological identity of a NPs depends on the composition of the surrounding biological medium[165]. It has also been shown that increasing NPs incubation time may induce NPs aggregation and changes in protein corona composition that subsequently determine cellular uptake mechanisms[165]. We further explored cell types as a factor influencing the NPs entry pathways. We showed that the potential to take up NPs is highly different for BMDM, 293T epithelial cells and L929 fibroblasts, being highest for macrophages followed by fibroblasts for 20 nm NPs, indicating variability of uptake kinetics for the same material in different cell types. This finding is in line with a previous report by dos Santos et al. which showed that the uptake of different sizes of NPs varies in different cell lines, being highest in macrophages and lowest in the HeLa cells[96]. The differences in the uptake rates of BMDMs (professional phagocytes) and non-professional phagocytes (293T epithelial cells and L929 fibroblasts) may be due to differences in the number or type of endocytic pathways involved to internalize the NPs. In contrast to 293T epithelial cells and L929 fibroblasts, BMDMs may use multiple uptake routes simultaneously for relatively smaller particle sizes. In summary our data showed that cellular uptake of NPs is influenced by several factors associated with either physiochemical properties of the NPs or its surrounding environments.

Furthermore, we looked whether NPs import is influenced by microbial infection. We demonstrated that infection of BMDMs with *L. major* significantly decreased the cellular uptake of NPs. The effect of *L. major* infection on macrophages has been investigated by many researchers and demonstrated that the parasite can subvert macrophage responses by regulating different genes including those responsible for endocytosis and cell adhesion[21–23]. However, the mechanism(s) by which the parasites subvert macrophages is (are) still remain poorly understood. In our group, it was previously shown that the parasite induces down regulation or upregulation of cytokine and chemokine expression profiles as a mechanism of subversion[166]. It represses the production of inflammatory cytokines (TNF-α, IL-6, IL-12) which are very essential for the survival and multiplication of the parasites inside macrophages[166,167]. Moreover, it has been shown that some intracellular pathogens have inhibitory mechanisms to suppress macrophage physiological functions. Recently, it has been shown that macrophages infection with HIV-1 virus would result in impairment of its phagocytic function[168]. Similar to our findings, Basu et al. have showed a 2-fold decrease in uptake rate in *Leishmanai* infected macrophages through a decrease in endocytosis receptors after infection; whereas recovery of receptor activity and uptake potential were observed after elimination of parasites from macrophages[169]. Thus, these findings suggest that the decreased uptake of NPs by *L. major*-infected macrophages may be associated with a kind of "silencing effect" of the intracellular parasite on BMDMs. We also showed that the activation status of macrophages has a significant effect on their uptake potential. The uptake of NPs was significantly enhanced in CpG ODN-activated macrophages as compared to non-activated control cells. It shows that CpG ODN could rescue the decrease in NPs uptake of BMDMs due to *L. major* infection. These results are also in agreement with the previous findings. Gupta et al. showed that CpG-ODN has a promising efficacy against *L. major in vivo* rodent experiments through activation of host immune responses and consequently, could revert the

effect of the parasite on macrophages[114]. Similarly, it has also been shown that endocytic activity of macrophages is enhanced in response to CpG ODN[170,171]. As a result, the observed effect of CpG-ODN could be either through activation of the macrophages to increase the uptake of the NPs or to kill the intercellular parasite in order to decrease the parasite effect on BMDMs.

The distinct endocytic pathways are highly regulated to control all aspects of intercellular communications and have been associated with many factors[134,172]. However, it has not yet been fully known whether a single cell or cell type uses several uptake pathways simultaneously for a given NPs. As can be clearly seen in our TEM and inhibitor studies results, a cell may utilize multiple endocytic pathways simultaneously to internalize a given type of particles. Interestingly, all these distinct uptake routes were observed in the same BMDM after treating with 100 nm NPs sizes for 30 min, confirming the use of several routes by cells to uptake a given NPs. Our TEM analysis revealed that an uptake pathway that requires a larger size of NPs (phagocytosis or macropinocytosis) may be triggered by a number of smaller particles or their aggregates, approaching a specific area of the plasma membrane giving the uptake signal. This signal most probably controls the type of protein recruitment in the area of initiation and the type of endocytic pathway that should be in place for the uptake of NPs via protein-lipid and protein-protein interactions[92,135,173,174]. The sonication of NPs to generate single particles is very important in such type of studies since the uptake mechanisms for a specific NPs and their aggregate may differ. Even though it is believed that there are several endocytic pathways for uptake of various NPs by a given cell, to our knowledge this is the first evidence based on ultrastructural analysis documenting multiple uptake routes simultaneously to internalize a given type of NPs. Blocking distinct endocytosis pathways by inhibitors corroborated this conclusion. None of the treatments with different inhibitors fully inhibited NPs uptake but some inhibited more strongly in one cell

type than others. For instance, wortmannin, cytochalasin D and chlorpromazine inhibited the NP uptake in BMDMs more strongly than in L929 and 293T cells, suggesting that some pathway might be more sensitive to the inhibitors in one cell type than in the others. In line with our results, a recent study showed that polyelectrolyte multilayer capsules of a few micrometer size are taken up by cells via multiple pathways such as lipid rafts, macropinocytosis or phagocytosis[175]. The authors used larger particle sizes and, consequently, identified larger size uptake pathways such as macropinocytosis and phagocytosis. However, unlike in our study, they could not identify the smaller size uptake pathways like clathrin, caveolin or clathrin- and caveolin-independent uptake pathways. This difference can be explained by the fact that the sizes of the NPs used in this particular experiment for identification of different routes were 0.02 μm or 0.1 μm, while the sizes of the multilayer capsules were in the micrometer range.

Our TEM and co-localization studies further showed that the NPs localize in membrane-bound endosomal vesicles soon after their internalizations and are subsequently trafficked to late endosomes/lysosomes. Different from this finding, Johnston et al. reported that polystyrene NPs are not contained in early endosomes or lysosomes in hepatocytes[176]. On the other hand, many investigators described that the NPs enter a lysosome-associated membrane protein 1 (LAMP-1)-positive lysosomal compartment in macrophages[138,177]. These differences may be explained by the use of different cell types or methodology approaches. Generally, it has been shown that cells internalize NPs by different types of endocytosis, resulting in their accumulation in different endocytic vesicles or tubules after engulfing. NPs are then transported to early endosomes and either transported back to the membrane surface by exocytosis (not very common in NPs), or further transported through late endosomes or multivesicular bodies to lysosomes for attempting to degrade[88,178,179].

In conclusion, the results presented in this study provide a detailed analysis of multiple cellular uptake mechanisms of fluorescent polystyrene NPs and factors affecting their uptake mainly in BMDMs. The data showed that NPs are rapidly internalized and accumulated in endosomal compartments, indicating their ability to entry into different cell types. Once the NPs are internalized by host cells, they localize in endosomes and then traverse to acidic pH vesicles through the endolysosomal pathways. The NPs uptake is an energy-dependent process that highly depends on NPs' sizes, cell types and time. Cells may use several distinct types of endocytosis pathways simultaneously for the uptake of a given type of particles. Even though particles of larger size (a few micrometers) are usually taken up by phagocytosis or micropinocytosis, our findings suggest that smaller NPs are internalized by multiple endocytosis routes including macropinocytosis, phagocytosis, clathrin-mediated endocytosis, caveolae-mediated endocytosis, and clathrin- and caveolae-independent pathways. Our findings highlight the complexity of cell-nanoparticle interactions beyond the previous assumptions, and the need of case-by-case studies to achieve the goal of manipulating NPs to control their entry pathways. Furthermore, physicochemical properties of the NPs have been considered as the main factors determining the cellular uptake and intracellular pathways of NPs. However, our study showed that the type of infection or disease pathogenesis and/or the cell activation status also significantly affects the potential of BMDMs to take up NPs. Since this may consequently determine the application of NPs in biomedical delivery systems, our findings emphasize the need to understand the diseases' pathogenesis in order to establish effective and rationally designed drug delivery systems. These observations may enhance our understanding of the application of nanotechnology in biomedical sciences.

5.3 PHMB nanopolyplex therapy for CL

The prevalence of leishmaniasis is estimated to be 12 million in 98 countries across the globe, of which two-third of the cases are CL presentations[180]. CL is characterized by skin ulcers that carry significant scarring and causes a social stigmatization. Regardless of the enormous efforts made so far, there is still no new commercial drug available, and the existing therapies against CL are far from being satisfactory. Single therapy approach has often resulted in suboptimum clinical efficacies with high risk to benefit ratio, indicating the complex nature of the disease. It has been suggested that multidisciplinary and parallel synergistic approaches are important strategy to sustain the modern practice of medicine[181]. Thus, curative CL therapy may need combinations of multiple strategies including chemotherapy, modulation of host immunity and advanced drug delivery systems. Particularly, combination therapies that simultaneously kill the pathogen and manipulate the host immune system for overall synergistic therapeutic effect would be an ideal therapy for CL patients. Therefore, technologies that enhance delivery and antileishmanial immune responses may improve the overall outcomes of CL treatments. On the other hand, as well as eradication of the intracellular parasites causing the lesions, effective treatment of CL includes wound management caused by the parasites. In these contexts, we investigated PHMB and CpG ODN polyplexes as combined therapy as well as advanced drug delivery systems against CL. We clearly showed that PHMB and CpG ODN form self-assembled nanopolyplexes that are readily taken up by macrophages, increasing the uptake efficiency of CpG ODN and increasing the potency and selectivity of PHMB against *L. major*. This could probably provide potent and synergistic combination therapy for *Leishmania* infections, without the toxicities associated with currently used drugs. Moreover, our results suggest that PHMB could be potentially used as effective non-viral nucleic acid delivery vehicle. In principle, such nanopolyplex formulations are used for sustained long-term release rather than an

immediate quick release, which would also be beneficial for topical dermatological applications and controlling toxicity.

Recently, host-directed treatment strategies were suggested to improve treatment efficacy and outcome, represent feasible alternatives to conventional approaches[182]. It has been suggested that modulation of the immune microenvironment in CL is a potential therapeutic and prophylactic target[183]. Indeed, immune deviation towards Th1 responses by immune modulating agents show promising efficacy against leishmanaisis[114,184,185]. In this scenario, CpG ODN is a potent immune modulator that activates macrophages and dendritic cells to kill intracellular *L. major* parasites[146]. CpG ODN can also accelerate wound repair[186,187]. Moreover, polyplex formulation of CpG ODNs could also stabilize oligomers against degradation, increase killing within macrophages by enhancing uptake and aid wound repair. In line with the effect of CpG ODN on the host, it has recently been shown that the traditional antileishmanial drugs critically modifies the maturation, activation and development of phagocytes through a mechanism dependent on TLR9 and MyD88[29]. Moreover, it has been known that lipophosphoglycan (LPG), a virulence factor expressed by *Leishmania* parasites, activate TLR-2 to reduce antileishmanial immune responses of macrophages via cytokine-mediated decrease of TLR-9 expression[188]. Conversely, it has also been shown that activation of TLR-9 by CpG ODN have potential applications both as adjuvants and nonspecific immune modulators by triggering immunity against intracellular *L. major*[146]. Similarly, paromomycin is being used in combination with methylbenzethonium chloride (Leshcutan adjuvant) to increase the amount of drug that is delivered to the skin for local treatment of CL[107,189].

On the other hand, recent studies show that stimulating the innate immune system by CpG ODN may accelerates wound repair and represents a novel, inexpensive, safe and effective means of improving wound repair[186,187]. The CpG ODN induced the production of

cytokines, chemokines, and growth factors that act on inflammatory and epithelial cells at the wound site to enhance wound healing[186,190]. Moreover, it has been shown that CpG ODN and chemotherapeutic delivery system not only lowers the effective drug dose and toxicity but also synergizes with the upregulation of tumor necrosis factor alpha (TNF-α), interleukin-12 (IL-12), and inducible nitric oxide synthase and with the down regulation of transforming growth factor β (TGF-β), IL-10, and IL-4 in leishmanai infection models [72,191,192]. Evehtough CpG ODN has an important role in both producing antileishmanial immune responses and wound management, efficient delivery of nucleic acid-based immune modulators like CpG ODN is a key challenge. This has been overcome by enclosing CpG ODN within PHMB and could overcome the delivery challenges by improving passage across physiological or cell barriers. Such delivery strategies may also favor the creation of a drug reservoir in the dermis by sustained release systems or enhance skin penetration of drug. Thus, a technology that combines PHMB and CpG ODN could kill parasites directly through parasite membrane and chromosome disruption, and indirectly through modulation of host immunity.

Moreover, the wound healing and antileishmanial effects of PHMB may be further facilitated by immunomodulatory property of CpG ODN. The discovery of PHMB-nucleic acid interactions and formation of nanopolyplexes for efficient delivery into macrophages may have vast applications beyond the initial objectives of this study. Our study indicated that the efficacy and the selectivity of drugs for CL can be drastically improved through an advanced drug delivery system and a combination therapy. Taken together, our finding has great translational implications for the treatment of CL and nucleic acid-based therapy/vaccine.

6. SUMMARY AND OUTLOOK

Several infectious diseases caused by intracellular pathogens including leishmaniasis cause enormous suffering in many countries. The global burden of leishmaniasis is exacerbated by the lack of licensed vaccines. Current treatments of CL are poorly justified and have sub-optimal effectiveness. Traditional antileishmanial systemic agents such as antimonials, pentamidine and amphotericin are limited by toxic side effects, parenteral route of administration and emerging drug resistance[34]. Topical or local treatment has been recommended by the WHO as a first line treatment approach for CL patients; however, they have not yet provided a strong consistent result either. WHO recommended a simple wound management as a first line treatment approach for non-complicated CL cases. Overall, there is a lack of evidence for potential benefit of the current CL treatments. New efficacious, affordable and noninvasive therapeutic drugs are desperately needed. Among several drug discovery research strategies, repurposing or repositioning existing drugs from other diseases accounts for many currently used antiparasitic drugs, and thus, have historically played a great role in antiparastic drug discovery[193]. It has been a rationale for development of amphotericin B, miltefosine and paromomycin against leishmaniasis. This particular approach has a number of advantages including reduction in development times, costs, and overall risks. In this study, we discovered PHMB as a novel, affordable and potent antileishmanial agent that could potentially be used for topical treatments of CL patients. PHMB has long history of safe topical usage for several purposes including for dermatological and wound managements.

For effective targeting of intracellular pathogens including *Leishmania* parasites, an efficient uptake of drugs by phagocytes is an important prerequisite[40]. For intracellular localization of drugs in macrophage-rich organs such as liver, spleen and bone marrow, NPs holds great promise. When NPs are introduced into a medium, opsonin proteins are attached

to the surface of NPs, and they are then tend to be recognized by phagocytes as 'foreign'. Consequently, they are preferentially taken up by the intended target cells (phagocytes) much more effectively than their free drug counterparts[194]. Among various NPs platforms, cationic polymer NPs are known to improve cellular uptake, biodegradability and biocompatibility of drugs[195]. Moreover, they can also be used to manipulate or deliver immunologically active components to the target sites more effectively. Thus, understanding of biological pathways for internalization of the NPs can facilitate precise intracellular targeting with enhanced therapeutic outcomes. By using standardized commercial polystyrene NPs as model, we studied the interactions of NPs with biological systems. We showed that NPs are internalized by several endocytic routes. Moreover, there are also various physicochemical and biological factors that determine NPs-cell interactions.

Finally, we attempted to develop innovative NPs based host- and pathogen-directed therapy for successful treatment of CL. The treatment approach focused on a combination therapy that can simultaneously kill the pathogen selectively and manipulate the host immune system in favor of elimination of the parasite for overall synergistic effect against CL. In this scenario, we investigated the overall synergistic effect of a combined therapy comprising PHMB and CpG ODN against CL. Our results clearly showed that PHMB and CpG ODN form self-assembled nanostructures that act through the host immune modulation and directly killing the intracellular parasites. This suggests that PHMB can be potentially used as non-viral nucleic acid carrier and a combination therapy with CpG ODN for effective host- and pathogen-directed therapy against CL. Regardless of its excellent safety record, as expected for a cationic polymer, PHMB shows cell toxicity at high concentrations. However, our results suggested that PHMB toxicity could be effectively counteracted when interacting with negatively charged CpG ODN as a result of effective charge shielding upon complexation without minimizing its antileishmanial effect. This nanopolyplexes potentially provide

additional benefits through wound healing, immune modulation and cellular delivery. It is a novel idea that constitutes rationale-based combination therapy and an innovative nanotechnology strategy. Unlike other combination therapies, in this technology, PHMB condense nucleic acids into smaller particles forming nanopolyplexes for enhanced delivery, while allowing it to dissociate once inside the cell. Conclusively, our proof-of concept study showed that PHMB with or without the nucleic acid immunomodulator could be effectively used to challenge CL. Therefore, our findings have a great implication to combat human diseases by opening a new methodology for nucleic acid-based therapy and/or vaccine.

For several reasons such as low-cost, high-throughput, and accuracy in efficacious determination, *in vitro* experimental systems are ideal[196]. However, one of the main challenges in drug development research is many candidate drugs that are initially promising in cell culture may not retain the same efficacy in laboratory animals or in clinical trials. The additional barriers present in the physiological environment may prevent successful translation of *in vitro* study into animal study. Furthermore, the treatment strategies of CL and its outcomes differ based on the type of parasites causing the diseases[197]. Thus, the idea of using PHMB with or without CpG ODN for topical application against CL has to be further studied and evaluated in *in vivo* animal model(s). Moreover, the discovery should be evaluated against a range of *Leishmania genus,* species and strains. In summary, further appropriate *in vitro* and in *vivo* studies, and clinical trials are warranted to take the currently identified novel candidate drug to clinics.

7. REFERENCES

1. Kaye, P. & Scott, P. Leishmaniasis: complexity at the host-pathogen interface. *Nat. Rev. Microbiol.* **9,** 604–15 (2011).

2. Hartley, M.-A., Drexler, S., Ronet, C., Beverley, S. M. & Fasel, N. The immunological, environmental, and phylogenetic perpetrators of metastatic leishmaniasis. *Trends Parasitol.* **30,** 412–22 (2014).

3. Bañuls, A. L. *et al.* Clinical pleiomorphism in human leishmaniases, with special mention of asymptomatic infection. *Clin. Microbiol. Infect.* **17,** 1451–61 (2011).

4. Choi, C. M. & Lerner, E. A. Leishmaniasis as an emerging infection. *J. Investig. Dermatol. Symp. Proc.* **6,** 175–82 (2001).

5. World Health Organization. Technical Report Series on control of the leishmaniases. *Geneva, 22–26 March* **949,** 1–187 (2010).

6. Rodríguez, N. E. & Wilson, M. E. Eosinophils and mast cells in leishmaniasis. *Immunol. Res.* **59,** 129–41 (2014).

7. Murray, H. W., Berman, J. D., Davies, C. R. & Saravia, N. G. Advances in leishmaniasis. *Lancet* **366,** 1561–77 (2005).

8. Hartley, M.-A., Kohl, K., Ronet, C. & Fasel, N. The therapeutic potential of immune cross-talk in leishmaniasis. *Clin. Microbiol. Infect.* **19,** 119–30 (2013).

9. McCall, L.-I. & McKerrow, J. H. Determinants of disease phenotype in trypanosomatid parasites. *Trends Parasitol.* **30,** 342–9 (2014).

10. Monge-Maillo, B. & López-Vélez, R. Therapeutic options for old world cutaneous leishmaniasis and new world cutaneous and mucocutaneous leishmaniasis. *Drugs* **73,** 1889–920 (2013).

11. Peacock, C. S. *et al.* Comparative genomic analysis of three Leishmania species that cause diverse human disease. *Nat. Genet.* **39,** 839–47 (2007).

12. Hoyer, C., Mellenthin, K., Schilhabel, M., Platzer, M. & Clos, J. Use of genetic complementation to identify gene(s) which specify species-specific organ tropism of Leishmania. *Med. Microbiol. Immunol.* **190,** 43–6 (2001).

13. McCall, L.-I. & Matlashewski, G. Localization and induction of the A2 virulence factor in Leishmania: evidence that A2 is a stress response protein. *Mol. Microbiol.* **77,** 518–30 (2010).

14. Zhang, W.-W. *et al.* Comparison of the A2 gene locus in Leishmania donovani and Leishmania major and its control over cutaneous infection. *J. Biol. Chem.* **278,** 35508–15 (2003).

15. Zhang, W.-W. & Matlashewski, G. Screening Leishmania donovani Complex-Specific Genes Required for Visceral Disease. *Methods Mol. Biol.* **1201,** 339–61 (2015).

16. Ramanathan, R., Talaat, K. R., Fedorko, D. P., Mahanty, S. & Nash, T. E. A species-specific approach to the use of non-antimony treatments for cutaneous leishmaniasis. *Am. J. Trop. Med. Hyg.* **84,** 109–17 (2011).

17. Arevalo, J. *et al.* Influence of Leishmania (Viannia) species on the response to antimonial treatment in patients with American tegumentary leishmaniasis. *J. Infect. Dis.* **195,** 1846–51 (2007).

18. Schamber-Reis, B. L. F. *et al.* UNC93B1 and nucleic acid-sensing Toll-like receptors mediate host resistance to infection with Leishmania major. *J. Biol. Chem.* **288,** 7127–36 (2013).

19. Ramasawmy, R. *et al.* The -2518bp promoter polymorphism at CCL2/MCP1 influences susceptibility to mucosal but not localized cutaneous leishmaniasis in Brazil. *Infect. Genet. Evol.* **10,** 607–13 (2010).

20. Sakthianandeswaren, A., Foote, S. J. & Handman, E. The role of host genetics in leishmaniasis. *Trends Parasitol.* **25,** 383–91 (2009).

21. Dogra, N., Warburton, C. & McMaster, W. R. Leishmania major abrogates gamma interferon-induced gene expression in human macrophages from a global perspective. *Infect. Immun.* **75,** 3506–15 (2007).

22. Lemaire, J. *et al.* MicroRNA expression profile in human macrophages in response to Leishmania major infection. *PLoS Negl. Trop. Dis.* **7,** e2478 (2013).

23. Gregory, D. J., Sladek, R., Olivier, M. & Matlashewski, G. Comparison of the effects of Leishmania major or Leishmania donovani infection on macrophage gene expression. *Infect. Immun.* **76,** 1186–92 (2008).

24. Schurigt, U., Masic, A. & Moll, H. : Trypanosomatid Diseases - Molecular Routes to Drug Discovery. *T. Jäger, O. Koch L. Flohé (eds.), Wiley-VCH, Weinheim, Ger.* 105–119 (2013). doi:10.1002/9783527670383.ch6

25. Hurdayal, R. & Brombacher, F. The role of IL-4 and IL-13 in cutaneous Leishmaniasis. *Immunol. Lett.* **161,** 179–83 (2014).

26. Sacks, D. & Noben-Trauth, N. The immunology of susceptibility and resistance to Leishmania major in mice. *Nat. Rev. Immunol.* **2,** 845–58 (2002).

27. McMahon-Pratt, D. & Alexander, J. Does the Leishmania major paradigm of pathogenesis and protection hold for New World cutaneous leishmaniases or the visceral disease? *Immunol. Rev.* **201,** 206–24 (2004).

28. Gonzalez-Leal, I. J. *et al.* Cathepsin B in Antigen-Presenting Cells Controls Mediators of the Th1 Immune Response during Leishmania major Infection. *PLoS Negl. Trop. Dis.* **8,** e3194 (2014).

29. Das, S. *et al.* TLR9 and MyD88 are crucial for the maturation and activation of dendritic cells by paromomycin-miltefosine combination therapy in visceral leishmaniasis. *Br. J. Pharmacol.* **171,** 1260–74 (2014).

30. Ghosh, M., Roy, K. & Roy, S. Immunomodulatory effects of antileishmanial drugs. *J. Antimicrob. Chemother.* **68,** 2834–8 (2013).

31. Silverman, J. M. *et al.* Leishmania exosomes modulate innate and adaptive immune responses through effects on monocytes and dendritic cells. *J. Immunol.* **185,** 5011–22 (2010).

32. Schnitzer, J. K., Berzel, S., Fajardo-Moser, M., Remer, K. A. & Moll, H. Fragments of antigen-loaded dendritic cells (DC) and DC-derived exosomes induce protective immunity against Leishmania major. *Vaccine* **28,** 5785–93 (2010).

33. Kumar, R. & Engwerda, C. Vaccines to prevent leishmaniasis. *Clin. Transl. Immunol.* **3,** e13 (2014).

34. Ameen, M. Cutaneous leishmaniasis: therapeutic strategies and future directions. *Expert Opin. Pharmacother.* **8,** 2689–99 (2007).

35. Carneiro, G., Aguiar, M. G., Fernandes, A. P. & Ferreira, L. A. M. Drug delivery systems for the topical treatment of cutaneous leishmaniasis. *Expert Opin. Drug Deliv.* **9,** 1083–97 (2012).

36. Wortmann, G. *et al.* Lipsosomal amphotericin B for treatment of cutaneous leishmaniasis. *Am. J. Trop. Med. Hyg.* **83,** 1028–33 (2010).

37. Obonaga, R. *et al.* Treatment failure and miltefosine susceptibility in dermal leishmaniasis caused by Leishmania subgenus Viannia species. *Antimicrob. Agents Chemother*. **58,** 144–52 (2014).

38. Huh, A. J. & Kwon, Y. J. 'Nanoantibiotics': a new paradigm for treating infectious diseases using nanomaterials in the antibiotics resistant era. *J. Control. Release* **156,** 128–45 (2011).

39. Färber, K. & Moll, H. Vaccination as a control measure. In: Drug Resistance in Leishmania Parasites. *A. Ponte-Sucre, E. Diaz M. Padron-Nieves (eds.), Springer Verlag GmbH, Berlin, Ger.* 113–143 (2012).

40. Yameen, B. *et al.* Insight into nanoparticle cellular uptake and intracellular targeting. *J. Control. Release* **190,** 485–99 (2014).

41. Kim, B. Y. S., Rutka, J. T. & Chan, W. C. W. Nanomedicine. *N. Engl. J. Med.* **363,** 2434–43 (2010).

42. Smith, D. M., Simon, J. K. & Baker, J. R. Applications of nanotechnology for immunology. *Nat. Rev. Immunol.* **13,** 592–605 (2013).

43. Yin, H. *et al.* Non-viral vectors for gene-based therapy. *Nat. Rev. Genet.* **15,** 541–55 (2014).

44. Samal, S. K. *et al.* Cationic polymers and their therapeutic potential. *Chem. Soc. Rev.* **41,** 7147–94 (2012).

45. Carmona-Ribeiro, A. M. & de Melo Carrasco, L. D. Cationic antimicrobial polymers and their assemblies. *Int. J. Mol. Sci.* **14,** 9906–46 (2013).

46. Karve, S. *et al.* Revival of the abandoned therapeutic wortmannin by nanoparticle drug delivery. *Proc. Natl. Acad. Sci. U. S. A.* **109,** 8230–5 (2012).

47. Couvreur, P. Nanoparticles in drug delivery: past, present and future. *Adv. Drug Deliv. Rev.* **65,** 21–3 (2013).

48. Bertrand, N. & Leroux, J.-C. The journey of a drug-carrier in the body: an anatomo-physiological perspective. *J. Control. Release* **161,** 152–63 (2012).

49. Briones, E., Colino, C. I. & Lanao, J. M. Delivery systems to increase the selectivity of antibiotics in phagocytic cells. *J. Control. Release* **125,** 210–27 (2008).

50. Li, H., Li, Y., Jiao, J. & Hu, H.-M. Alpha-alumina nanoparticles induce efficient autophagy-dependent cross-presentation and potent antitumour response. *Nat. Nanotechnol.* **6,** 645–50 (2011).

51. Wicki, A., Witzigmann, D., Balasubramanian, V. & Huwyler, J. Nanomedicine in cancer therapy: Challenges, opportunities, and clinical applications. *J. Control. Release* **200,** 138–157 (2014).

52. Wang, A. Z., Langer, R. & Farokhzad, O. C. Nanoparticle delivery of cancer drugs. *Annu. Rev. Med.* **63,** 185–98 (2012).

53. Farokhzad, O. C. & Langer, R. Impact of nanotechnology on drug delivery. *ACS Nano* **3,** 16–20 (2009).

54. De la Torre, B. G. *et al.* A BODIPY-embedding miltefosine analog linked to cell-penetrating Tat(48-60) peptide favors intracellular delivery and visualization of the antiparasitic drug. *Amino Acids* **46,** 1047–58 (2014).

55. Das, S., Roy, P., Mondal, S., Bera, T. & Mukherjee, A. One pot synthesis of gold nanoparticles and application in chemotherapy of wild and resistant type visceral leishmaniasis. *Colloids Surf. B. Biointerfaces* **107,** 27–34 (2013).

56. Momeni, A. A. *et al.* Development of liposomes loaded with anti-leishmanial drugs for the treatment of cutaneous leishmaniasis. *J. Liposome Res.* **23,** 134–44 (2013).

57. Panzarini, E. & Dini, L. Nanomaterial-induced autophagy: a new reversal MDR tool in cancer therapy? *Mol. Pharm.* **11,** 2527–38 (2014).

58. Tang, S. *et al.* Co-delivery of doxorubicin and RNA using pH-sensitive poly (β-amino ester) nanoparticles for reversal of multidrug resistance of breast cancer. *Biomaterials* **35,** 6047–59 (2014).

59. Colombo, S., Zeng, X., Ragelle, H. & Foged, C. Complexity in the therapeutic delivery of RNAi medicines: an analytical challenge. *Expert Opin. Drug Deliv.* **11,** 1481–95 (2014).

60. Ganju, A. *et al.* Nanoways to overcome docetaxel resistance in prostate cancer. *Drug Resist. Updat.* **17,** 13–23 (2014).

61. Jhaveri, A., Deshpande, P. & Torchilin, V. Stimuli-sensitive nanopreparations for combination cancer therapy. *J. Control. Release* **190,** 352–70 (2014).

62. Zafar, N., Fessi, H. & Elaissari, A. Colloidal particles containing labeling agents and cyclodextrins for theranostic applications. *Int. J. Pharm.* **472,** 118–29 (2014).

63. Du, H., Yang, X. & Zhai, G. Design of chitosan-based nanoformulations for efficient intracellular release of active compounds. *Nanomedicine (Lond).* **9,** 723–40 (2014).

64. Van Riet, E., Ainai, A., Suzuki, T., Kersten, G. & Hasegawa, H. Combatting infectious diseases; nanotechnology as a platform for rational vaccine design. *Adv. Drug Deliv. Rev.* **74,** 28–34 (2014).

65. Swartz, M. A., Hirosue, S. & Hubbell, J. A. Engineering approaches to immunotherapy. *Sci. Transl. Med.* **4,** 148rv9 (2012).

66. Tsai, N. *et al.* Nanomedicine for global health. *J. Lab. Autom.* **19,** 511–6 (2014).

67. Sahdev, P., Ochyl, L. J. & Moon, J. J. Biomaterials for nanoparticle vaccine delivery systems. *Pharm. Res.* **31,** 2563–82 (2014).

68. Shima, F., Uto, T., Akagi, T. & Akashi, M. Synergistic stimulation of antigen presenting cells via TLR by combining CpG ODN and poly(γ-glutamic acid)-based nanoparticles as vaccine adjuvants. *Bioconjug. Chem.* **24,** 926–33 (2013).

69. Kasturi, S. P. *et al.* Programming the magnitude and persistence of antibody responses with innate immunity. *Nature* **470,** 543–7 (2011).

70. Karlson, T. D. L., Kong, Y. Y., Hardy, C. L., Xiang, S. D. & Plebanski, M. The signalling imprints of nanoparticle uptake by bone marrow derived dendritic cells. *Methods* **60,** 275–83 (2013).

71. Sanjuan, M. A. *et al.* Toll-like receptor signalling in macrophages links the autophagy pathway to phagocytosis. *Nature* **450,** 1253–7 (2007).

72. De Titta, A. *et al.* Nanoparticle conjugation of CpG enhances adjuvancy for cellular immunity and memory recall at low dose. *Proc. Natl. Acad. Sci. U. S. A.* **110,** 19902–7 (2013).

73. Knuschke, T. *et al.* Immunization with biodegradable nanoparticles efficiently induces cellular immunity and protects against influenza virus infection. *J. Immunol.* **190,** 6221–9 (2013).

74. Zaman, M., Good, M. F. & Toth, I. Nanovaccines and their mode of action. *Methods* **60,** 226–31 (2013).

75. Stano, A., Nembrini, C., Swartz, M. A., Hubbell, J. A. & Simeoni, E. Nanoparticle size influences the magnitude and quality of mucosal immune responses after intranasal immunization. *Vaccine* **30,** 7541–6 (2012).

76. Fratila, R. M., Mitchell, S. G., Del Pino, P., Grazu, V. & de la Fuente, J. M. Strategies for the biofunctionalization of gold and iron oxide nanoparticles. *Langmuir* **30,** 15057–71 (2014).

77. Gdowski, A., Ranjan, A. P., Mukerjee, A. & Vishwanatha, J. K. Nanobiosensors: role in cancer detection and diagnosis. *Adv. Exp. Med. Biol.* **807,** 33–58 (2014).

78. Neely, L. A. *et al.* T2 magnetic resonance enables nanoparticle-mediated rapid detection of candidemia in whole blood. *Sci. Transl. Med.* **5,** 182ra54 (2013).

79. Lazarovits, J., Chen, Y. Y., Sykes, E. A. & Chan, W. C. W. Nanoparticle-blood interactions: the implications on solid tumour targeting. *Chem. Commun. (Camb).* (2014). doi:10.1039/c4cc07644c

80. Jiang, W., Kim, B. Y. S., Rutka, J. T. & Chan, W. C. W. Nanoparticle-mediated cellular response is size-dependent. *Nat. Nanotechnol.* **3,** 145–50 (2008).

81. Tenzer, S. *et al.* Rapid formation of plasma protein corona critically affects nanoparticle pathophysiology. *Nat. Nanotechnol.* **8,** 772–81 (2013).

82. Monopoli, M. P., Aberg, C., Salvati, A. & Dawson, K. A. Biomolecular coronas provide the biological identity of nanosized materials. *Nat. Nanotechnol.* **7,** 779–86 (2012).

83. Lundqvist, M. *et al.* Nanoparticle size and surface properties determine the protein corona with possible implications for biological impacts. *Proc. Natl. Acad. Sci. U. S. A.* **105,** 14265–70 (2008).

84. Monopoli, M. P. *et al.* Physical-chemical aspects of protein corona: relevance to in vitro and in vivo biological impacts of nanoparticles. *J. Am. Chem. Soc.* **133,** 2525–34 (2011).

85. Walkey, C. D., Olsen, J. B., Guo, H., Emili, A. & Chan, W. C. W. Nanoparticle size and surface chemistry determine serum protein adsorption and macrophage uptake. *J. Am. Chem. Soc.* **134,** 2139–47 (2012).

86. Dobrovolskaia, M. A. *et al.* Interaction of colloidal gold nanoparticles with human blood: effects on particle size and analysis of plasma protein binding profiles. *Nanomedicine* **5,** 106–17 (2009).

87. Caracciolo, G. Liposome-protein corona in a physiological environment: challenges and opportunities for targeted delivery of nanomedicines. *Nanomedicine* (2014). doi:10.1016/j.nano.2014.11.003

88. Iversen, T.-G., Skotland, T. & Sandvig, K. Endocytosis and intracellular transport of nanoparticles: Present knowledge and need for future studies. *Nano Today* **6,** 176–185 (2011).

89. Chou, L. Y. T., Ming, K. & Chan, W. C. W. Strategies for the intracellular delivery of nanoparticles. *Chem. Soc. Rev.* **40,** 233–45 (2011).

90. Hansen, C. G. & Nichols, B. J. Molecular mechanisms of clathrin-independent endocytosis. *J. Cell Sci.* **122,** 1713–21 (2009).

91. Xu, S., Olenyuk, B. Z., Okamoto, C. T. & Hamm-Alvarez, S. F. Targeting receptor-mediated endocytotic pathways with nanoparticles: rationale and advances. *Adv. Drug Deliv. Rev.* **65,** 121–38 (2013).

92. Sandvig, K., Pust, S., Skotland, T. & van Deurs, B. Clathrin-independent endocytosis: mechanisms and function. *Curr. Opin. Cell Biol.* **23,** 413–20 (2011).

93. Conner, S. D. & Schmid, S. L. Regulated portals of entry into the cell. *Nature* **422,** 37–44 (2003).

94. Yan, Y., Such, G. K., Johnston, A. P. R., Best, J. P. & Caruso, F. Engineering particles for therapeutic delivery: prospects and challenges. *ACS Nano* **6,** 3663–9 (2012).

95. Falcone, S. *et al.* Macropinocytosis: regulated coordination of endocytic and exocytic membrane traffic events. *J. Cell Sci.* **119,** 4758–69 (2006).

96. Dos Santos, T., Varela, J., Lynch, I., Salvati, A. & Dawson, K. A. Quantitative assessment of the comparative nanoparticle-uptake efficiency of a range of cell lines. *Small* **7,** 3341–9 (2011).

97. Saha, K. *et al.* Surface functionality of nanoparticles determines cellular uptake mechanisms in mammalian cells. *Small* **9,** 300–5 (2013).

98. Albanese, A., Tang, P. S. & Chan, W. C. W. The effect of nanoparticle size, shape, and surface chemistry on biological systems. *Annu. Rev. Biomed. Eng.* **14,** 1–16 (2012).

99. Herd, H. *et al.* Nanoparticle geometry and surface orientation influence mode of cellular uptake. *ACS Nano* **7,** 1961–73 (2013).

100. Underhill, D. M. & Goodridge, H. S. Information processing during phagocytosis. *Nat. Rev. Immunol.* **12,** 492–502 (2012).

101. Nowak, J. S. *et al.* Silica nanoparticle uptake induces survival mechanism in A549 cells by the activation of autophagy but not apoptosis. *Toxicol. Lett.* **224,** 84–92 (2014).

102. Yu, J., Baek, M., Chung, H. E. & Choi, S. J. Effects of physicochemical properties of zinc oxide nanoparticles on cellular uptake. *J. Phys. Conf. Ser.* **304,** 012007 (2011).

103. Castellucci, L. *et al.* Wound healing genes and susceptibility to cutaneous leishmaniasis in Brazil. *Infect. Genet. Evol.* **12,** 1102–10 (2012).

104. Bailey, M. S. Editorial commentary: local treatments for cutaneous leishmaniasis. *Clin. Infect. Dis.* **57,** 381–3 (2013).

105. Morizot, G. *et al.* Travelers with cutaneous leishmaniasis cured without systemic therapy. *Clin. Infect. Dis.* **57,** 370–80 (2013).

106. Moreno, E. *et al.* Nanoparticles as multifunctional devices for the topical treatment of cutaneous leishmaniasis. *Expert Opin. Drug Deliv.* **11,** 579–97 (2014).

107. Ben Salah, A. *et al.* Topical paromomycin with or without gentamicin for cutaneous leishmaniasis. *N. Engl. J. Med.* **368,** 524–32 (2013).

108. Carneiro, G. *et al.* Topical delivery and in vivo antileishmanial activity of paromomycin-loaded liposomes for treatment of cutaneous leishmaniasis. *J. Liposome Res.* **20,** 16–23 (2010).

109. Gupta, S., Pal, A. & Vyas, S. P. Drug delivery strategies for therapy of visceral leishmaniasis. *Expert Opin. Drug Deliv.* **7,** 371–402 (2010).

110. Romero, E. L. & Morilla, M. J. Drug delivery systems against leishmaniasis? Still an open question. *Expert Opin. Drug Deliv.* **5,** 805–23 (2008).

111. Barratt, G. & Legrand, P. Comparison of the efficacy and pharmacology of formulations of amphotericin B used in treatment of leishmaniasis. *Curr. Opin. Infect. Dis.* **18,** 527–30 (2005).

112. Glasser, J. S. & Murray, C. K. Central nervous system toxicity associated with liposomal amphotericin B therapy for cutaneous leishmaniasis. *Am. J. Trop. Med. Hyg.* **84,** 566–8 (2011).

113. Saha, P., Mukhopadhyay, D. & Chatterjee, M. Immunomodulation by chemotherapeutic agents against Leishmaniasis. *Int. Immunopharmacol.* **11,** 1668–79 (2011).

114. Gupta, S., Sane, S. A., Shakya, N., Vishwakarma, P. & Haq, W. CpG oligodeoxynucleotide 2006 and miltefosine, a potential combination for treatment of experimental visceral leishmaniasis. *Antimicrob. Agents Chemother.* **55,** 3461–4 (2011).

115. O'Malley, L. P., Hassan, K. Z., Brittan, H., Johnson, N. & Collins, A. N. Characterization of the biocide polyhexamethylene biguanide by matrix-assisted laser desorption ionization time-of-flight mass spectrometry. *J. Appl. Polym. Sci.* **102,** 4928–4936 (2006).

116. Gerit D. Mulder, Joseph P. Cavorsi, D. K. L. Polyhexamethylene Biguanide (PHMB): An Addendum to Current Topical Antimicrobials. *Wounds,* **19,** 173–182 (2007).

117. Kaehn, K. Polihexanide: a safe and highly effective biocide. *Skin Pharmacol. Physiol.* **23 Suppl,** 7–16 (2010).

118. Wessels, S. & Ingmer, H. Modes of action of three disinfectant active substances: a review. *Regul. Toxicol. Pharmacol.* **67,** 456–67 (2013).

119. Walls, G., Noonan, L., Wilson, E., Holland, D. & Briggs, S. Successful use of locally applied polyhexamethylene biguanide as an adjunct to the treatment of fungal osteomyelitis. *Can. J. Infect. Dis. Med. Microbiol.* **24,** 109–12 (2013).

120. Patel, D. V & McGhee, C. N. Presumed late recurrence of Acanthamoeba keratitis exacerbated by exposure to topical corticosteroids. *Oman J. Ophthalmol.* **6,** S40–2 (2013).

121. Rusciano, G. *et al.* Raman microspectroscopy analysis in the treatment of acanthamoeba keratitis. *PLoS One* **8,** e72127 (2013).

122. Firdessa, R., Oelschlaeger, T. A. & Moll, H. Identification of multiple cellular uptake pathways of polystyrene nanoparticles and factors affecting the uptake: Relevance for drug delivery systems. *Eur. J. Cell Biol.* **93,** 323–37 (2014).

123. Chekeni, F. B. *et al.* Pannexin 1 channels mediate 'find-me' signal release and membrane permeability during apoptosis. *Nature* **467,** 863–7 (2010).

124. Bringmann, G. *et al.* A novel Leishmania major amastigote assay in 96-well format for rapid drug screening and its use for discovery and evaluation of a new class of leishmanicidal quinolinium salts. *Antimicrob. Agents Chemother.* **57,** 3003–11 (2013).

125. Lang, T., Goyard, S., Lebastard, M. & Milon, G. Bioluminescent Leishmania expressing luciferase for rapid and high throughput screening of drugs acting on amastigote-harbouring macrophages and for quantitative real-time monitoring of parasitism features in living mice. *Cell. Microbiol.* **7,** 383–92 (2005).

126. Ponte-Sucre, A. *et al.* Structure-activity relationship and studies on the molecular mechanism of leishmanicidal N,C-coupled arylisoquinolinium salts. *J. Med. Chem.* **52,** 626–36 (2009).

127. Hellman, L. M. & Fried, M. G. Electrophoretic mobility shift assay (EMSA) for detecting protein-nucleic acid interactions. *Nat. Protoc.* **2,** 1849–61 (2007).

128. Rebong, R. A. *et al.* Polyhexamethylene biguanide and calcineurin inhibitors as novel antifungal treatments for Aspergillus keratitis. *Invest. Ophthalmol. Vis. Sci.* **52,** 7309–15 (2011).

129. Ikeda, T., Tazuke, S. & Watanabe, M. Interaction of biologically active molecules with phospholipid membranes. I. Fluorescence depolarization studies on the effect of polymeric biocide bearing biguanide groups in the main chain. *Biochim. Biophys. Acta* **735,** 380–6 (1983).

130. Allen, M. J., Morby, A. P. & White, G. F. Cooperativity in the binding of the cationic biocide polyhexamethylene biguanide to nucleic acids. *Biochem. Biophys. Res. Commun.* **318,** 397–404 (2004).

131. El-Sayed, A., Futaki, S. & Harashima, H. Delivery of macromolecules using arginine-rich cell-penetrating peptides: ways to overcome endosomal entrapment. *AAPS J.* **11,** 13–22 (2009).

132. Küsters, M., Beyer, S., Kutscher, S., Schlesinger, H. & Gerhartz, M. Rapid, simple and stability-indicating determination of polyhexamethylene biguanide in liquid and gel-like dosage forms by liquid chromatography with diode-array detection. *J. Pharm. Anal.* **3,** 408–414 (2013).

133. Van Gisbergen, P. A. C., Esseling-Ozdoba, A. & Vos, J. W. Microinjecting FM4-64 validates it as a marker of the endocytic pathway in plants. *J. Microsc.* **231,** 284–90 (2008).

134. Kumari, S., Mg, S. & Mayor, S. Endocytosis unplugged: multiple ways to enter the cell. *Cell Res.* **20,** 256–75 (2010).

135. McMahon, H. T. & Boucrot, E. Molecular mechanism and physiological functions of clathrin-mediated endocytosis. *Nat. Rev. Mol. Cell Biol.* **12,** 517–33 (2011).

136. Vercauteren, D. *et al.* The use of inhibitors to study endocytic pathways of gene carriers: optimization and pitfalls. *Mol. Ther.* **18,** 561–9 (2010).

137. Moscatelli, A. *et al.* Distinct endocytic pathways identified in tobacco pollen tubes using charged nanogold. *J. Cell Sci.* **120,** 3804–19 (2007).

138. Fernando, L. P. *et al.* Mechanism of cellular uptake of highly fluorescent conjugated polymer nanoparticles. *Biomacromolecules* **11,** 2675–82 (2010).

139. Khalil, I. A., Kogure, K., Akita, H. & Harashima, H. Uptake pathways and subsequent intracellular trafficking in nonviral gene delivery. *Pharmacol. Rev.* **58,** 32–45 (2006).

140. Kirchhausen, T., Macia, E. & Pelish, H. E. Use of dynasore, the small molecule inhibitor of dynamin, in the regulation of endocytosis. *Methods Enzymol.* **438,** 77–93 (2008).

141. Sato, K., Nagai, J., Mitsui, N., Ryoko Yumoto & Takano, M. Effects of endocytosis inhibitors on internalization of human IgG by Caco-2 human intestinal epithelial cells. *Life Sci.* **85,** 800–7 (2009).

142. Roth, M. G. Integrating actin assembly and endocytosis. *Dev. Cell* **13,** 3–4 (2007).

143. Nagahama, M. *et al.* Cellular vacuolation induced by Clostridium perfringens epsilon-toxin. *FEBS J.* **278,** 3395–407 (2011).

144. Park, M. C., Kim, D., Lee, Y. & Kwon, H.-J. CD83 expression induced by CpG-DNA stimulation in a macrophage cell line RAW 264.7. *BMB Rep.* **46,** 448–53 (2013).

145. Castillo, B. *et al.* Intracellular Delivery of siRNA by Polycationic Superparamagnetic Nanoparticles. *J. Drug Deliv.* **2012,** 218940 (2012).

146. Ramírez-Pineda, J. R., Fröhlich, A., Berberich, C. & Moll, H. Dendritic cells (DC) activated by CpG DNA ex vivo are potent inducers of host resistance to an intracellular pathogen that is independent of IL-12 derived from the immunizing DC. *J. Immunol.* **172,** 6281–9 (2004).

147. Creppy, E. E., Diallo, A., Moukha, S., Eklu-Gadegbeku, C. & Cros, D. Study of Epigenetic Properties of Poly(HexaMethylene Biguanide) Hydrochloride (PHMB). *Int. J. Environ. Res. Public Health* **11,** 8069–92 (2014).

148. The Scientific Committee on Consumer Safety of the European Commission. Opinion on the safety of poly(hexamethylene) biguanide hydrochloride (PHMB). *Eur. Union, SCCS/1535/14* **ISSN 1831-,** 1–72 (2014).

149. Novo, L. *et al.* Decationized polyplexes as stable and safe carrier systems for improved biodistribution in systemic gene therapy. *J. Control. Release* **195,** 162–75 (2014).

150. Hübner, N.-O. & Kramer, A. Review on the efficacy, safety and clinical applications of polihexanide, a modern wound antiseptic. *Skin Pharmacol. Physiol.* **23 Suppl,** 17–27 (2010).

151. Müller, G., Koburger, T. & Kramer, A. Interaction of polyhexamethylene biguanide hydrochloride (PHMB) with phosphatidylcholine containing o/w emulsion and consequences for microbicidal efficacy and cytotoxicity. *Chem. Biol. Interact.* **201,** 58–64 (2013).

152. Jebran, A. F. *et al.* Rapid healing of cutaneous leishmaniasis by high-frequency electrocauterization and hydrogel wound care with or without DAC N-055: a randomized controlled phase IIa trial in Kabul. *PLoS Negl. Trop. Dis.* **8,** e2694 (2014).

153. Hirsch, T. *et al.* [A comparative in vitro study of cell toxicity of clinically used antiseptics]. *Hautarzt.* **60,** 984–91 (2009).

154. Gentile, A., Gerli, S. & Di Renzo, G. C. A new non-invasive approach based on polyhexamethylene biguanide increases the regression rate of HPV infection. *BMC Clin. Pathol.* **12,** 17 (2012).

155. Sahay, G., Alakhova, D. Y. & Kabanov, A. V. Endocytosis of nanomedicines. *J. Control. Release* **145,** 182–95 (2010).

156. Salvati, A. *et al.* Experimental and theoretical comparison of intracellular import of polymeric nanoparticles and small molecules: toward models of uptake kinetics. *Nanomedicine* **7,** 818–26 (2011).

157. Mu, Q. *et al.* Mechanism of cellular uptake of genotoxic silica nanoparticles. *Part. Fibre Toxicol.* **9,** 29 (2012).

158. Kim, J. A., Åberg, C., Salvati, A. & Dawson, K. a. Role of cell cycle on the cellular uptake and dilution of nanoparticles in a cell population. *Nat. Nanotechnol.* **7,** 62–8 (2012).

159. Shima, F., Uto, T., Akagi, T., Baba, M. & Akashi, M. Size effect of amphiphilic poly(γ-glutamic acid) nanoparticles on cellular uptake and maturation of dendritic cells in vivo. *Acta Biomater.* **9,** 8894–901 (2013).

160. Li, K. & Schneider, M. Quantitative evaluation and visualization of size effect on cellular uptake of gold nanoparticles by multiphoton imaging-UV/Vis spectroscopic analysis. *J. Biomed. Opt.* **19,** 101505 (2014).

161. Hu, Y., Xie, J., Tong, Y. W. & Wang, C.-H. Effect of PEG conformation and particle size on the cellular uptake efficiency of nanoparticles with the HepG2 cells. *J. Control. Release* **118,** 7–17 (2007).

162. Kulkarni, S. A. & Feng, S.-S. Effects of particle size and surface modification on cellular uptake and biodistribution of polymeric nanoparticles for drug delivery. *Pharm. Res.* **30,** 2512–22 (2013).

163. Kettler, K., Veltman, K., van de Meent, D., van Wezel, A. & Hendriks, A. J. Cellular uptake of nanoparticles as determined by particle properties, experimental conditions, and cell type. *Environ. Toxicol. Chem.* **33,** 481–92 (2014).

164. Liu, H. *et al.* The effect of surface charge of glycerol monooleate-based nanoparticles on the round window membrane permeability and cochlear distribution. *J. Drug Target.* **21,** 846–54 (2013).

165. Albanese, A. *et al.* Secreted biomolecules alter the biological identity and cellular interactions of nanoparticles. *ACS Nano* **8,** 5515–26 (2014).

166. Steigerwald, M. & Moll, H. Leishmania major modulates chemokine and chemokine receptor expression by dendritic cells and affects their migratory capacity. *Infect. Immun.* **73,** 2564–7 (2005).

167. Olivier, M., Gregory, D. J. & Forget, G. Subversion mechanisms by which Leishmania parasites can escape the host immune response: a signaling point of view. *Clin. Microbiol. Rev.* **18,** 293–305 (2005).

168. Jambo, K. C. *et al.* Small alveolar macrophages are infected preferentially by HIV and exhibit impaired phagocytic function. *Mucosal Immunol.* **7,** 1116–26 (2014).

169. Basu, N., Sett, R. & Das, P. K. Down-regulation of mannose receptors on macrophages after infection with Leishmania donovani. *Biochem. J.* **277 (Pt 2,** 451–6 (1991).

170. Wang, J., Huang, W.-L. & Liu, R.-Y. CpG-ODN enhances ingestion of apoptotic neutrophils by macrophages. *Clin. Exp. Med.* **9,** 37–43 (2009).

171. Utaisincharoen, P. *et al.* CpG ODN enhances uptake of bacteria by mouse macrophages. *Clin. Exp. Immunol.* **132,** 70–5 (2003).

172. Scita, G. & Di Fiore, P. P. The endocytic matrix. *Nature* **463,** 464–73 (2010).

173. Le Roy, C. & Wrana, J. L. Clathrin- and non-clathrin-mediated endocytic regulation of cell signalling. *Nat. Rev. Mol. Cell Biol.* **6,** 112–26 (2005).

174. Olsson, A. Wortmannin, an Inhibitor of Phosphoinositide 3-Kinase, Inhibits Transcytosis in Polarized Epithelial Cells. *J. Biol. Chem.* **270,** 28425–28432 (1995).

175. Kastl, L. *et al.* Multiple internalization pathways of polyelectrolyte multilayer capsules into mammalian cells. *ACS Nano* **7,** 6605–18 (2013).

176. Johnston, H. J. *et al.* Evaluating the uptake and intracellular fate of polystyrene nanoparticles by primary and hepatocyte cell lines in vitro. *Toxicol. Appl. Pharmacol.* **242,** 66–78 (2010).

177. Injury, M. *et al.* Cationic polystyrene nanosphere toxicity depends on cell-specific endocytic and mitochondrial injury pathways. *ACS Nano* **2,** 85–96 (2008).

178. Al-Rawi, M., Diabaté, S. & Weiss, C. Uptake and intracellular localization of submicron and nano-sized SiO_2 particles in HeLa cells. *Arch. Toxicol.* **85,** 813–26 (2011).

179. Kang, B. *et al.* Intracellular uptake, trafficking and subcellular distribution of folate conjugated single walled carbon nanotubes within living cells. *Nanotechnology* **19,** 375103 (2008).

180. Alvar, J. *et al.* Leishmaniasis worldwide and global estimates of its incidence. *PLoS One* **7,** e35671 (2012).

181. Nathan, C. Fresh approaches to anti-infective therapies. *Sci. Transl. Med.* **4,** 140sr2 (2012).

182. Mayer-Barber, K. D. *et al.* Host-directed therapy of tuberculosis based on interleukin-1 and type I interferon crosstalk. *Nature* **511,** 99–103 (2014).

183. Jabbour, M. N. *et al.* The immune microenvironment in cutaneous leishmaniasis. *J. Eur. Acad. Dermatol. Venereol.* (2014). doi:10.1111/jdv.12781

184. Lima-Junior, D. S. *et al.* Inflammasome-derived IL-1β production induces nitric oxide-mediated resistance to Leishmania. *Nat. Med.* **19,** 909–15 (2013).

185. Datta, N., Mukherjee, S., Das, L. & Das, P. K. Targeting of immunostimulatory DNA cures experimental visceral leishmaniasis through nitric oxide up-regulation and T cell activation. *Eur. J. Immunol.* **33,** 1508–18 (2003).

186. Yamamoto, M., Sato, T., Beren, J., Verthelyi, D. & Klinman, D. M. The acceleration of wound healing in primates by the local administration of immunostimulatory CpG oligonucleotides. *Biomaterials* **32,** 4238–42 (2011).

187. Sato, T., Yamamoto, M., Shimosato, T. & Klinman, D. M. Accelerated wound healing mediated by activation of Toll-like receptor 9. *Wound Repair Regen.* **18,** 586–93 (2010).

188. Srivastava, S., Pandey, S. P., Jha, M. K., Chandel, H. S. & Saha, B. Leishmania expressed lipophosphoglycan interacts with Toll-like receptor (TLR)-2 to decrease TLR-9 expression and reduce anti-leishmanial responses. *Clin. Exp. Immunol.* **172,** 403–9 (2013).

189. El-On, J., Jacobs, G. P., Witztum, E. & Greenblatt, C. L. Development of topical treatment for cutaneous leishmaniasis caused by Leishmania major in experimental animals. *Antimicrob. Agents Chemother.* **26,** 745–751 (1984).

190. Hergert, B., Grambow, E., Butschkau, A. & Vollmar, B. Effects of systemic pretreatment with CpG oligodeoxynucleotides on skin wound healing in mice. *Wound Repair Regen.* **21,** 723–9 (2013).

191. Daftarian, P. M. *et al.* A targeted and adjuvanted nanocarrier lowers the effective dose of liposomal amphotericin B and enhances adaptive immunity in murine cutaneous leishmaniasis. *J. Infect. Dis.* **208,** 1914–22 (2013).

192. Asthana, S. *et al.* Immunoadjuvant chemotherapy of visceral leishmaniasis in hamsters using amphotericin B-encapsulated nanoemulsion template-based chitosan nanocapsules. *Antimicrob. Agents Chemother.* **57,** 1714–22 (2013).

193. Andrews, K. T., Fisher, G. & Skinner-Adams, T. S. Drug repurposing and human parasitic protozoan diseases. *Int. J. Parasitol. Drugs Drug Resist.* **4,** 95–111 (2014).

194. Kunjachan, S. *et al.* Physicochemical and biological aspects of macrophage-mediated drug targeting in anti-microbial therapy. *Fundam. Clin. Pharmacol.* **26,** 63–71 (2012).

195. Grijalvo, S., Aviñó, A. & Eritja, R. Oligonucleotide delivery: a patent review (2010 - 2013). *Expert Opin. Ther. Pat.* **24,** 801–19 (2014).

196. Whitehead, K. A. *et al.* In vitro - In vivo translation of lipid nanoparticles for hepatocellular siRNA delivery. *ACS Nano* **6,** 6922–6929 (2012).

197. De Vries, H. J. C., Reedijk, S. H. & Schallig, H. D. F. H. Cutaneous Leishmaniasis: Recent Developments in Diagnosis and Management. *Am. J. Clin. Dermatol.* **16,** 99–109 (2015).

8. ABSTRACT

Despite huge suffering caused by cutaneous leishmaniasis (CL), there is no effective and affordable treatment strategy against CL and no licensed vaccines. The current treatments show limited efficacy and high toxicity. Improved therapies through discovery of novel drugs and/or an alternative treatment approaches are/is urgently needed. We aimed at identifying a novel antileishmanial agent and developing an innovative nanoparticle (NP) based platform for safe and effective treatments against CL. We discovered that polyhexanide (PHMB), a widely used antimicrobial polymer and wound antisepsis, shows an inherent antileishmanial activity at submicromolar concentrations. PHMB appears to kill *L. major* parasites via a dual mechanism involving disruption of membrane integrity and selective chromosome condensation. However, host chromosomes binding appear to be limited by exclusion from mammalian cell nuclei. Moreover, we attempted to establish effective drug delivery systems that overcome the various shortcomings in the present treatment of CL. In this scenario, we initially studied the cellular interactions of NPs and their uptake mechanisms into mammalian cells before applying them in drug delivery system. We obtained clear evidence for the involvement of multiple endocytic routes to internalize NPs. Physicochemical properties of NPs, cell type, temperature and pathogenesis of the target diseases were shown to be determinant factors. Thereafter, a mechanism based host- and pathogen-directed combination therapy comprising PHMB and CpG ODN immunomodulator was established for overall synergistic effect against CL. It simultaneously targets the pathogen and the host immunity with effective delivery system. The results show that PHMB binds to CpG ODN and form stable nanopolyplexes for efficient cell entry and therapy. The nanopolyplexes displayed enhanced cellular uptake and antileishmanial potency while drastically reducing the toxicity against mammalian cells. In conclusion, our findings clearly indicate that PHMB can be used as effective candidate drug against CL and as non-viral delivery of immunomodulatory

nucleic acids. Moreover, our proof-of concept study showed nanomedicine approaches are effective strategy to challenge CL and other human diseases.

Zusammenfassung

Obgleich enorme Leiden mit der kutanen Leishmaniose einhergehen stehen bis dato keine wirkungsvollen und erschwinglichen Therapien oder zugelassene Impfstoffe zur Verfügung. Die derzeitigen Behandlungsmethoden sind kaum effektiv und zeichnen sich vor allem durch ihre enormen Nebenwirkungen aus. Aus diesem Grund ist die Erforschung neuartiger Wirkstoffe und Therapieansätze gegen kutane Leishmaniose zwingend notwendig. Die vorliegende Arbeit beschreibt die Entdeckung eines neuen antileishmanialen Wirkstoffes und die Etablierung eines innovativen und auf Nanopartikeln basierenden Verfahrens zur sicheren und effizienten Behandlung der kutanen Leishmaniose. Das Polyhexanid, welches bereits Verwendung als antimikrobielles Polymer und als Wundantiseptikum findet, weist bereits in submikromolaren Konzentrationen eine immanente antileishmaniale Wirkung auf. Den Beobachtungen zu Folge beeinflusst das Polyhexanid die Integrität der parasitären Zellmembran und führt zur selektiven Chromosomenkondensation des Parasiten *Leishmania major*. Eine potentielle Chromosomenmodifikation in der Säugetierzelle wird durch den Ausschluss des Polyhexanides aus dem Zellkern verhindert. Um die zahlreichen Mängel der aktuellen Behandlungsmethoden gegen kutane Leishmaniose zu überwinden, wurde zudem ein effizientes System der Wirkstoffabgabe etabliert. Diesbezüglich wurden zunächst die zellulären Wechselwirkungen der Nanopartikel und deren Aufnahme in die Säugtierzelle untersucht ehe diese als Vehikel für den Wirkstoff verwendet wurden. Es konnte gezeigt werden, dass die Nanopartikel über mehrere endozytische Wege internalisiert werden. Physikochemische Eigenschaften der Nanopartikel, der Zelltyp, die Temperatur und erregerspezifische Pathogenese gehören zu den beeinflussenden Faktoren. Daraufhin wurde

eine Kombinationstherapie bestehend aus Polyhexaniden und dem unmethylierten Immunmodulator Zystein-Phosphat-Guanin Oligodeoxynukleotid mit synergistischen antileishmanialen Auswirkungen, etabliert. Dies gestattet eine gegen den Erreger zielgerichtete Behandlung und die zeitgleiche Stimulierung der Wirtsimmunität. Die Bildung eines stabilen Nanopolyplexes bestehend aus dem Polyhexanid und dem oben genannten Immunmodulator befähigen die effiziente Aufnahme in die Zelle und somit die Behandlung. Der Nanopolyplex ermöglicht eine verbesserte Aufnahme in die Zelle und antileishmaniale Wirksamkeit wohingegen die Toxizität gegenüber Säugetierzellen drastisch reduziert ist. Zusammenfassend lässt sich feststellen, dass Polyhexanide als effizienter Wirkstoffkandidat gegen kutane Leishmaniose und als nicht-viraler Träger von immunmodulatorischen Nukleinsäuren zu betrachten sind. Zugleich wurde gezeigt, dass die Nanomedizin einen wertvollen Beitrag zur Bekämpfung der kutanen Leishmaniose und sicherlich auch anderer Krankheitserregern leisten kann.

9. AFFIDAVIT

I herby confirm that my thesis entitled “Use of polyhexanide and nanomedicine approach for effective treatment of cutaneous leishmaniasis” is the result of my own work. I did not receive any help or support from commercial consultants. All sources and /or materials applied are listed and specified in the thesis. Furthermore, I confirm that this thesis has not yet been submitted as part of another examination process neither in identical nor in similar form.

Würzburg, 23.03.2015 Rebuma Firdessa Fite

Eidesstattliche Erklärung

Hiermit erkläre ich an Eides statt, die Dissertation “ Die Verwendung von Polyhexaniden und Konzepten der Nanomedizin zur effektiven Behandlung kutaner Leishmaniose” eigenständig, d.h. insbesondere selbständig und ohne Hilfe eines kommerziellen Promotionsberaters angefertigt und keine andere als die von mir angegebenen Quellen und Hilfsmittel verwendet zu haben. Ich erkläre außerdem, dass die Dissertation weder in gleicher noch in ähnlicher Form bereits in einem anderen Prüfungsverfahren vorgelegen hat.

Würzburg, 23.03.2015 Rebuma Firdessa Fite

10. ABBREVIATIONS

APC	Antigen-presenting cell
BMDC	Bone marrow-derived dendritic cell
BMDM	Bone marrow-derived macrophages
CD	Cluster of differentiation
CL	Cutaneous leishmaniasis
CpG ODN	Cytosine-phosphate-guanosine oligodeoxynucleotide
CpG-R	R hodamine -red CpG ODN
DCL	Diffuse cutaneous leishmaniasis
DMEM	Dulbecco's modified eagle medium
DNA	Deoxyribonucleic acid
ELS	Electrophoretic light scattering
ELISA	Enzyme-linked immunosorbent assay
EMSA	Electrophoretic mobility shift assay
FACS	Fluorescence activated cell sorting
FITC	Fluorescein isothiocyanate
FM4-64FX	Fei Mao fixative form
gDNA	Genomic DNA
HPV	Human papilloma virus
IFN-γ	Interferon gamma
IL	Interleukin
ITC	Isothermal titration calorimetry
L. major	*Leishmania major*
LPG	Lipophosphoglycan
M-CSF	Macrophage-colony stimulating factor
MDR	Multidrug resistance
MFI	Mean fluorescence intensity
MHC	Major histocompatibility complex

NF-κB	the transcription factor nuclear factor kappa B
NP	Nanoparticle
PBS	Phosphate-buffered saline
PFA	Paraformaldehyde
PHMB	Polyhexamethylene biguanide
PRRs	Pattern-recognition receptors
PI3K	Phosphatidylinositol 3-kinase
RPMI	Roswell park memorial institute
RNA	Ribose nucleic acid
TEM	Transmission electron microscopy
TGFβ	Transforming growth factor β
Th	T helper
TLR	Toll-like receptor
TNF-α	Tumor necrosis factor alpha
VL	Visceral leishmaniasis
WHO	World health organization

11. ACKNOWLEDGEMENT

Above all, I would like to thank God, the creator of the Universe, my Lord and my saviour, Jesus Christ for giving me the patience, health and ability to conduct my PhD study.

My great appreciation and thank goes to Prof. Dr. Heidrun Moll for giving me the chance to do my PhD in her esteemed infection immunology laboratory at Institute for Molecular Infection Biology (IMIB), University of Würzburg. I particularly thank for her overall guidance, care and support throughout my PhD study period. I also thank for her meticulous corrections during the preparation of the doctoral thesis and manuscripts for publication, and for providing an enjoyable place to work in. An extra thank to Prof. Dr. Heidrun Moll for giving me extra chance and freedom to generate my own research idea, work independently and explore my hidden potential to convert a great challenge into great opportunity. Dear Prof. Dr. Moll, the entire study and its productive outcome wouldn't have been possible without your presence.

I would like to express my deepest thank to my other two supervisors, AOR Dr. Tobias Ölschläger, IMIB, Würzburg and Prof. Dr. Richard Lucius, Molecular Parasitology, Humboldt University, Berlin, for their scientific support and guidance, sharing their busy time to discuss on my progress reports, positive feedbacks and overall guidance. I am very lucky to have them in my supervisory committee and express my special thank for their invaluable input into my research when most needed. I am very grateful to Prof. Dr. Thomas Hünig for his willingness to chairperson my doctoral thesis.

During my PhD study, I had a great opportunity to collaborate with different institutes and laboratories. In this scenario, I was privileged to have Dr. Liam Good, Royal Veterinary College, University of London and thank him for sending me PHMB regularly, his discussions on each result comes out of every experiment over Skype and telephone, and his support in the preparation for a publication and a patent. Similarly, I thank Prof. Dr. Dr.

Lorenz Meinel and his laboratory members, Institute for Pharmacy and Food Chemistry, University of Würzburg for the excellent collaboration we had for physicochemical characterizations of our nanopolyplexes. I extent my gratefully thank to Prof. Dr. Anke Krüger, Institute for Organic Chemistry, University of Würzburg and Dr. Uta Schurigt, IMIB, for the initiation and inspiration into the field of nanomedicine and the collaboration we had during the first two years of my PhD study. Moreover, I thank Dr. Conor Caffrey, Department of Pathology, School of Medicine, University of California, San Francisco, for the opportunity and collaboration we had during my research stays in his laboratory.

I would also like to thank Dr. Gabriele Blum-Oehler for sharing my challenges and concerns during the difficult period of my PhD study. In general, Graduate School of Life Sciences (GSLS) administration office is appreciated for the opportunity, support and organizations to participate in many workshops, transferable skills, courses and retreats. Moreover, I am very grateful for the PhD fellowship supports from the German Excellence Initiative to GSLS and DAAD STIBET Abschlussbeihilfe, University of Würzburg, Germany.

I would like to thank all members of Prof. Dr. Heidrun Moll and the IMIB/ZINF for their technical or administrative supports. Particularly, I thank our wonderful technical assistants namely: Martina Schultheis, Bianca Röger, Elena Katzowitsch and Christina Daumberger for their technical assistance. Special thank to Dr. Anita Masic for support in translating the abstract of this thesis from English to German.

At last but not the least, I would like to thank my parents and whole family who didn't have a chance to learn modern education but understood its value and straggled a lot to send me to school, taught me to be respectfully to all human kind and made me who I am today. Thank you for everything. Very special thank to my wife, Atsede Bekele Hisa (Lali), for her love, care, encouragement and prayer during my PhD period. For whatever challenge I might have faced, she was there for me with her smiley face and made me cool down by her Godly

advice and then at the end confronted the challenge with maturity. Moreover, thank you sweet Lali for your nice foods and hot drinks after every long day laboratory work. I don't have enough word to express my feeling, but I say that you are really a blessing and a vital to my life. My PhD study and life without you would have been very boring or some time meaningless. As you are part of my life, we also share this PhD like any other things, cheers and love you much Lali!! Ati gonfoo kooti! Galata baay'ees narraa qabda!!

Finally, I am grateful to my friend Dr. Dejene Milkessa Tufa, Hannover Medical School, Germany, for correcting part of my thesis and to everyone who has involved in my studies in one way or another and supported my journey towards the finished line.

12. LISTS OF PUBLICATIONS AND CURICULUM VITAE

All my publications and their citations can be seen in pubmed and google scholar through the following links (http://www.ncbi.nlm.nih.gov/pubmed/?term=Firdessa+R; http://scholar.google.com/citations?user=6KNJFMwAAAAJ&hl=en)

1. Thilo Waag[+], **Rebuma Firdessa**[+], Lena Winner, Uta Schurigt, Anke Krueger: Nanodiamond for targeted drug release using pH sensitive linkers. [+]These authors contributed equally to this work (in preparation)
2. **Rebuma Firdessa**, Liam Good, Maria Cecilia Amstalden, Martina Schultheis, Bianca Röger, Nina Hecht, Tobias A. Oelschlaeger, Lorenz Meinel, Tessa Lühmann, Heidrun Moll: Pathogen and host directed antileishmanial effects mediated by PHMB. **PLOS Neglected Tropical Diseases** (in revision).
3. Stefan Berg[+], Esther Schelling[+], Elena Hailu[+], **Rebuma Firdessa**[+], Balako Gumi, Girume Erenso, Endalamaw Gadisa,Araya Mengistu, Meseret Habtamu, Jemal Hussein, Teklu Kiros, Shiferaw Bekele, Wondale Mekonnen, Yohannes Derese,Jakob Zinsstag, Gobena Ameni, Sebastien Gagneux, Brian D Robertson, Rea Tschopp, Glyn Hewinson, Lawrence Yamuah, Stephen V Gordon and Abraham Aseffa. Investigation of the high rates of extrapulmonary tuberculosis in Ethiopia reveals no single driving factor and minimal evidence for zoonotic transmission of *Mycobacterium bovis* infection. [+]Equal contributors. ***BMC Infectious Diseases*** **2015**, 15:112 doi: 10.1186/s12879-015-0846-7
4. **Rebuma Firdessa,** Tobias A. Oelschlaeger, Heidrun Moll: Multiple cellular uptake pathways of polystyrene nanoparticles and factors affecting the uptake: Relevance for drug delivery systems. **European Journal of Cell Biology**, **2014**, 93(8-9):323-337. Doi: 10.1016/j.ejcb.2014.08.001.
5. **Rebuma Firdessa,** Stefan Berg, Elena Hailu, Esther Schelling, Balako Gumi, Girume Erenso, Endalamaw Gadisa, Teklu Kiros, Meseret Habtamu, Jemal Hussein, Jakob Zinsstag, Brian D. Robertson, Gobena Ameni, Amanda J. Lohan, Brendan Loftus, Iñaki Comas, Sebastien Gagneux, Rea Tschopp, Lawrence Yamuah, Glyn Hewinson, Stephen V. Gordon, Douglas B. Young, and Abraham Aseffa. Mycobacterial Lineages Causing Pulmonary and Extrapulmonary Tuberculosis, Ethiopia. **Emerging Infectious Diseases**, **2013**, 19(3):460-3. Dio: 10.3201/eid1903.120256
6. Balako Gumi, **Rebuma Firdessa**, Lawrence Yamuah, Teshale Sori, Tadele Tolosa, Abraham Aseffa, Jakob Zinsstag and Esther Schelling. Seroprevalence of Brucellosis and

Q-Fever in Southeast Ethiopian Pastoral Livestock. **Journal of Veterinary Science & Medical Diagnosis**, **2013**, 2(1). Doi: 10.4172/2325-9590.1000109

7. Abraham Mekibeb, Tadele Tolosa Fulasa**,** **Rebuma Firdessa** and Elena Hailu. Prevalence study on bovine tuberculosis and molecular characterization of its causative agents in cattle slaughtered at Addis Ababa municipal abattoir, Central Ethiopia. **Tropical Animal Health and Production, 2013**, 45(3):763-9. Doi: 10.1007/s11250-012-0287-x
8. Legesse Garedew, Adane Mihret, Gezahagne Mamo,Tamrat Abebe, **Rebuma Firdessa**, Yonas Bekele, Gobena Ameni. Strain diversity of mycobacteria isolated from pulmonary tuberculosis patients at Debre Birhan Hospital, Ethiopia. **The International Journal of Tuberculosis and Lung Disease, 2013**, 17(8):1076-81. Doi: 10.5588/ijtld.12.0854
9. **Rebuma Firdessa,** Rea Tschopp, Alehegne Wubete, Melaku Sombo, Elena Hailu, Girume Erenso, Teklu Kiros, Lawrence Yamuah, Martin Vordermeier, R. Glyn Hewinson, Douglas Young, Stephen V. Gordon, Mesfin Sahile, Abraham Aseffa, and Stefan Berg. High prevalence of bovine tuberculosis in dairy cattle in central ethiopia: implications for the dairy industry and public health. **PLoS One**, **2012** doi:10.1371/journal.pone.0052851
10. Balako Gumi, Esther Schelling, Stefan Berg, **Rebuma Firdessa,** Girume Erenso, Wondale Mekonnen, Elena Hailu, Ermias Melese, Jemal Hussein, Abraham Aseffa, and Jakob Zinsstag. Zoonotic transmission of tuberculosis between pastoralists and their livestock in South-East Ethiopia. **Ecohealth, 2012**, 9(2):139-49. Doi: 10.1007/s10393-012-0754-x
11. Balako Gumi, Esther Schelling, **Rebuma Firdessa,** Girume Erenso, Demelash Biffa, Abraham Aseffa, Rea Tschopp, Lawrence Yamuah, Douglas Young, and Jakob Zinsstag. Low prevalence of bovine tuberculosis in Somali pastoral livestock, southeast Ethiopia. **Tropical Animal Health and Production, 2012,** 44(7):1445-1450. Doi: 10.1007/s11250-012-0085-5
12. Rea Tschopp, Kidist Bobosha, Abraham Aseffa, Esther Schelling, Meseret Habtamu, Rahel Iwnetu, Elena Hailu, **Rebuma Firdessa**, Jemal Hussein, Douglas Young, and Jakob Zinsstag. Bovine tuberculosis at a cattle-small ruminant-human interface in Meskan, Gurage region,Central Ethiopia. **BMC Infectious Diseases, 2011**, 11:318. Doi: 10.1186/1471-2334-11-318
13. Balako Gumi, Esther Schelling, **Rebuma Firdessa,** Abraham Aseffa, Rea Tschopp, Lawrence Yamuah, Douglas Young and Jakob Zinsstag. Prevalence of bovine tuberculosis in pastoral cattle herds in the Oromia region, southern Ethiopia. **Tropical**

Animal Health and Production, 2011, 43(6):1081-1087. Doi: 10.1007/s11250-010-9777-x

14. Stefan Berg, M. Carmen Garcia-Pelayo, Borna Müller, Elena Hailu, Benon Asiimwe, Kristin Kremer, James Dale, M. Beatrice Boniotti, Sabrina Rodriguez, Markus Hilty, Leen Rigouts, **Rebuma Firdessa,** Adelina Machado, Custodia Mucavele, Bongo Nare Richard Ngandolo, Judith Bruchfeld, Laura Boschiroli, Annélle Müller, Naima Sahraoui, Maria Pacciarini, Simeon Cadmus, Moses Joloba, Dick van Soolingen, Anita L. Michel, Berit Djønne, Alicia Aranaz, Jakob Zinsstag, Paul van Helden, Françoise Portaels, Rudovick Kazwala, Gunilla Källenius, R. Glyn Hewinson, Abraham Aseffa, Stephen V. Gordon, and Noel H. Smith. African 2, a clonal complex of Mycobacterium bovis epidemiologically important in East Africa. **Journal of Bacteriology, 2011**,193(3):670-678. Doi: 10.1128/JB.00750-10
15. Gobena Ameni, Martin Vordermeier, **Rebuma Firdessa,** Abraham Aseffa, Glyn Hewinson, Stephen V. Gordon, and Stefan Berg. Mycobacterium tuberculosis infection in grazing cattle in central Ethiopia. **Veterinary Journal, 2011**, 188(3):359-361. Doi: 10.1016/j.tvjl.2010.05.005
16. Gobena Ameni, Desta F, and **Rebuma Firdessa.** Molecular typing of Mycobacterium bovis isolated from tuberculosis lesions of cattle in north eastern Ethiopia. **Veterinary Record, 2010**,167(4):138-41. Doi: 10.1136/vr.b4881.
17. Stefan Berg, **Rebuma Firdessa**, Meseret Habtamu, Endalamaw Gadisa, Araya Mengistu, Lawrence Yamuah, Gobena Ameni, Martin Vordermeier, Brian D. Robertson, Noel H. Smith, Howard Engers, Douglas Young, R. Glyn Hewinson, Abraham Aseffa, and Stephen V. Gordon. The burden of mycobacterial disease in ethiopian cattle: implications for public health. **PLoS One**, **2009**, 4(4):e5068.doi: 10.1371/journal.pone.0005068

PATENT

A patent on activity of PHMB against *Leishmania* and the use of PHMB as carrier for immunomodulatory molecules has been submitted by University of Würzburg and University of London, Royal Veterinary Medicine to World Intellectual Property Organization, London Office, 2015.

SELECTED SCIENTIFIC PRESENATIONS

Year	*Institute and Descriptions*
10/14	Nanomedicine: an alternative approaches to challenge human diseases (poster presentation). Graduate School of Life Sciences, University Würzburg, Rudolf-Virchow-Zentrum, Würzburg, Germany.
05/14	Nanotechnology as an approach to challenge infectious Diseases. 3rd Molecular Microbiology Meeting, Institute for Molecular Infection Biology, Würzburg, Germany.
03/14	Multiple cellular uptake mechanisms of nanoparticle and intracellular trafficking: relevance in drug delivery systems. 5th International Congress NanoBioMed, 2014, Krems, Austria.
01/14	Role of nucleic acid-sensing toll-like receptors in Th1/Th2 polarizations. Institute for Molecular Infection Biology, University Würzburg, Würzburg Germany.
11/13	Peptide nucleic acids and its application in biomedical sciences, PhD Student Seminar, Institute for Molecular Infection Biology, University Würzburg, Würzburg, Germany.
05/13	Nanovaccine as an approach to challenge human diseases. Institute for Molecular Infection Biology, University Würzburg, Würzburg Germany.
01/13	Cellular uptake mechanisms and intracellular trafficking of fluorescent polystyrene nanoparticles: relevance in controlled drug release. Institute for Molecular Infection Biology, University Würzburg, Würzburg Germany.
10/12	Global molecular epidemiology of tuberculosis**,** PhD Student Seminar, Institute for Molecular Infection Biology, University Würzburg, Würzburg Germany.
10/12	Mechanisms of nanodiamonds cellular uptake and their implication in drug delivery system, Institute for Molecular Infection Biology, University Würzburg, Würzburg Germany.
03/12	Functional analysis of novel compounds and drug delivery systems against *Leishmania major* on the 6th short course for Young Parasitologist, Heidelberg organized by Germany Society for parasitology

	and University of Heidelberg , Heidelberg, Germany.
01/12	Nanoparticles based delivery systems, PhD Student Seminar, Institute for Molecular Infection Biology, University Würzburg, Würzburg Germany.
11/11	Functional analysis of compounds and effective drug delivery systems against *Leishmania major* and *Mycobacterium tuberculosis.* Institute for Molecular Infection Biology, University Würzburg, Würzburg Germany.

SCHOLARSHIPS AND AWARDS

Years	***Funding and Descriptions***
09/14 –02/15	DAAD STIBET Fellowship Abschlussbeihilfe fellowship for a total of five months
03/11 –09/14	German Excellent Initiatives PhD fellowship to Graduate School of Life Science, University of Würzburg, Germany. It includes 5000 Euro for research grant and 750 Euro for conferences transport cost each year, and 1460 Euro monthly stipendium for a total of 3 and half years.
01/11	Keystone Symposium International Travel awards, travel to Vancouver, Canada covering round trip flight ticket from Ethiopia, accommodation for one week, symposiums costs and pocket money.
08/10	Full sponsorship from European and Developing Countries Clinical Trials Partner (EDCTP) through East African Consortium for Clinical Research to attend workshop on tuberculosis epidemiology and microbiology for one week held at National Institute for Medical, Dar es Salaam, Tanzania.
01/10	50% bursary from Wellcome Trust Fellowship for short term training (one week) on Genomics and Clinical Microbiology, Wellcome Trust Advanced Course at Sanger Institute, Wellcome trust Genome campus Cambridge, UK.
01/10 – 02/ 10	Wellcome Trust fellowships for short term training on molecular biology and immunological techniques at Veterinary Laboratory Agency, London, UK. The fellowship included round flight tick from Ethiopia to UK, course fee, daily allowance pocket money and accommodation expenses.

09/08 –08/10	Sponsorship research project grant from Wellcome Trust fund to AHRI for my Master of Science in Tropical and Infectious Diseases study at Addis Ababa University, Ethiopia.

NATIONAL SHORT TERM TRAINING AND WORKSHOPS

Years	***Institutes and Descriptions***
09/10	Advanced Epidemiology training for three days organized by Swiss Tropical Institute, Switzerland in collaboration with Armauer Hansen Research Institute (AHRI), held at Addis Ababa, Ethiopia.
10/09	Strategic Quality Management(SQM) in Biomedical Research organized by World Health Organization, Tropical Disease Research (WHO/TDR) in collaboration with AHRI, held at Addis Ababa, Ethiopia.
12/07	Operational Health Research in Epidemiology for one week organized by AHRI/ALER in collaboration with WHO held at Addis Ababa, Ethiopia.
11/07 – 12/07	Wet training on molecular typing techniques: Deletion typing, Spoligotyping and Variable Number Tandem Repeats (VNTR Organized by AHRI in collaboration with Veterinary Laboratories Agency, UK held at Addis Ababa, Ethiopia.
06/07	Workshop on application of genetics to disease control for three days organized by AHRI, Ethiopia, Imperial College London, UK, Trinity College Dublin, Ireland, and Veterinary Laboratories Agency, UK which was sponsored by Wellcome Trust UK held at Addis Ababa, Ethiopia.

INTERNATIONAL WORKSHOPS /RESEARCH STAY

Years	***Institutes and Descriptions***
07/14	MicroScale Thermophoresis, organized by Graduate School of Life Science, University of Würzburg, Würzburg, Germany.
11/13	Grant Proposal Writing workshop for one day, organized by Graduate School of Life Science, University of Würzburg, Würzburg, Germany.
10/13	Patent Law in Life Sciences workshop for two days, organized by Graduate School of Life Science, University of Würzburg, Würzburg, Germany.

06/12 – 08/12 Research stay at Dr. Conor Caffrey, Department of Pathology, School of Medicine, University of California, San Francisco, USA.

03/12 Intercultural training organized by Graduate School of Life Science, University of Würzburg, Würzburg, Germany.

03/12 The 6th short course for Young Parasitologist (one week), Heidelberg organized by Germany Society for parasitology and University of Heidelberg , Heidelberg, Germany.

02/12 Poster Design and Presentation organized by Grduate School of Life Science, University of Würzburg, Würzburg, Germany.

09/11 Laboratory animal sciences course CAT. B FELASA for one week in Berlin, Germany.

08/11 Information Technologies in Health Care and Life Sciences Graduate School of Life Science, University of Würzburg, Germany.

08/10 Tuberculosis Epidemiology and Microbiology, workshop for one week, organized by European and Developing countries clinical Trials Initiatives held at National Institute for Medical Research though (EDCTP), Dar es Salaam, Tanzania.

02/10 *M. tuberculosis* drug resistance, DNA Microarray, Sequencing, and other molecular and immunological techniques training organized by Veterinary laboratory Agency, held at London, UK.

01/10 Wellcome Trust Advanced Course on Genomics and Clinical Microbiology organized by Sanger Institute, held at Wellcome trust Genome campus Cambridge, UK.

JOURNAL EDITOR AND REVIEWER

Assistant editor for De Gruyter Open Publishing in Medicine, Pharmacy and Public Health (http://degruyteropen.com/people/rfirdessa/), reviewer to European Journal of Cell Biology and BMC Veterinary Journal.

TECHNICAL SKILLS

Nanomedicine and nanotechnology: Strong knowledge and research experience in nanoparticle/drug formulations and their physicochemical characterizations: determinations of size, zeta potential and binding affinity of nanoparticles or nanopolyplexes by dynamic light

scattering (DLS), electrophoretic light scattering (ELS), transmission electron micrscopy (TEM), electrophoretic mobility shift assay (EMSA), isothermal titration calorimetry (ITC) and microscale thermophoresis (MST); polymer nanoparticle-based delivery of small molecules, immune modulators and nucleic acids**,** and testing for efficacy (IC_{50} determination), biocompatibility with reporter gene assays (Luciferase transgenic strains) and MTT assay.

Laboratory animal handling: General anaesthesia by isoflurane inhalation via anaesthetic machine; over all handling and sampling; taking general clinical parameters including footpads swelling and weight; administration of drugs with/without nanoparticle formulations intravenous (tail vein), subcutaneous (foot pad and neck fold) and intraperitoneal; experience with mouse surgery, taking organs and stem cells for cell generation; in vivo imaging systems (IVIS) of mice infected with reporter gene strains of microbes for determination of drug efficacy and longitudinal infection progression studies.

Molecular biology and immunology techniques: cell and tissue culture, bone marrow derived macrophages and dendritic cells generations, cell isolation from mice organs (lymph nodes, spleen), TEM, confocal microscopy and fluorescent microscopy with image processing tools like Imagej, immunocytochemistry, flow cytometry**,** western blotting**,** biological sample collection, microbiological culture, biochemical tests, gamma interferon assay, ELISA, complement fixation test, competitive ELISA, RT-PCR, DNA extraction, transformation or transfection, restriction fragment length polymorphism (RFLP), variable number tandem repeats, spoligotyping, multi-locus sequencing, DNA microarray, bioinformatics tools for proteomics and genomics and, single nucleotide polymorphisms analysis.

Würzburg, 23.03.2015 Rebuma Firdessa Fite